1971

An investigation of the radiation polymerization of methyl methacrylate-kaolin clay composites

James Jackson Beeson

Department: Chemical and Biochemical Engineering

111

AN INVESTIGATION OF THE RADIATION POLYMERIZATION OF METHYL METHACRYLATE-KAOLIN CLAY COMPOSITES

by

JAMES JACKSON BEESON, 1945-

A DISSERTATION

Presented to the Faculty of the Graduate School of the

UNIVERSITY OF MISSOURI-ROLLA

In Partial Fulfillment of the Requirements for the Degree

DOCTOR OF PHILOSOPHY

in

CHEMICAL ENGINEERING

1971

K. G. Mayhan
Advisor

Gary L. Rutland

Otto H. Hill

E. W. Dorf

G. Ray Edwards

ABSTRACT

A kinetic and characterization study has been made on the effects of gamma-rays (Co^{60}) on the polymerization of a 50-50 weight mixture methyl methacrylate (MMA) kaolin clay system. The effect of dose rate (7.35 - 24.9 rads per second), temperature (25 to 75^{o}C) and total dose on the percentage conversion of monomer to polymer was studied. The rate of formation of polymer at 25^{o}C in the composite system was found to be faster when compared to a bulk MMA system at the same experimental conditions. This acceleration showed that the clay had a catalytic effect on the formation of polymer. The effect decreased as temperature increased. Rate data and apparent activation energies are reported.

Two types of polymethylmethacrylate (PMMA) were formed in the composite. One type was called homopolymer and could be removed from the composite by extraction with organic solvents. The other type was called inserted polymer and could only be removed by dissolving the clay matrix with hydrofluoric acid. Characterization studies showed that the homo and inserted polymer exhibited the following characteristics:

1. NMR spectra showed that both polymers had increased isotacticity as compared to bulk polymer

2. the viscosity average molecular weights of the homopolymer ranged from (0.4×10^{6} to 5×10^{6}) depending upon the dose rate, temperature and total dose received.

3. gel permeation chromatography studies confirmed the increase of molecular weight for the homopolymer and showed the same peak molecular weights and distribution for the inserted polymer.

4. infrared spectroscopy showed no differences in the structure of either type of polymer.

X-ray, particle size gravimetric thermal analysis (DTA-TGA) and surface area measurements were used to characterize the clay. Mechanical tests, DTA-TGA and scanning electron microscopy were used to characterize the entire composite.

A discussion on the potential uses of PMMA-kaolin clay composites is presented along with suggested future work in this area of research.

ACKNOWLEDGEMENTS

The author wishes to acknowledge Dr. K. G. Mayhan, his advisor, and his advisory committee, Doctors E. L. Park, O. H. Hill, G. L. Bertrand and D. R. Edwards, for their assistance given throughout the duration of the research. The author acknowledges the United States Atomic Energy Commission for their financial support of this project. Thanks are extended to the personnel at the Reactor Center, University of Missouri-Columbia, Columbia, Missouri and at the Nuclear Reactor, University of Missouri-Rolla, Rolla, Missouri for their cooperation and assistance in the irradiation of the samples. The author also wishes to thank the personnel at the Graduate Center for Materials Research, University of Missouri-Rolla for their cooperation and assistance in constructing the many devices used in this work.

TABLE OF CONTENTS

Table of Contents (continued) Page

Table of Contents (continued) Page

Table of Contents (continued) Page

Table of Contents (continued) Page

LIST OF FIGURES

List of Figures (continued) Page

List of Figures (continued) Page

LIST OF TABLES

List of Tables (continued) Page

I. INTRODUCTION

Radiation initiated polymerization studies have been investigated since 1938. However, until 1958 most work dealt with the effects on and polymerization of solution and pure (bulk) polymers by radiation. Since 1958, a new type of material which incorporates the use of polymer with inorganic additives to form composites has been studied. General studies have been performed using various types of monomers and inorganic additives to give systems including polymer-concrete and polymer-clay composites. These systems make use of the fact that either the polymer was already formed or the inorganic material has been made and the monomer is impregnated into the material and then polymerized.

The purpose of this work was to investigate the radiation polymerization of a vinyl type monomer (methyl methacrylate) with a kaolin clay inorganic additive. This study was directed toward the determination of the kinetic parameters which govern the formation of polymer in the presence of kaolin clay and the characterization of the resulting polymer. The effects of dose rate, total dose and reaction temperature on the rate of polymer formation and on the properties of the polymer formed were investigated. The system studied was a 50 - 50 weight per cent mixture which was subjected to Co^{60} radiation in air. The resulting characterization and

testing of the properties of the composite have led to an understanding of the radiation polymerization of this composite, a material which may have practical engineering applications.

II. REVIEW OF THE LITERATURE

The initiation of polymerizations by ionizing radiation has been known since about 1938 when Hopwoods and Phillips* polymerized methyl methacrylate (MMA), styrene and vinyl acetate using gamma-rays and fast neutrons. After World War II Dainton* studied the X-ray and gamma-ray polymerization of acrylonitrile, methacrylonitrile and acrylamide and Magat* used gamma-rays, mixed reactor flux and X-rays to study the polymerization of vinyl monomers. From this work, the first kinetic data and possible mechanisms of radiation polymerization were obtained. From the post war era until 1958, the main area of study was the radiation polymerization of monomers in bulk and in solution. A historical review through 1961 given by Chapiro[1] includes all the above references of this type of work.

The two basic fields of kinetic study for polymer-inorganic reactions are the postulated ionic and free radical mechanisms. The work done with these mechanisms and how they pertain to the polymerization of monomer-inorganic solid reactions will be discussed separately. A special section on the characterization of polymer formed on the inorganic surface of similar compounds found in this work will also be discussed.

A. Postulated Ionic Mechanism

In 1958, Worrall and Charlesby[2] were the first to study the effects of gamma radiation (dose rate = 5.58×10^4 rads per hour) on the polymerization

*Referenced from Chapiro[1].

of polymer-inorganic additives. In their study of the low temperature ($-78.5^{o}C$) polymerization of isobutene, they found that for a total dose of one Mrad, an increase of 400 to 1400 per cent of polymer converted occurred when inorganic additives such as ZnO, CaO, MgO, Aerosil (silica gel) and $NaHCO_3$ were added to the monomer as compared to the bulk system (pure monomer). Other additives such as carbon black and polyethylene powder had no effect or actually decreased the percentage yield. As the concentration of inorganic additive (ZnO) increased, the rate of polymerization increased up to a maximum for 41 per cent by weight of additive. Low dose experiments showed that the viscosity average molecular weight ($\overline{M}_v = 388 - 541 \times 10^3$) was not appreciably affected by the presence of the additive ZnO which indicated to the authors that the main effect caused by the additive was to increase the initiation step.

Charlesby, Pinner and Worrall[3], using previously published and new data, postulated an ionic mechanism for the low temperature ($-78.5^{o}C$) polymerization of isobutene in bulk, solution (good and poor solvent), and as composites in the presence of solid additives (powdered glass, ZnO). Dose rates from a Co^{60} source of $2.64 - 9.78 \times 10^4$ rads per hour were used for the solution experiments, while dose rates of $4.5 - 4.8 \times 10^4$ rads per hour were used for the solid additive (powdered glass). For a given dose, the percentage conversion for the solution polymerization (good solvent = n-pentane, poor solvent = propane) was less than the conversion for the bulk polymer. The glass powder, as did the ZnO, greatly increased the yield of polymer for a given dose.

The analysis of the polymerization took into account the observations that:

1. the polymer yield per unit dose decreased as total dose increased
2. the $\overline{M}_v$ of the polymer starts to decrease after 0.2 Mrads of irradiation
3. the yield was independent of dose rate and increased with decreasing temperature.

A reaction scheme for the bulk polymerization was proposed which took into account the initiation, propagation and termination reaction steps and which included unimolecular, chain transfer and termination reactions by an inhibitor. The increase in observed yield due to the additives was attributed to an increase in the initiation rate caused by the additives. The cause of this increase was attributed to ionization of the monomer and stabilization of the ejected electron on the inorganic particle or initiation of an ionic reaction on the solid surface.

Dalton, Glawitsch and Roberts[4] continued the investigation of the polymerization by gamma-rays of the isobutene-zinc oxide system at $-78^{o}C$ and dose rates of 1.9×10^{4} and 4.1×10^{2} rads per hour. The surface area of the ZnO was varied from 0.2 to 17.4 m^2 per gram by varying the temperature at which the oxide was heated. Removal of surface oxygen on the ZnO by heating in vacuum increased the polymerization rate approximately five times as much as when a vacuum was pulled on the oxide at room temperature. Viscosity average molecular weights

ranged from 1 - 4 x 10^6 depending upon the conditions of the polymerization. The rate of polymerization at the same dose rate was unchanged in all cases as the surface area was varied, except at the very lowest surface area (0.2 m^2 per gram). For this surface area, the rate was reduced for both dose rates. By stirring the mixture containing the lowest surface area of oxide, it was found that the rate increased to that of the other mixtures. High $G_{initiation}$ values were obtained, which along with the high molecular weights obtained, indicated to the authors a strong possibility for chain transfer with complete suppression of termination by the additive.

Mezhirova, Sheinker and Abkin[5] did low temperature gamma ray studies on the effects of various semiconductor oxides on the polymerization of MMA and acrylonitrile at a dose rate of 28.8 x 10^4 rads per hour. In the acrylonitrile polymerization, N-type semiconductors (ZnO, TiO_2, Cr_2O_3) had no effect on the polymerization rates. P-type additives (cuprous oxide, nickel monoxide, lithiated nickel monoxide) sharply increased the acrylonitrile polymerization rate and $\overline{M}_v$ of acrylonitrile at -78°C compared to the bulk polymerization, but had no effect at 0°C which would indicate an anionic mechanism. MgO had an analogous effect; however, it could not be explained why MgO had the same effect on both the cationic polymerization of isobutylene[6] and the postulated anionic mechanism of this work. The rate of polymerization of MMA at - 52.5°C exhibited a 30 - 35 fold increase in the presence of MgO. No further work was done on the MMA polymerization.

In 1963, Charlesby and Morris[7] investigated the radiation polymerization of styrene in the presence and absence of air using dried and undried monomer in methylene chloride and in the presence of glass and silica powders at $-78^{o}C$ and dose rates of $10 - 720 \times 10^{3}$ rads per hour. The variation of $\overline{M}_v$ and polymer yield per hour with dose rate indicated that an ionic mechanism occurs in the absence of inorganic additives, but with the additives present, the styrene yield per hour varied with the square root of the dose rate which is plausible for a free radical mechanism. The number average molecular weight ($\overline{M}_n$) varied as $C^{0.5}$ in the absence of additives and as $C^{.125}$ in their presence (C is the weight concentration of styrene in solution). Increased initiation was again postulated to be the rate determining step for the increase in polymerization yield. No attachment of polystyrene to the powders was found and traces of water were determined to increase the termination rate and inhibit the polymerization. Some work was also done with surface treated silicas. Charlesby and Morris[8] continued their study of the low temperature radiation polymerization of styrene in the presence of surface modified Aerosils (surface silanol groups replaced to give organic-silyl groups). Increasing the surface coverage with a particular organic group or increasing the length of the modified species resulted in decreases of the molecular weight and yield of the polymer.

Kristal'nyi and Medvedev[9] also studied the low temperature polymerization of isobutylene in the presence of inorganic additives. At $-78^{o}C$ numerous oxides were tried and the $\overline{M}_v$ ($500 - 800 \times 10^{3}$) with and without

the additives was unchanged in agreement with Charlesby[2]. As the weight of inorganic additive and surface area increased (percentage conversion as a function of surface area of glass per gram of monomer), the yield of polymer increased. Special emphasis was placed on the isobutylene-ZnO system from -127 to 0°C. ZnO increased the yield of polymer at all temperatures. The $\overline{M}_v$ was independent of the presence of ZnO and increased as the temperature decreased. The method of purification of monomer determined the rate of polymerization at all temperatures. The copolymerization of the isobutylene-vinylidene chloride-ZnO system showed that the reactivity ratios were of the same magnitude as the ionic bulk polymer system from -78 to -39°C. This study was an indication that an ionic mechanism prevails.

B. Postulated Radical Mechanism

In 1959, Worrall and Pinner[6] continued their low temperature (-78°C) study of isobutene and also investigated the room temperature heterogenous polymerization of the MMA-polyethylene and MMA-silica systems using two MeV. electrons (6.0×10^9 rads per hour). The conversion per megarad in the MMA-polyethylene system increased as the weight fraction of solid increased. The silica had no effect on the system. This effect is not in agreement with results reported by Kornienko[10] and Uskov[11]. The amount of degradation of PMMA was small up to four Mrads. The increase in rate observed for the MMA-polyethylene system was determined to be caused by a decrease in the bimolecular termination rate constant. The possible mechanisms of radiation polymerization are discussed.

In 1960, Tsetlin, Rafikov, Plotnikova, and Glazunov[12] grafted vapors of MMA at 40°C onto carbon black, silica gel and MgO using a 700 Kv electron accelerator. The available surface area of the inorganic materials decreased rapidly as polymer was formed. Two types of polymer were formed. One type (homopolymer) was typical of the bulk polymer, while the polymer which was grafted to the surface had different characteristics. A difference in the $\overline{M}_v$ was found between the homopolymer formed ($\overline{M}_v$ = 310,000) and the polymer grafted to the MgO ($\overline{M}_v$ = 65,000). The total yield of polymer was found to increase with decreasing dose rate and to vary with the reciprocal of the square root of the dose rate. This type of polymer yield indicated to the authors a free radical mechanism with termination by a bimolecular mechanism.

Nahin[13] performed exploratory experiments with the grafting of polyethylene to organomontmorillonites and kaolinites using two MeV electrons and gamma-rays. The grafted polyethylene had greater thermal stability, tensile strength and insolubility than the control bulk polyethylene. The insolubility was taken as an indication that the polyethylene was crosslinked with the clays.

Kornienko, Polishchuk, Zelenchukova, and Polyakov[10] studied the effect of high gamma dose rate (50 - 150 rads per second) on the polymerization of styrene and MMA in bulk and in the presence of ZnO and silica gel at 20°C. The bulk polystyrene and grafted polystyrene yields per unit time varied as a function of the square root of the dose rate. Benzoquinone inhibited the reaction of all systems to the same degree.

MMA was irradiated in a nitrogen atmosphere at room temperature in the presence of ZnO, MgO, silica gel and NiO. All oxides increased the yield except NiO which had no effect. The reaction was also found to continue and be increased by the presence of the solid additives after the irradiation was discontinued. No substantial difference in $\overline{M}_v$ (190 - 290 x 10^3) was found between the polymer formed in bulk and as a composite immediately after irradiation. However, the $\overline{M}_v$ increased with time in the presence of the additives after irradiation compared to the bulk polymer (200 x 10^3 increased to 2042 x 10^3). The mechanism of the radiation polymerization for the grafted polymers was determined to be free radical by comparison with the bulk polymer systems.

Uskov, Tertykh, Solomko and Polishchuk[11] investigated the radiation polymerization of MMA in the presence of silica gel, kaolin (Glukovetshii), asbestos and glass fibers using Co^{60} as an initiator (dose rate = 50 and 100 rads per second). At room temperature, silica gel and kaolin increased the rate of polymerization of styrene, but only silica gel increased the rate for PMMA. They also found that at higher temperatures (70°C) the yields of PMMA at the same dose increased more in the presence of the silica gel than with the bulk polymer (64 per cent with silica gel compared to 41 per cent with the bulk polymer). Some of the polymer (both polystyrene and PMMA) was grafted and could not be removed by solvent extraction. PMMA was grafted to a much greater extent than polystyrene.

Morozov, Plotnikova, Rafikov and Tsetlin[14] continued the study of the kinetics of the vapor phase radiation grafting of MMA and styrene onto MgO

and Aerosil using X-rays at dose rates to 500 rads per second. They studied the dependence of reaction rate on temperature, dose rate, vapor pressure, and degree of adsorption of monomer on the inorganic substrate. The rate of grafting was found to be strongly dependent on the change of absorption characteristics of the substrate and change of chemical nature of the substrate. The adsorption of monomer vapor decreased during the reaction and the reaction rate reached a limiting value indicating a complete coating of polymer on the surface of the substrate. The reaction rate decreased as temperature increased due to a decrease in the equilibrium adsorption of monomer. Activation energies were found which were close to those of the bulk activation (MgO-styrene = 6.9, MgO-MMA = 7.0, Aerosil-styrene = 4.5 kilocalories per mole) except for the grafting of Aerosil-MMA system which was close to zero. The polymerization rate was dependent on dose rate to the 0.5 power. The rate of polymerization is proportional to the concentration of adsorbed monomer between the second and fifth power.

Yuan, Hsu, Wang, Wu, Shieh and Chang[15] studied the radiation polymerization of unsaturated polyester-styrene and red mud-fiber system at a dose rate of 7.13×10^4 rads per hour. The rate of polymerization was found to be dependent on the dose rate with an increase in the rate of polymerization as the dose rate decreased. DTA, IR and X-ray analyses were also performed which showed possible chemical bonding of polymer and red mud. The physical properties including hardness (Shore), impact strength, compression strength and tensile strength, self-extinguishing,

water absorption and thermal stability tests were reported. A regression analysis correlating the process variables to impact strength was also reported.

Kornienko and Zelenchukova[16] studied the radiation copolymerization (dose rate = 40 rads per second) of styrene-MMA system in a nitrogen atmosphere in the presence of the inorganic additives SiO_2 and MgO (40 per cent by weight of the monomer). Solvents of differing electronic nature were mixed with the system in order to define the mechanism of the process. Pure SiO_2 had a much greater influence on the rate than the pure MgO especially as the concentration of MMA increased. However, all solvents when mixed with the monomer and inorganic additives had the effect of lowering the percentage conversion and intrinsic viscosity for the same dose rate and total dose. The authors concluded that the solvents therefore had no effect on the mechanism except to act as chain transfer agents. Copolymerization rate constants found were close to the rate constants of chemically initiated copolymerization systems. There was no mention of graft copolymer onto the additives and no mechanism was given for the adsorption of the monomer to the inorganic surface.

C. Characterization

In a series of papers Blumstein and coworkers have characterized the methyl acrylate (MA), MMA and MMA-crosslinked systems polymerized in the presence of sodium montmorillonites. They were especially interested in the polymer grafted to the clay which was called inserted polymer. In Blumstein's first paper[17] on the preparation of the inserted

polymer, both free radical catalysts (benzoyl peroxide, azobis-isobutyronitrile) and gamma rays (0.4 Mrads per hour) were used as initiators. Blumstein states that the bulk monomer is almost entirely polymerized at an intensity of 0.1 Mrad while the composite needs much higher doses (six Mrads). Composites which initially contain up to 25 per cent MMA polymerize and only inserted polymer is recovered. Composites containing higher initial percentages of MMA polymerize and contain both inserted and homopolymer (polymer which can be recovered by extraction with normal solvents). No spontaneous polymerization occurred in the system. The thermal degradation at 215°C[18] of the complex showed that the inserted polymer resisted degradation even when the conventional bulk polymer was totally destroyed. This fact was attributed to the steric structure of the clay which restricted the thermal motion of the polymer. Oxygen greatly accelerated the degradation process. Blumstein and Billmeyer[19] in their study of the dilute solution properties of the three systems found that the poly(methyl acrylate) (PMA) and crosslinked insertion PMMA systems had quite different properties from the conventional bulk polymer. The differences included high light scattering molecular weights combined with low viscosities, low second virial coefficients, large variations of k' (Huggins constant) with time and temperature and low sedimentation velocities. The insertion PMMA made without crosslinking had dilute solution properties similar to conventional bulk PMMA. In continuing the study Blumstein[20] calculated the polydispersity parameter $\overline{M}_w/\overline{M}_n$ of the inserted polymer and found that

it varied between three and six from gel permeation chromatography (GPC) data. The insertion polymer[21] was found to be more isotactic than the bulk reference polymer. This type of tacticity was explained to be caused by the interaction of the carbonyl group of the ester with the positive exchangeable ions on the surface of the substrate.

Raff[22] has prepared a review of the general grafting of organic polymers onto inorganic surfaces. This review includes chemical, mechanical and radiation polymerization onto these surfaces.

The literature reveals that a great deal of work has been reported by other investigators involving the effects of gamma initiated polymerization of vinyl monomers in the presence of various inorganic surfaces. However, there has not been a detailed study performed which considered both the kinetic parameter (such as concentration, dose rate, total dose and temperature) and characterization of the subsequent products of polymerization. In addition, the procedures and experimental parameters, reported by other workers, as of now could not be utilized easily in a commercial process. The results reported in this dissertation encompass a detailed kinetic and characterization study of MMA and kaolin clay which have both scientific and engineering significance.

III. EXPERIMENTAL

A. System Design

The irradiation system was essentially in three parts, (1) a source, (2) a controlled temperature bath and (3) auxillary equipment to control the bath, record temperatures and serve as a reference point for temperature. This system allowed for the control of the three main parameters of investigation, that is temperature, dose rate and total dose.

1. Source. The Co^{60} source at the University of Missouri-Columbia of original strength of 5650 curies (1965) and present strength of 3000 curies (January 1971) consisted of 10 stainless steel tubes arranged in a cylindrical pattern 5.5 inches in diameter and was normally situated under 16 feet of water which served as a biological shield. A restraining shield 7.5 inches in diameter and 12.3 inches in height was around the outside of the cylindrical pattern of the Co^{60} tubes. The source could be used in two positions, (1) "in water" and (2) "in air." The Co^{60} source was placed on a platform (14.5 inches square) attached to a mechanical hoist. The hoist was used to raise the source from the "in water" position to the "in air" position and back again into the "in water" position. All trials were made using the source in the "in air" position. A schematic representation of the source assembly is shown in Figure 1.

2. Sample containers. The disposable aluminum sample cylinders and caps were obtained from the Nuclear Reactor, University of Missouri,

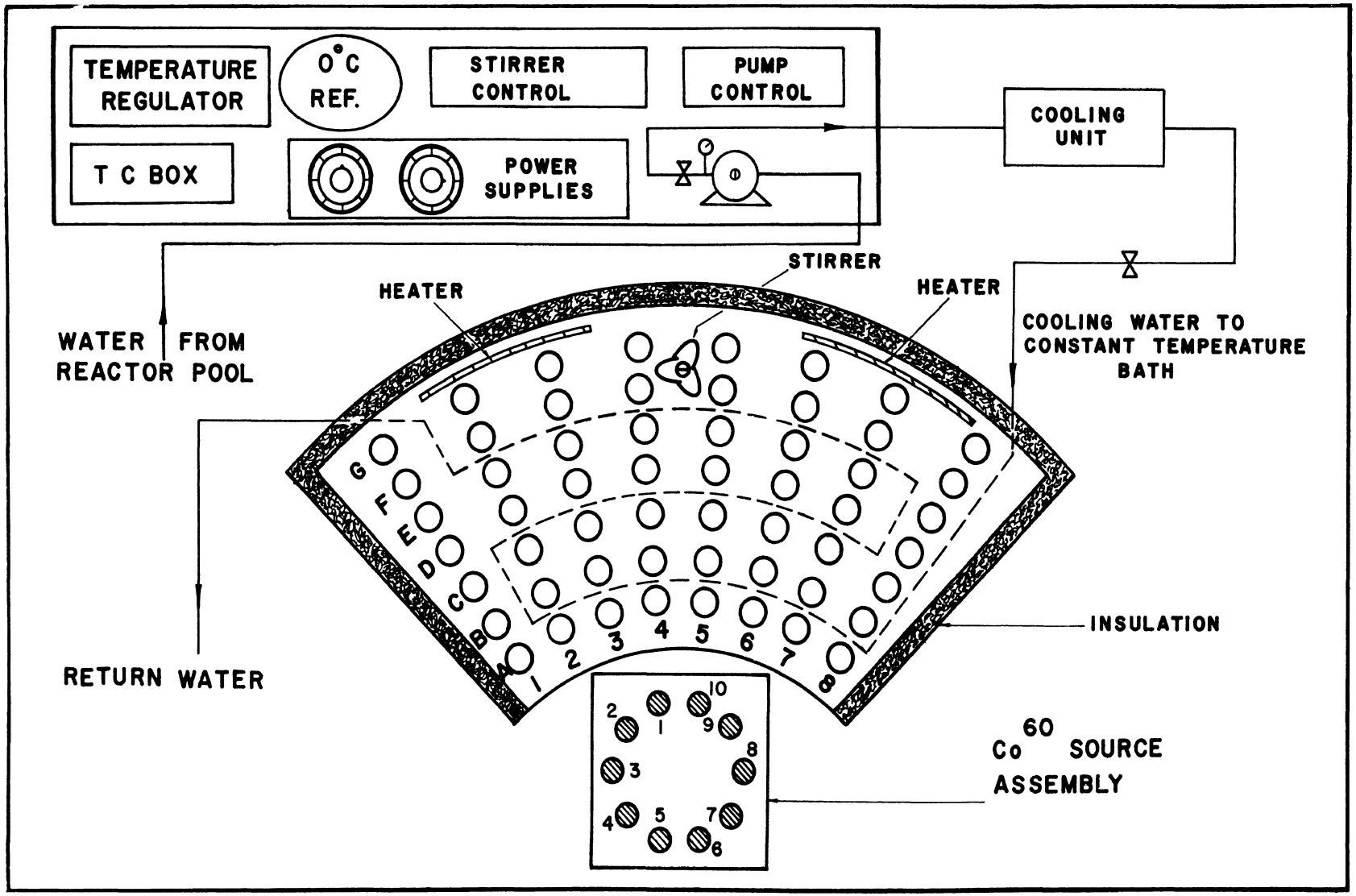

Figure 1. Source Assembly.

Rolla. The dimensions of the cylinders were 5.375 inches in length, .75 inches in diameter and had a wall thickness of 0.015 inches. The pretreatment of the containers consisted of washing in acetone and drying in an oven at 100°C.

Some of the containers had thermocouples inserted into them to measure the temperature change of the polymerization process. A hole 0.117 inches in diameter was drilled into the side of the container 2.5 inches from the bottom of the cylinder. An iron-constantan thermocouple (#26 gauge) was epoxied (epoxy-amine system) into a glass insulation tube and then sealed into the aluminum cylinder so that the bead of the thermocouple was in the geometrical center of the tube (Figure 2). The epoxied thermocouple was cured in an oven at 100°C to insure quick and proper placement of the thermocouple.

3. Constant temperature bath. A schematic representation of the bath can be seen in Figure 1. The bath is shaped as "1/3 of a cylindrical annulus" made of galvanized sheet steel (15.2 inches high), with an inner radius of 6.0 inches and outer radius of 16.0 inches as measured from its zero radius. A covering of insulation on the outside of the bath (except for the inner radius) was used to help maintain temperature control. Copper coils (1/4 inch I.D.) were bent into the desired shape of the bath. Water from the Co^{60} pool was used as cooling water. A schematic diagram of the sample holder is shown in Figure 3 and consisted of three aluminum sheets (.08 inches in thickness) machined so that the sheets fit snugly on

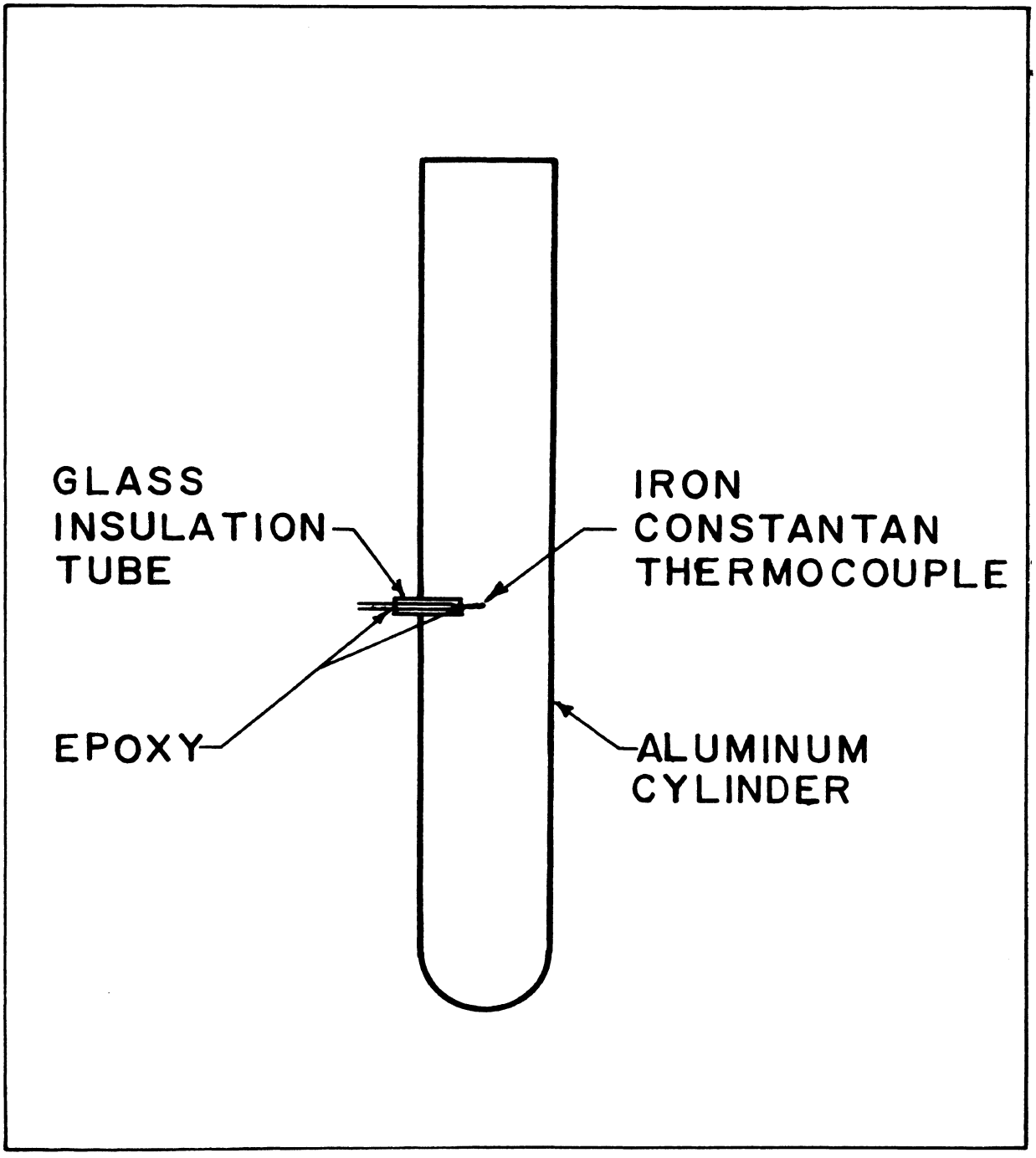

Figure 2. Sample Container with Temperature Probe

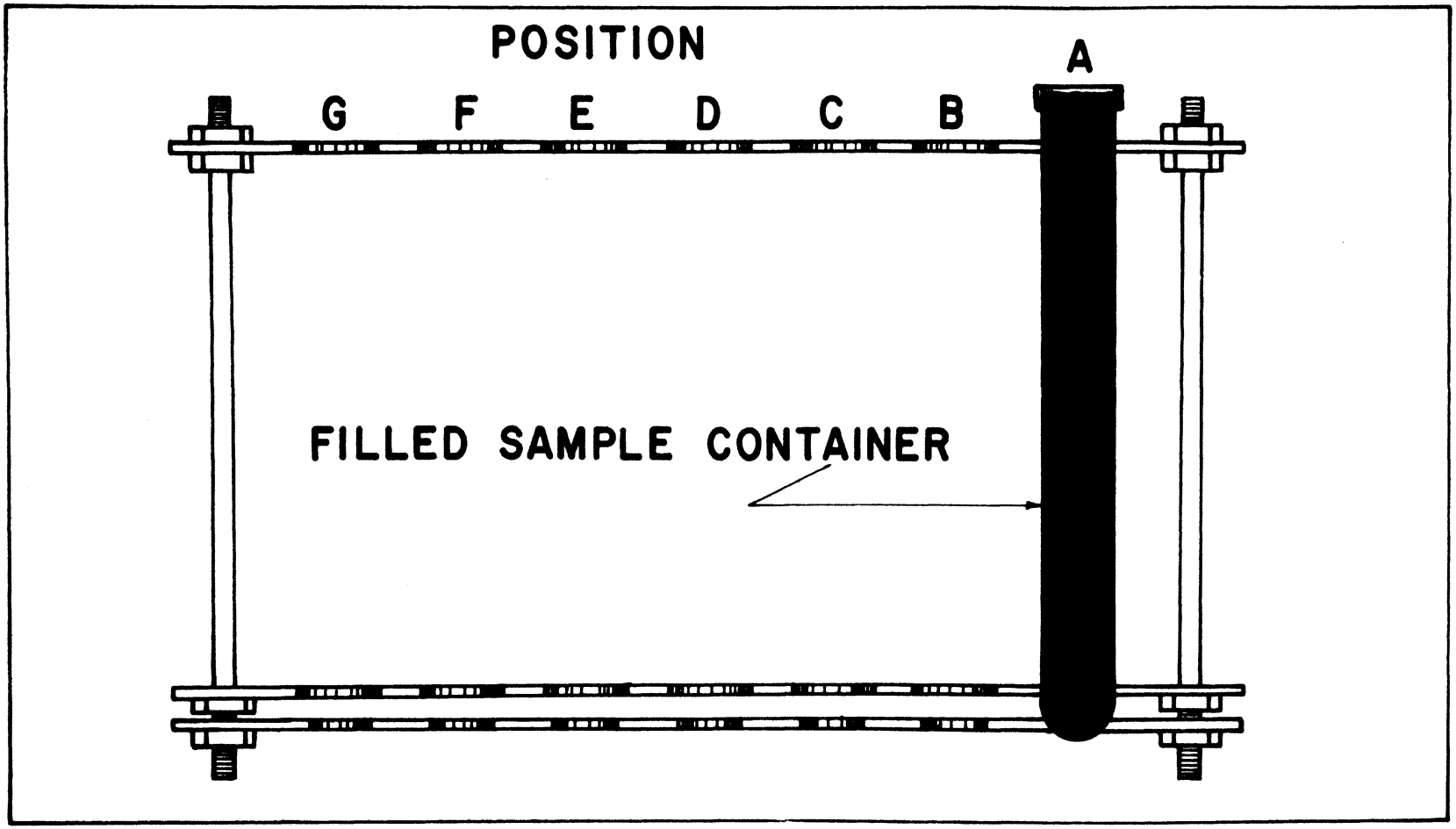

Figure 3. Side View of Sample Holder

the inside of the bath. Holes were drilled at intervals of an angle of 12^{o} around the geometrical center and one inch apart from the center of each hole in depth. Two of the plates were drilled with 3/4 inch diameter holes in order to allow the sample containers to fit through them snugly. The third plate was drilled with 5/8 inch diameter holes and provided a base for the sample cylinders to sit upon. The plates were drilled with all holes concentrically aligned. Seven rows of holes were drilled around the geometrical center of the holder consisting of eight holes each on the 12^{o} angle from the zero radius. This arrangement allowed for the irradiation of eight samples at once at any of seven different distances away from the source and thus at seven different dose rates.

4. Auxillary equipment. The auxillary equipment used for a thermocouple reference and for controlling the bath temperature is also shown in Figure 1. The equipment consisted of a Jabsco self-priming pump used for circulating the cooling water, two temperature controlling units, a $0^{o}C$ thermocouple reference bath, various stirrers, a refrigeration unit used only if necessary to cool the cooling water, five direct current heaters totaling 3500 watts of power and other rheostats used to control the heaters. A lead wall separated this equipment from the constant temperature bath and protected it from the gamma-rays. This equipment controlled the water temperature of the bath from a minimum deviation of $\pm 0.05^{o}C$ at $25^{o}C$ to a maximum deviation of $\pm .2^{o}C$ at $75^{o}C$.

The polymerization temperatures and bath temperature were recorded using a variable span (0.1 millivolts - 100 volts), variable suppression

(+100 to -1000 per cent of span), variable chart speed, two pen, wide chart Honeywell Electronik 194 recorder and a single pen, variable span, variable chart speed, narrow chart Honeywell 193 recorder which had the same specifications as the two pen recorder. Four sets of lead wires were strung from the equipment using Thermoelectric quick disconnect plugs through a cement-lead protection maze to the recorders. These lead wires allowed for the recording of three different sample polymerization temperatures plus the bath temperature by simply switching leads to the recorders.

B. Materials.

1. Monomer. The monomer used was methyl methacrylate (MMA) red label [10 ppm 4-methoxy phenol (MEHQ)] obtained from Rohm and Haas Company, Philadelphia, Pennsylvania.

2. Clay. The clay used was Ajax P Georgia Kaolin clay obtained from the Georgia Kaolin Company, Elizabeth, New Jersey 07207. A chemical analysis obtained from Georgia Kaolin is given in Table I.

3. Solvents. All solvents used were CP grade reagents and were used without further purification.

C. Dosimetry

The dosimetry was accomplished using the modified Fricke dosimeter[23]. The solution consisted of 0.001 M $Fe(NH_4)_2(SO_4)_2$ dissolved in an air saturated 0.8 N H_2SO_4 with 0.001 M NaCl added to decrease the effect of organic impurities. Doubly distilled water was used to make up all

TABLE I

CHEMICAL ANALYSIS OF AJAX
P JIGGER KAOLIN CLAY

Component	Chemical Analysis
SiO_2	45.20
Al_2O_3	38.08
FeO	.49
TiO_2	1.52
CaO	.26
MgO	.30
Na_2O	.02
K_2O	.04
Loss on ignition	13.51

solutions. All dosimetry irradiations were done in eight milliliter polyethylene vials which were 2.0 inches in height, 0.58 inches in diameter with a wall thickness of .05 inches. The vials were initially filled with the dosimetry solution and then refilled with fresh solution immediately before irradiation. The vials were placed inside the aluminum sample containers which contained pieces of coiled lead 1.5 inches in length. The coils of lead allowed the vials to sit in the middle of the tube and thus receive the dose which was proportional to the dose the sample received. All dosimetry was done at 25 $\pm$ .05^{o}C, in the constant temperature bath. The oxidation of ferrous to ferric ion was measured at 304 millimicrons using a Hitachi Perkin-Elmer UV-Visible spectrophotometer with a constant temperature cell regulated to 25 $\pm$ 0.3^{o}C.

Calculation of the absorbed dose in the Fricke dosimeter was made according to the following equation[24]:

$$D = \frac{N[\Delta(A)]\ 100}{(\Delta\epsilon)\,(10^{3})\,G(Fe^{+3})\,f\,\rho\,l}$$

where: D = absorbed dose (rads)

N = Avagadro's Number 6.023×10^{23} (molecules per gram-mole)

Δ(A) = difference in peak absorbance between irradiated solution and control

$\Delta\epsilon$ = difference in molar absorptivity (moles per centimeter) between ferric and ferrous ions at the wavelength used for the absorbance measurements

ρ = density of irradiated solution

l = optical path length (cm)

f = 6.24×10^{13} electron volt per rad

$G(Fe^{+3})$ = 15.6 molecules per 100 electron volts[25].

Calculations were made to determine the absorbed dose in the bulk polymer and the composite to determine for any necessary corrections. Mass energy absorption coefficients were calculated (Appendix A) and are shown in Table II.

The absorbed dose in the bulk polymer and composite was obtained by assuming that charged particle equilibrium existed and that the average gamma radiation exposures in the volumes of the two systems were equal. The absorbed dose for the 50-50 composite was calculated according to the following equation[26]:

$$D_{composite} = \frac{(\mu_{en}/\rho)_{composite} D_{Fricke}}{(\mu_{en}/\rho)_{Fricke}}$$

where: $D_{composite}$ = absorbed dose in composite (rads)

D_{Fricke} = absorbed dose in Fricke solution (rads)

$(\mu_{en}/\rho)_{composite}$ = mass energy absorption coefficient-composite (centimeters^2 per gram)

$(\mu_{en}/\rho)_{Fricke}$ = mass energy absorption coefficient-Fricke solution (centimeters^2 per gram)

and was found to be:

$$D_{composite} = 0.945\ D_{Fricke}$$

TABLE II

MASS ENERGY ABSORPTION COEFFICIENTS
FOR VARIOUS COMPONENTS[a]

Component	μ / ρ_{en} ($cm.^2/gm.$)
Fricke Solution	.0294
Bulk PMMA	.0288
Kaolin Clay	.0268
50-50 Composite	.0278

[a] See Appendix A.

The percentage error in reproducing the dosimetry for the various trials, differences in actual dose rate at any of the seven samples positions around the source, and obtaining the percentage conversion was greater than the differences between the absorbed dose for the Fricke and that of the composite. The mass energy absorption coefficient for the PMMA and Fricke solution were equal and within the range of experimental error. Therefore, the dose absorbed by the Fricke solution will be considered as the dose absorbed by the 50 - 50 composite and the bulk polymer.

D. Sample Preparation

1. Monomer preparation.

a. In air. For all tests, the MMA was distilled at 100^{o}C at atmospheric pressure. For all trials, the middle 1/2 was retained and the beginning 1/4 and end 1/4 discarded.

b. Inert atmosphere. The purified monomer from the atmospheric distillation was frozen in liquid nitrogen. A vacuum was then applied to the flask and the flask was allowed to slowly warm to room temperature in order to degas the monomer. This procedure was repeated at least three times. A teflon stopcock was fitted to the flask to allow for sealing of the flask. This stopcock was necessary for transferring the degassed monomer from vacuum to an inert atmosphere. The inert atmosphere was used to determine the effects of a deoxygenated system on the polymerization rate.

c. Testing of monomer. In all cases the purified monomer was protected from light by wrapping the flasks in aluminum foil. Before any monomer was used, a test was made for formation of polymer by adding normal hexane to a test portion and noting any precipitation. In all cases, no precipitate was observed.

2. Clay preparation.

a. In air. The pretreatment of the Georgia Kaolin clay consisted of heating in a muffle furnace at 300°C for four hours. Three hundred°C was chosen because this temperature insures removal of all unbound surface water, but does not effect the bound hydroxyl groups of the clay. The clay was then allowed to cool to 100°C and then placed in a descicator to cool to room temperature until needed.

b. Inert atmosphere. The clay was heated as in the "in air" treatment just before use. It was then placed in the vacuum chamber of a dry box and oxygen removed by use of a fore pump followed by purging at least three times with argon.

3. Mixing.

a. Bulk.

(1) In air. The purified monomer was placed in the sample cylinders, covered with aluminum cap and sealed with a quick drying (three hour cure time) epoxy.

(2) Inert atmosphere. The degassed purified monomer was placed into a dry box containing an argon atmosphere. The monomer was then filled as "in air" and the container was sealed with the quick drying epoxy.

b. Composite mixing. The basic mixture of monomer and clay was in the proportion of 50 per cent by weight of monomer to 50 per cent by weight of dried clay. Batches were made up on a basis of 250 grams of dried clay for the kinetic and mechanical studies. This weight is equivalent to 268 milliliters $\pm$ 1 milliliter of monomer (density of monomer = .936 grams per milliliter 20^{o}C).

(1) In air. The dried clay was removed from the descicator at room temperature, weighed and placed in a mixing container. The measured amount of pure monomer was then poured over the clay, covered with aluminum foil and allowed to stand for approximately three minutes to allow the monomer to begin penetrating into the clay. The mixing was then accomplished using a spatula until a smooth fluid mixture was obtained. The mixing process took approximately three to four minutes. The mixture was then placed into the sample container with continuous tapping to insure a homogeneous mixture. The aluminum cylinder was then capped and sealed with epoxy and allowed to stand until the epoxy was cured. A maximum of 24 hours was allowed to elapse between mixing and time of irradiation.

(2) Inert atmosphere. The same procedure was used as the "in air" mixing except that the degassed purified monomer and clay were mixed in a dry box in an argon atmosphere.

E. Kinetic Evaluation

1. Parameters. There were four initial parameters of interest in the kinetic investigation. These were concentration, dose rate, total dose

and temperature. In preliminary studies, it was determined that a 50 per cent monomer to 50 per cent dried clay (weight basis) mixture could be easily handled and had very little separation of phases. Above 50 per cent concentration of monomer, the clay settled from the mixture and below 50 per cent the clay adsorbed all monomer and no uniformity of mixture could be obtained. Therefore the concentration was held constant at 50 - 50 by weight and there were only the three remaining parameters for investigation.

2. Initial kinetic trials. A basis was required for determining an endpoint for the kinetic trials. This endpoint was found by following the exothermic temperature profile of the mixture as shown in Figure 4. The endpoint was arbitrarily assigned as the apex of the exotherm peak. Conversion data was then based on times from the beginning of polymerization to the endpoint.

3. Kinetic trials. An overall kinetic study as well as the necessary initial rate study was desired. It was decided to choose the "pull points" as 1/3, 1/2, 2/3 and 7/8 of the endpoint as well as at the endpoint and two points after. These "pull points" can also be seen in Figure 4.

In order to study the effect of dose rate on the polymerization, three different dose rates were chosen. The rates, based on Fricke dosimetry, are shown in Table III.

The temperature study was done at the three temperatures of $25 \pm .05$, $50 \pm .1$, and $75 \pm .2^{o}C$.

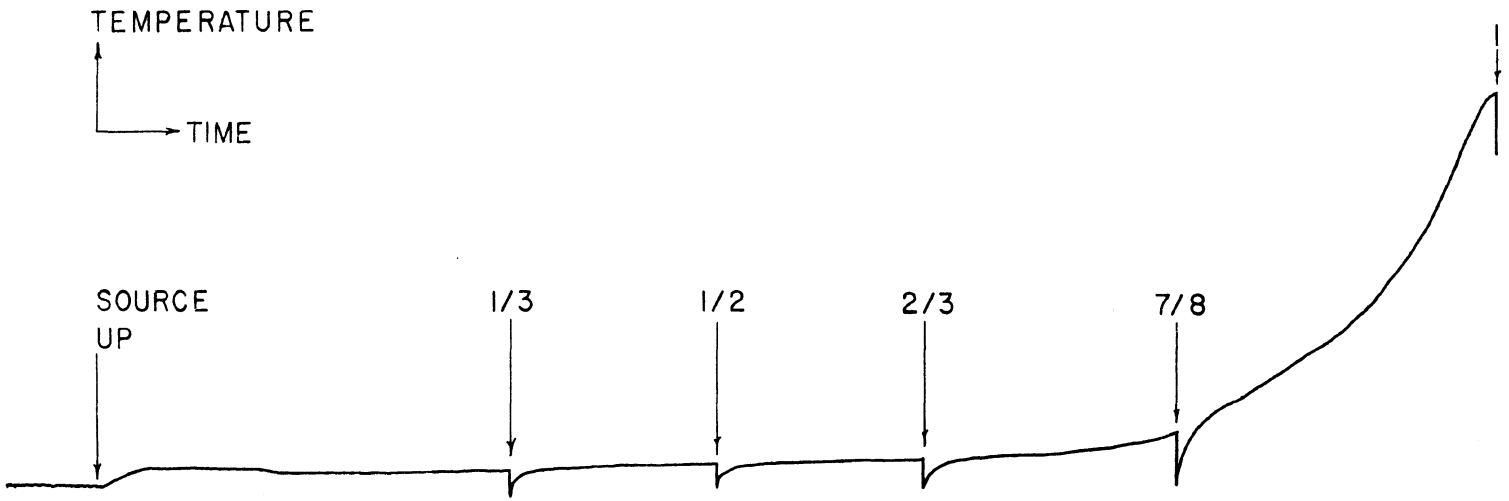

Figure 4. Temperature Profile and "Pull Points" of Samples

TABLE III

DOSIMETRY DATA

Bath Position[a]	Average Dose Rate[b] (rads/sec.)	Standard Deviation (rads/sec.)
A	24.9	1.2
C	12.9	0.6
E	7.35	0.2

[a] As shown in Figure 1.

[b] Based on molar extinction coefficient of 2198 $\pm$ 3.

4. Conversion data. The conversion data for the study was obtained by determining the per cent conversion of monomer to polymer. There were two types of polymer formed in the composite. The first type, "homopolymer" could be solvent extracted (dissolved) from the clay at ambient temperature. The second type of polymer was "inserted" and could not be dissolved from the composite by normal solvents.

a. Homopolymer of composite. Immediately after a sample was "pulled" from the irradiation source, an aliquot of the composite was taken from the middle of the sample tube, placed into a stoppered 250 milliliter Erylenmeyer flask, weighed and 150 milliliters ofdichloromethane was placed into the flask. An initial weight of composite for a "1/3 (of endpoint)" pull was approximately ten grams of composite, but this weight was decreased as the amount of polymer present in the total sample increased. The composite was kept in dichloromethane for at least two weeks in order to allow maximum polymer dissolution. The solution with dissolved composite was then centrifuged at 0^{o}C at 10,000 RPM for twenty minutes. One hundred milliliters of fresh dichloromethane were added to the solids and the solution allowed to stand for one more week and then recentrifuged. The centrifugate was then allowed to evaporate to dryness to remove the dichloromethane. The "homopolymer" was then redissolved in benzene, freeze-dried and the resulting white, fluffy polymer weighed and per cent conversion determined (Appendix B).

Specific samples were tested to insure that all homopolymer was being extracted. This test was accomplished by adding fresh solvent for a third

time and repeating the above procedure. The results of the tests shown in Table IV indicate that two washings of the composite removed all homopolymer within a ± two per cent error.

b. Inserted polymer of composite. The quantitative analysis of inserted polymer remaining on the clay was determined by calcination of a portion of the composite from which the soluble homopolymer had been extracted. The clay was dried at 100°C for one hour, weighed and thenignited to 1000°C in a muffle furnace. The composite was then reweighed and the amount and per cent conversion of insoluble polymer determined according to the calculations found in Appendix B.

An attempt was made to dissolve the clay from the polymer by use of hydrofluoric acid as was done by Blumstein[19]. Approximately one gram of the insoluble part of the remaining composite was weighed, and placed into a polyethylene beaker. Approximately ten milliliters of 52 per cent technical hydrofluoric acid was added. The reaction mixture was allowed to set for at least one hour in an ice bath. The remaining mixture was then filtered into polyethylene filter and washed until neutral with distilled water. The composite complex was then placed in an oven at 70°C for at least one hour or until dry. The complex was then redissolved in dichloromethane, allowed to stand for at least one day and then centrifuged for 1/2 hour at 10,000 RPM. Fresh solvent was again added and the solution was allowed to stand for one more day. Once again the solution was centrifuged and the decantant from both centrifugings allowed to evaporate. Benzene was

TABLE IV

EXTRACTION RESULTS OF HOMOPOLYMER

Trial	Days Extracted	Total % Conversion	Total Days Extracted	Total % Conversion	% Excess Conversion
50-50 COMPOSITE-INERT GAS @ 25°C @ 12.9 RADS/SEC.					
69-1B-C	20	6.4	34	6.4	0.0
69-2B-C	20	10.0	34	10.1	0.1
69-6B-C	30	58.1	34	59.0	0.9
69-7B-C	30	60.2	34	61.4	1.2
50-50 COMPOSITE - AIR @ 50°C @ 24.9 RADS/SEC.					
74-7-A	30	60.3	40	62.0	1.7
74-6-A	30	75.5	40	77.0	1.5
74-5-A	30	88.7	40	90.0	1.3
50-50 COMPOSITE - AIR @ 50°C @ 7.35 RADS/SEC.					
74-3D-B	30	55.0	40	57.5	2.5
74-2D-B	30	69.3	40	71.5	2.2

added to the flask and the polymer was freeze-dried and weighed to obtain the percentage of polymer recovered.

F. Characterization

1. Analysis of clay.

a. X-ray analysis. Samples of non-dried, dried and dried-irradiated clay were investigated using X-ray techniques to determine if changes had occurred in the clay at various stages of preparation and irradiation. A Siemens Crystalloflex IV, Type V-13 diffraction system equipped with a copper X-ray tube, operating at 35 kilovolts and a current of 20 milliamperes, was used.

b. DTA-TGA analysis. Thermal analysis for weight loss and transition regions was performed on samples of dried clay. Thermogravimetry (TGA) measures the weight loss of a sample as a function of temperature. In differential thermal analysis (DTA), the sample and an inert reference (alumina) are heated at the same rate. As endothermic or exothermic changes or heat capacity changes occur in the sample, a temperature difference between sample and reference occurs and this temperature difference is measured and plotted as a function of sample temperature. A Mettler Thermal Analyzer was used for all measurements. An air atmosphere was used with a flow rate of one liter per hour of air, and a temperature rise of 10^{o} per minute to a temperature of 1000^{o}C.

c. Particle size distribution analysis. Particle size distributions were made on dired, undried and dried-irradiated kaolin clays using the

United States Bureau of Mines Sharples Micromerograph. The clays were screened through a 200 mesh sieve, mixed with an anti-static agent (20 per cent by volume Anstac M and 80 per cent isopropyl alcohol), vacuum dried, placed in the injection port and forced through a deagglomerator (set at 250 microns) using nitrogen pressure at a 100 pounds per square inch. The distribution was calculated using the application of a corrected form of Stokes' Law of Fall for the velocity of particles falling in a gas.

d. Surface area analysis. The surface area was determined with a three point B.E.T. determination[27] using a Perkin-Elmer Model 212D Sorptometer. A continuous flow of a known mixture of nitrogen and helium was passed over a known weight of sample in a sample tube and the effluent gas was monitored by a thermal conductivity detector. The sample tube was cooled by immersing in a liquid nitrogen bath. This cooling causes a certain amount of nitrogen to be adsorbed from the gas stream and the change in the mixture results in a peak on a recorder. After equilibrium is established, the liquid nitrogen is removed from the sample tube and a desorption peak was recorded as the sample warmed. When desorption is complete, a known volume of nitrogen is added to the nitrogen-helium stream and a calibration peak is formed.

By comparing the integrated areas of the desorption and calibration peaks, the volume of nitrogen adsorbed by the sample was calculated. From this, the surface area of the sample was determined.

2. Analysis of total composite.

a. DTA-TGA. The analysis of the total composite was performed as on the clay samples (Section F, Part 1-b).

b. Scanning electron microscopy. Samples of total composite were investigated using the Jeolco JSM-2 scanning electron microscope. All samples were fractured at room temperature and mounted on a copper disc using a silver conducting paste. A thin film of gold was vapor deposited under vacuum on the samples because they were non-conductors.

c. Mechanical tests. Mechanical tests were performed on bulk and 50 - 50 composite specimens using a Tinius Olsen compression tester. The middle range was used which had a maximum compression of 12,000 pounds. The sample specimens were cut and machined on a lathe and had the dimensions of 0.5 inches in diameter (compression area = .1963 in^2) and 1.0 inches in length. An average compression rate of 1000 pounds per minute was applied with the tests being performed at ambient temperature. The yield point for the composite was taken when the composite fractured and a maximum value was indicated on the gauge while still applying compression. The yield point for the bulk polymer was determined when the indicator hesitated at a point while continuing to apply compression and then increased very swiftly to maximum compression on the gauge.

3. Analysis of homopolymer.

a. DTA-TGA. Thermal analysis was performed on selected samples of homopolymer using the same procedure as the clay analysis (Section F, Part 1-b).

b. Gel permeation chromatography. The molecular weight and molecular weight distribution of all polymers was obtained using a Waters Ana-prep gel permeation chromatograph (GPC). A description of this standard technique is given in Appendix C. All samples were in the concentration range of 0.15 - 0.4 grams per deciliter. Four milliliters of sample were filtered through a glass fiber syringe filter before injection into the GPC. The results of standard calibration curves of polystyrene used for calibration of peak molecular weight is given in Figure 5.

c. Infrared spectroscopy (IR). All infrared spectra were obtained using a Beckman IR-12 spectrophotometer. The polymer was dissolved in dichloromethane, placed in an aluminum dish and allowed to evaporate. The spectra were obtained from the film which remained.

d. Viscosity measurements. The intrinsic viscosities and viscosity average molecular weights of selected samples dissolved in benzene were determined using a Cannon-Ubbelohde Semi-Micro Dilution Viscometer (Number 50) at $30^{o} \pm .02^{o}C$. The efflux times of solvent and solutions were greater than 100 seconds; therefore kinetic effects were neglected. The viscosity calculations can be found in Appendix D.

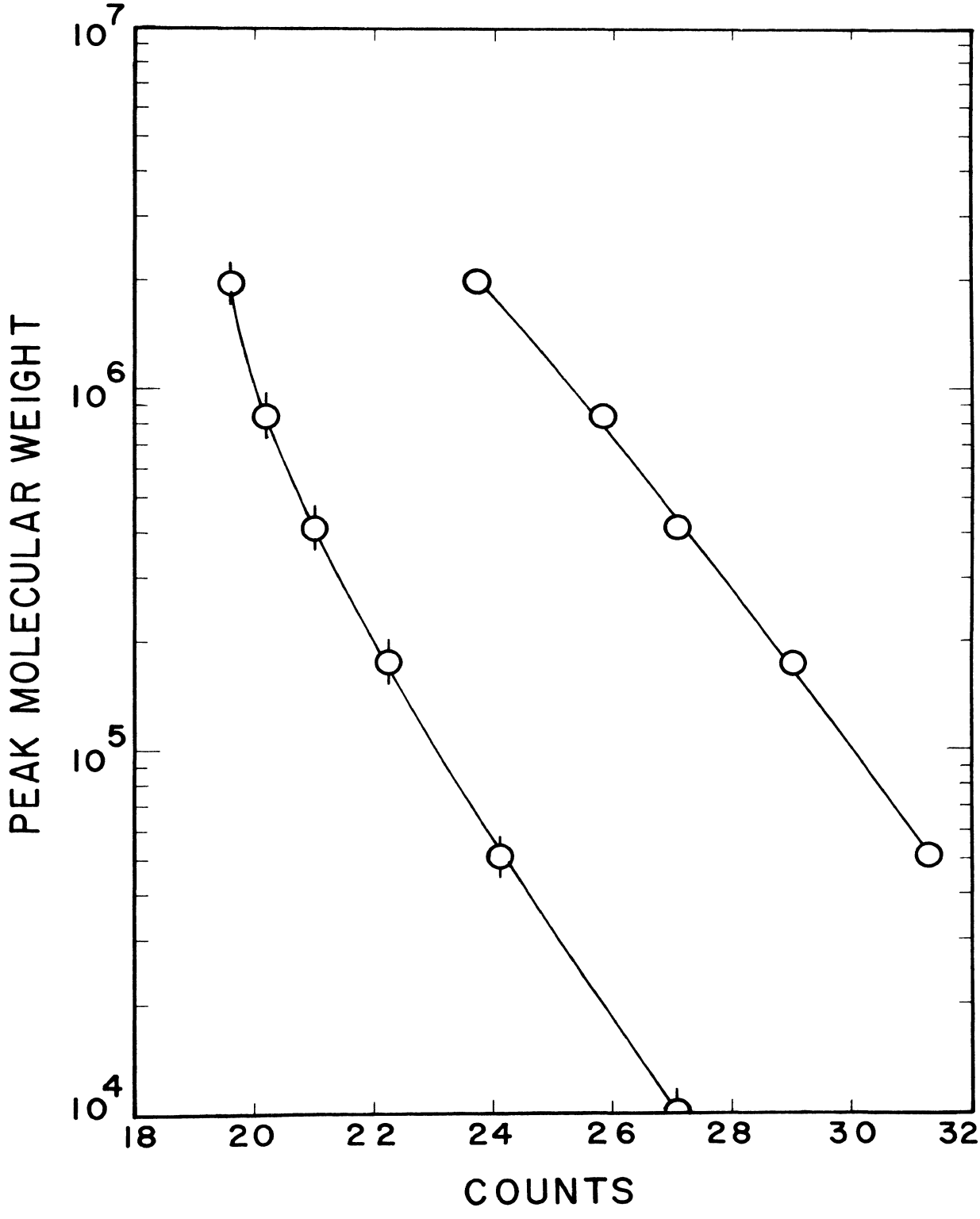

Figure 5. GPC Calibration Curves for A (○) and B (⏀) Columns.

e. Nuclear magnetic resonance measurements (NMR). NMR spectra were obtained using a Varian A-60 Nuclear Magnetic Resonance Spectrometer. The freeze-dried polymer was dissolved in o-dichlorobenzene. Due to the high molecular weights of the polymers and the subsequent high viscosities of the polymer solutions, only five to seven per cent solutions could be transferred to the NMR tubes. The solutions were frozen in NMR tubes using liquid nitrogen and sealed under vacuum. Spectra were obtained at approximately 150°C. Interpretation of the spectra was based upon statistical correlations reported by Reinmoller and Fox[28, 29].

4. Analysis of inserted polymer. Selected samples of inserted polymer were investigated using GPC, IR and NMR using the same techniques as with the homopolymer.

IV. RESULTS AND DISCUSSION-PART 1

A. Dosimetry

The dosimetry was performed according to Experimental Section C. The results of the dosimetry at the three dose rates used, with their standard deviations, are shown in Table III. These results are the average of all trials preformed over a four month period. The differences in the dose rates at any one distance away from the source was the largest source of error (± 4 per cent). This error was caused by the differences in the geometry of the source itself and positioning of the bath about the source. The basis for the determination of absorbed radiation is presented in the Experimental Section C and will not be reiterated here.

B. Endpoint Studies

A series of initial kinetic trials were made where the extent of polymerization was followed by recording the temperature at the geometrical centers of the samples as a function of time. The apex of the exotherm then served as a basis upon which to obtain conversion data. The temperatures at the apexes of the exotherm as seen in Table V showed that the polymerization temperatures of the composite at the same dose rate were substantially lower than the bulk polymerization temperatures. The temperature profile of both bulk and composite systems was also dependent upon the dose rate and decreased as dose rate decreased at a constant temperature.

TABLE V

AVERAGE ENDPOINT TEMPERATURES OF
BULK AND COMPOSITE SYSTEMS

Temp. (^{o}C)	Bulk Polymer			Composite Polymer		
Dose Rate (rads/sec.)	25	50	75	25	50	75
24.9	51.7			28.6	55.8	83.5
12.9	42.1	71.6	100.6	27.6	53.5	80.1
7.35	34.9			27.3	54.0	78.8

Table VI shows the total radiation dose necessary to reach a given endpoint under a variety of experimental conditions. As can be seen from the table, the major portion of this part of the study was done at 25^{o}C. The bulk polymerization (monomer distilled and inhibited) and the 50-50 composite (monomer distilled and inhibited) were compared in the inert gas and in air. Based upon the endpoint data for both bulk and composite polymer the following general statements may be made:

1. between dose rates of 7 and 25 rads per second, the total conversion dose needed decreased as dose rate decreased,

2. as the temperature increased between 25-75^{o}C at the same dose rate, the total conversion dose needed decreased,

3. as the temperature increased between 25-75^{o}C at the same dose

TABLE VI

TOTAL DOSES NECESSARY TO REACH ENDPOINTS
FOR VARIOUS SYSTEMS

Dose Rate (rads/sec.)	Bulk Distilled (rads $\times 10^{-3}$)	Bulk Inhibited (rads $\times 10^{-3}$)	50-50 Composite Distilled (rads $\times 10^{-3}$)	50-50 Composite Inhibited (rads $\times 10^{-3}$)	60-40 Composite Distilled (rads $\times 10^{-3}$)	60-40 Composite Inhibited (rads $\times 10^{-3}$)
			INERT GAS - TEMPERATURE = 25°C			
24.9	531	568	437	471		
12.9	384	394	309	303		
7.35	256	278	203	236		
			AIR - TEMPERATURE = 25°C			
24.9	638	636	457	471	450	481
12.9	457	518	300	325	324	336
7.35	278	403	220	243	247	248
			INERT GAS - TEMPERATURE = 50°C			
12.9			180			
			AIR - TEMPERATURE = 50°C			
24.9			264			
12.9	210		182			
7.35			140			
			INERT GAS - TEMPERATURE = 75°C			
12.9	124		124			
			AIR - TEMPERATURE = 75°C			
12.9	130		120			
7.35			90			

rate the difference in the amount of actual irradiation time needed between the composite and bulk polymerization decreased,

4. the inert gas and air composite systems at a constant dose rate and temperature showed little difference in total dose needed to reach the endpoint,

5. the temperature increase of the exotherm at a constant temperature and dose rate was considerably less for the composite than for the bulk polymer.

In comparing the bulk polymerization, the ratio of the different doses needed to reach the endpoint was used as a criteria for comparison as seen in Table VII. In this comparison, the ratio of the addition of one poison (inhibitor or oxygen) or both poisons was made to the bulk polymer-distilled-inert gas (B-D-IG). Two of the systems (columns 1 and 2) compared the introduction of the inhibitor (MEHQ) or of the retarder air while holding the other parameter constant. The endpoint of these systems with the inhibitor or retarder added reached its endpoint with a total dose needed of 1.02 to 1.2 times the dose necessary for the B-D-IG system regardless of dose rate. Detrick and Kelly[30] found a ratio of 1.24 was necessary in their studies for the addition of inhibitor (hydroquinone) at dose rates ranging from 1×10^4 to 3.2×10^5 rads per hour. The comparison of the systems which included both inhibitor and oxygen (column 3), showed that the total dose necessary to reach the endpoint was a function of the dose rate. It is seen that the ratio of the dose needed increased as dose rate decreased. The addition

TABLE VII

RATIO OF TOTAL DOSES NECESSARY TO REACH ENDPOINTS FOR VARIOUS BULK SYSTEMS

Dose Rate (rads/sec.)	(1) $\frac{\text{B-D-A}^a}{\text{B-D-IG}}$	(2) $\frac{\text{B-I-IG}^a}{\text{B-D-IG}}$	(3) $\frac{\text{B-I-A}^a}{\text{B-D-IG}}$
24.9	1.20	1.07	1.20
12.9	1.19	1.02	1.35
7.35	1.09	1.08	1.57

[a]where: B = Bulk polymer
D = Distilled monomer
I = Inhibited monomer
IG = Inert gas (Argon)

of both poisons has a much greater effect on the system than the addition of only one poison. Detrick and Kelly[30] found that oxygen influenced the retardation of the polymerization to a much greater extent than did the hydroquinone (60 PPM). These ratios only show a relative trend and can not be used to quantitatively account for the addition of one type of poison or adding of both poisons.

A study was made to determine the effects of the kaolin clay on the adsorption of the inhibitor hydroquinone (a similar inhibitor to MEHQ). A 20 per cent by weight kaolin clay to monomer ratio was used with 0.01

per cent hydroquinone added. The hydroquinone transmittance peak at 295 mμ was used as an indicator of any change in the concentration of hydroquinone. The absorptivity and cell path length were assumed constant. The test mixture was placed in a glass stoppered flask and aliquots removed for testing were returned to the test mixture to keep the material balance intact. As can be seen from Table VIII, the hydroquinone decreased in concentration in the supernatant monomer as the testing time increased and therefore must be adsorbed by the clay. In a 50-50 mixture of the monomer-clay system, the clay should have even a more pronounced effect and probably the bulk of the inhibitor would be adsorbed on the clay.

TABLE VIII

ADSORPTION OF HYDROQUINONE (HQ) BY KAOLIN CLAY AS A FUNCTION OF TIME

Time (hrs.)	Transmittance	Absorbance	Amount of HQ Remaining (gms./l. MMA)	% Adsorbed
0.0	.425	.372	.0936	0.0
7.5	.510	.292	.0736	21.4
21.0	.575	.240	.0604	35.5
72.0	.890	.051	.0128	86.3

In comparing the distilled and inhibited composite systems at the same dose rate and temperature, only slight differences in total dose were observed (6 to 15 per cent for all composite systems). As shown in Table VI, the inhibitor (MEHQ) and especially the retarder (air) have less effect on the composite system than on the bulk system.

The comparison of the distilled-bulk and distilled-composite in both atmospheres at 25°C showed a distinct acceleration of the endpoint in the composite polymerization. This acceleration, whether it be due to chemical or physical reactions, could only be caused by the clay. However, when the temperature of the system was increased, there occurs a narrowing of the differences between the endpoints. The same differences occurred with the inhibited-bulk and inhibited-composite systems with overall slight increases in total dose as compared to the distilled system. This behavior was an indication that the addition of the ten parts per million MEHQ had little effect when the monomer-composite system was irradiated.

C. Kinetic Analysis

The kinetic analysis of the system will be considered in three parts: (1) homopolymer from the composite, (2) inserted polymer from the extracted composite and, (3) total polymer (homopolymer and inserted polymer) of the composite. In each case the system will be compared to results obtained for the bulk polymer under the same conditions. The kinetic data reported represent the net result of polymer formation an polymer degradation during the irradiation process.

1. Homopolymer. The percentage conversion of monomer to polymer for the homopolymer and bulk polymer in air and argon as a function of total dose and dose rate are shown in Figures 6, 7, 8 and 9. The rate of polymerization at any specified total dose of homopolymer increased in all cases as the temperature increased and dose rate decreased (between 24.9 and 7.35 rads per second).

At 25°C the rate of formation of bulk polymer at 12.9 rads per second in air was less than the composite homopolymer in either air or inert gas. However, as the reaction temperature increased, the difference in the conversion curves lessened and finally coincided at 75°C. It must be remembered that these rates of conversion do not include the inserted polymer from the composite. At a dose rate of 12.9 rads per second and at all reaction temperatures, the fraction of homopolymer formed in the composite was equal to or greater than that of the bulk polymer to conversions of 60 per cent.

The percentage conversion of homopolymer was greater in the inert gas atmosphere at 25°C and 12.9 rads per second than in air system by 1 to 6 per cent at the same total dose. This percentage differential decreased as the temperature increased until at 75°C, there was no difference between the inert gas and air system. Clay, which has a large surface area, was difficult to degas. Actually, such a procedure would be impractical. Even though precautions were taken in this work to condition the clay for a specific experiment, it was likely that the clay surfaces in all of the

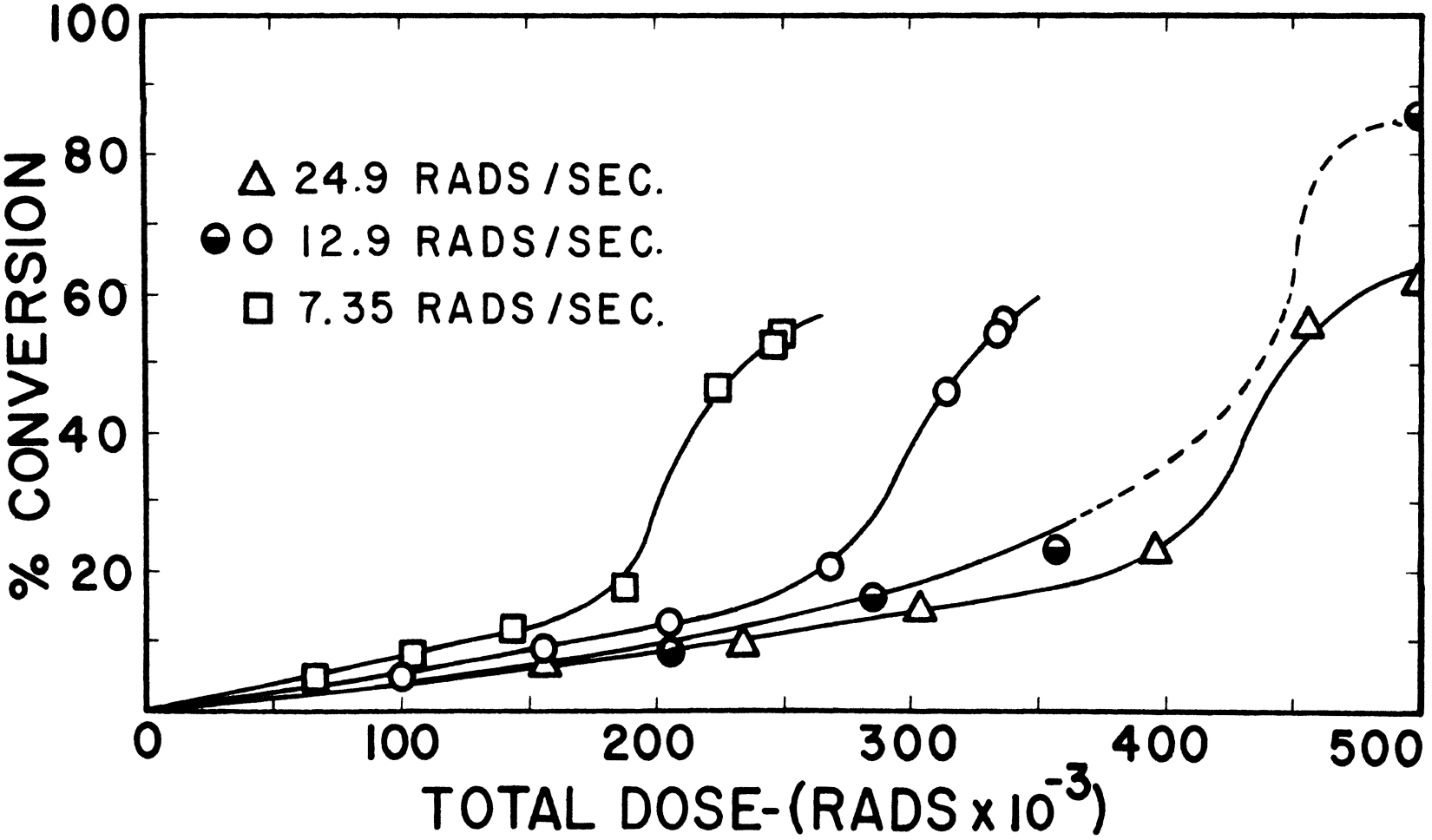

Figure 6. Formation of Homopolymer (△ , ○ , □) and Bulk Polymer (◒) in Air as a Function of Dose Rate @ 25°C.

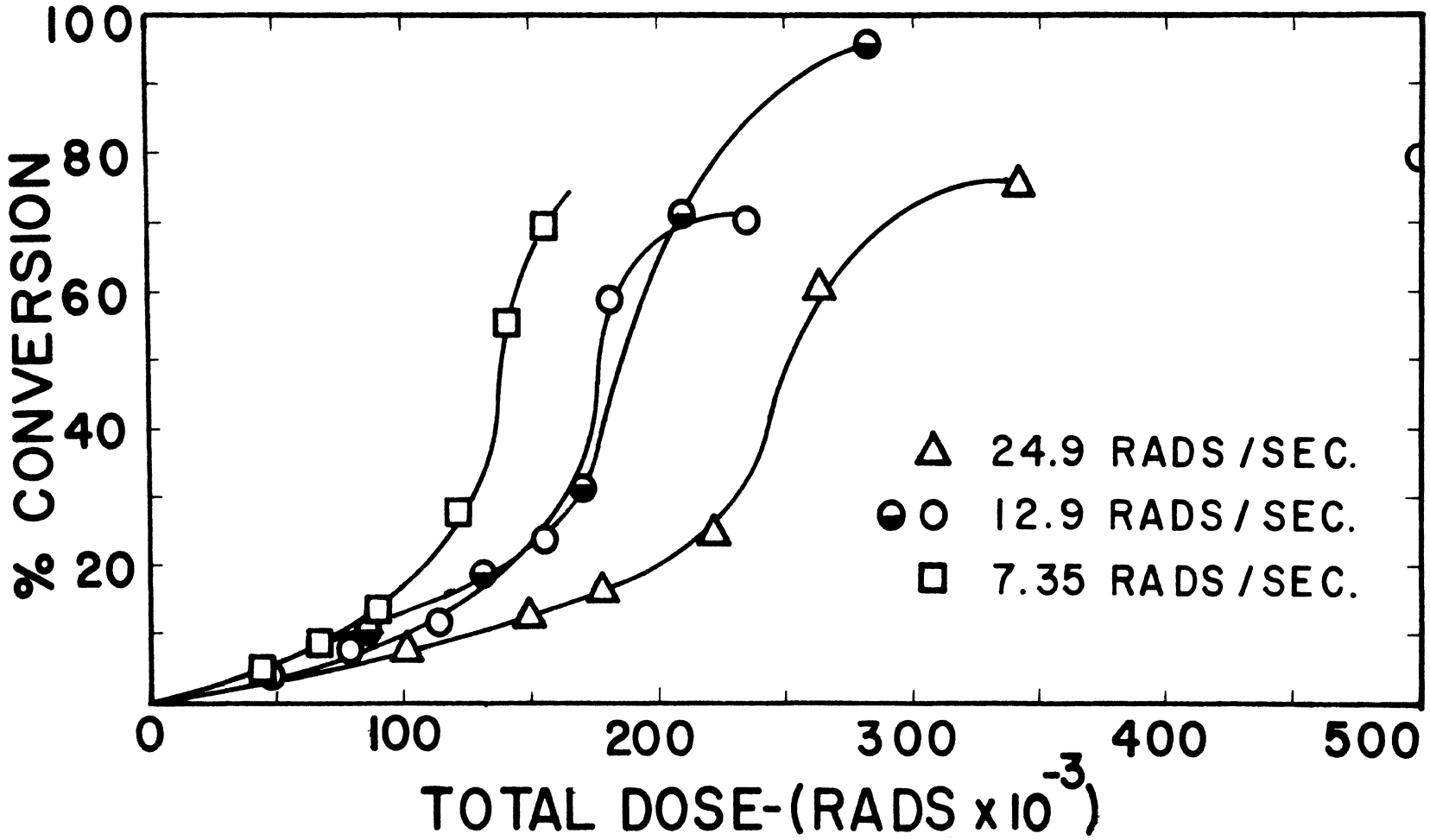

Figure 7. Formation of Homopolymer (△ , ○ , □) and Bulk Polymer (◒) in Air as a Function of Dose Rate @ 50°C.

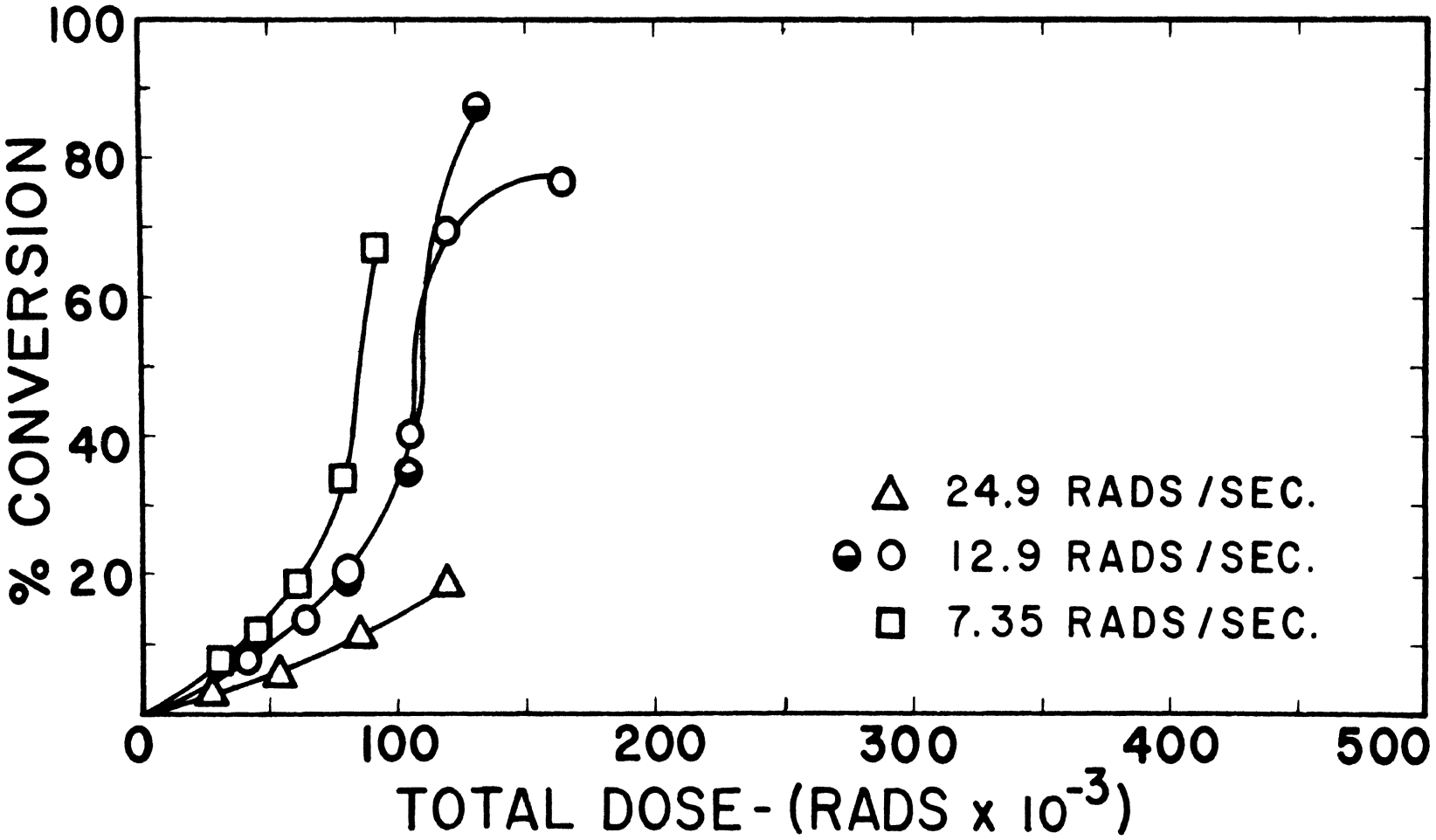

Figure 8. Formation of Homopolymer (△ , ○ , □) and Bulk Polymer (◒) in Air as a Function of Dose Rate @ 75° C.

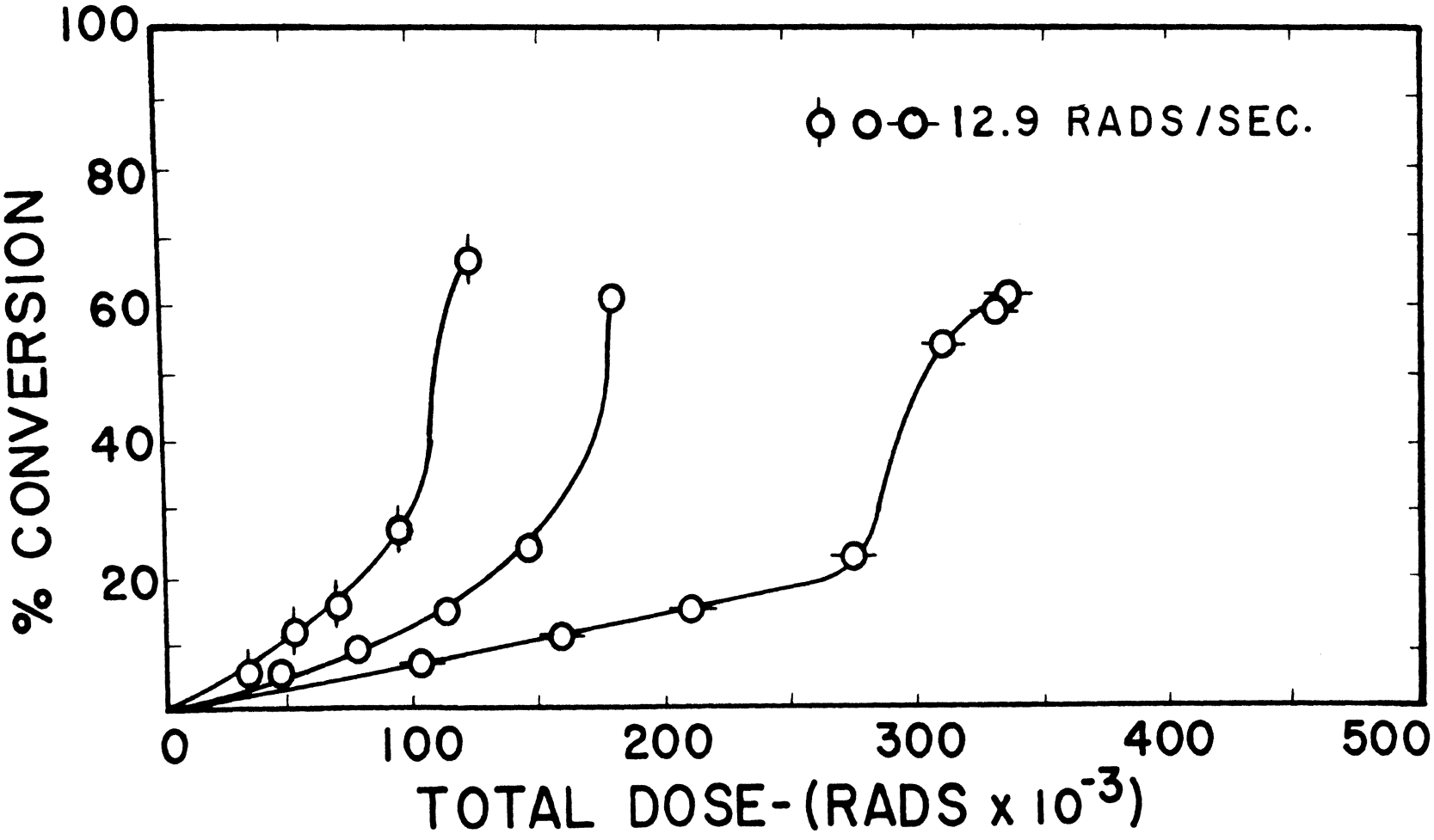

Figure 9. Formation of Homopolymer in Inert Gas at 25 (-O-), 50 (O) and 75°C (ϕ).

experiments had appreciable quantities of atmospheric gases still adsorbed on them. The various results and calculations obtained from the homopolymer conversion data will be discussed below.

a. Dose rate dependence. At low doses, the conversion curves for bulk and homopolymer were linear and can be described by an equation of the type:

$$\frac{dP}{dD} = kI^n$$

where: $\frac{dP}{dD}$ = initial polymerization rate (per cent conversion per rad)

I = absorbed dose rate in ferrous sulfate and system under study (rads per second)

k = apparent reaction rate constant

n = apparent reaction order

Data for the composite are shown in Figure 10. The apparent reaction orders calculated from this data are reported in Table IX. These reaction orders are close to the reaction order -0.5 predicted by the simplified kinetic scheme for bulk free radical initiated polymerization[31] for linear polymers. The minus signs are used in the plotting of dP/dD. If a plot of dP/dt were done where t is irradiation time, the reaction order would be positive and equal to n + 1.

b. Energy of activation. An equation of the Arrhenius type

$$\frac{dP}{dD} = Ae^{-\Delta E^*/RT}$$

where: $\frac{dP}{dD}$ = initial reaction rate (per cent conversion per rad)

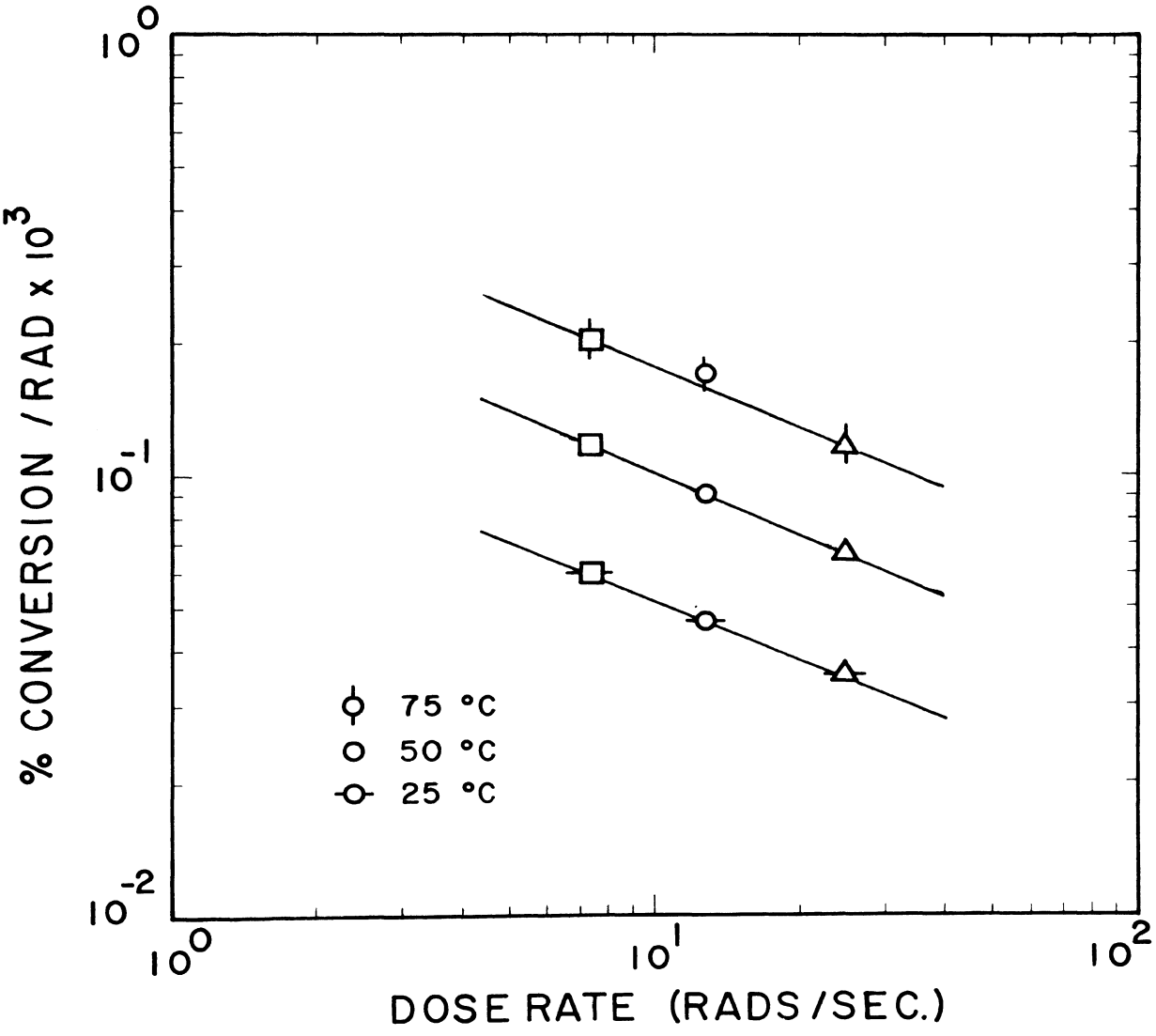

Figure 10. Per Cent Conversion vs. Dose Rate of Homopolymer in Air

ΔE^* = apparent activation energy (kilocalories per mole)

R = gas constant (kilocalories per mole ^oK)

T = temperature (^oK)

shown in Figure 11 indicates that for the homopolymer and bulk polymer, the reaction occurs within an isokinetic range and therefore the activation energy is independent of temperature. These data also show that the activation energy is dose rate dependent but that the net mechanism is essentially the same at the different dose rates studied. Within the temperature range studied, Table X shows the calculated activation energies for homopolymer-air (three dose rates), homopolymer-inert atmosphere and bulk polymer-air. The bulk polymer activation energy of 6.6 kilocalories per mole was 1.3 as great as the activation energy reported by Ballantine[32] and Okamura[33] (4.9 kilocalories per mole). However, their trials were done in an inert atmosphere while this trial was done in air.

TABLE IX

APPARENT REACTION ORDERS OF HOMOPOLYMERS AT VARIOUS TEMPERATURES

Temperature ^oC	Apparent Reaction Order n
25	-0.44
50	-0.46
75	-0.47

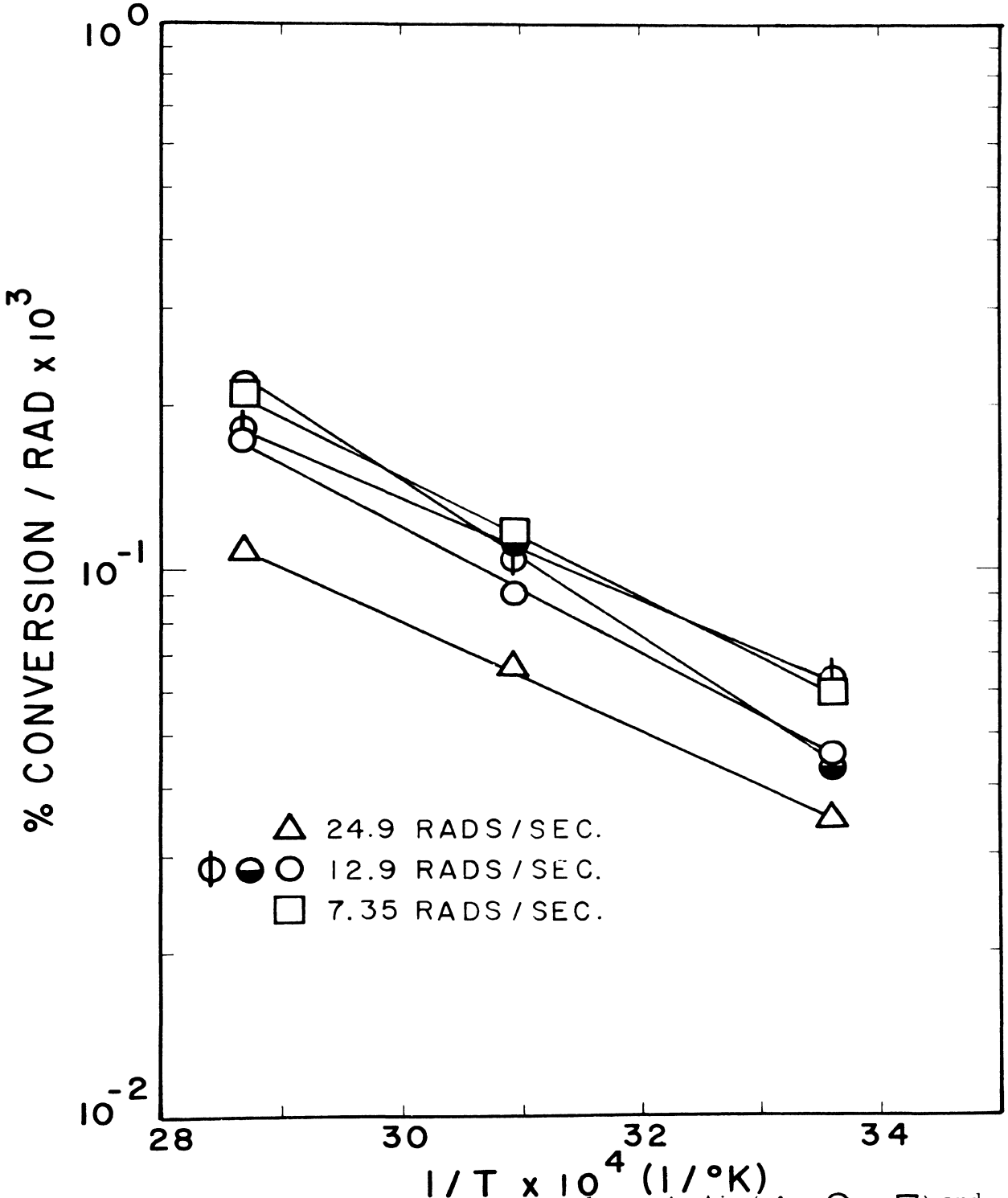

Figure 11. Activation Energy of Homopolymer in Air (△ , ○ , □) and Inert Gas (ϕ) and Bulk Polymer (◒) in Air.

TABLE X

ACTIVATION ENERGY OF HOMOPOLYMER AND BULK POLYMER AT VARIOUS DOSE RATES

System	Dose Rate (rads/sec.)	dP/dD[a] 25°C	50°C	75°C	ΔE^* (kcal./mole)	ΔE^* n = 0.5
Homopolym.-Air	24.9	.035	.066	.115	5.0	5.2
	12.9	.046	.090	.191	5.4	
	7.35	.059	.116	.204	4.6	
Homopolym.-Inert Gas	12.9	.062	.101	.178	4.2	4.4
Bulk Polymer-Air	12.9	.043	.112	.206	6.6	6.5
Bulk-Inert Gas[32,33]					4.9	

[a] dP/dD are initial reaction rates (% conversion per rad x 10^3).

Based on data in Table IX, the apparent reaction order was assumed to be -0.5. Values of the reaction rate constants were calculated using this assumption and the experimental values of the initial rates from Table X. The constants were shown to be independent of dose rate. These rate constant values were plotted as a function of 1/T and the activation energy calculated. The comparison of the experimental activation energies and calculated energies using n = -0.5 is shown in Table X. The small differences in activation energy show that the mechanism of polymerization is free radical for the homopolymer.

The homopolymer activation energy in air was essentially the same as the bulk activation energy in nitrogen (4.9 kilocalories per mole). The inert gas-homopolymer had an even lower activation energy (4.2 kilocalories per mole). These values indicate that the clay does exert a catalytic influence on the polymerization and has an even greater influence on the initial rate in the absence of air.

2. Inserted polymer. The inserted polymer conversion curves as a function of dose and dose rate in air shown in Figures 12, 13, 14 and 15 have the same general shape as the homopolymer except for the initial slope. From all data shown, the shape of conversion curves give two possible starting points. One fact that must be considered is that polymer can form before irradiation begins (due to the ambient catalytic nature of the clay) and if this is the case the conversion curves would not pass through zero conversion at time zero. The other possibility is that if the curves do pass through zero there is an initial acceleration caused by the catalytic effect of

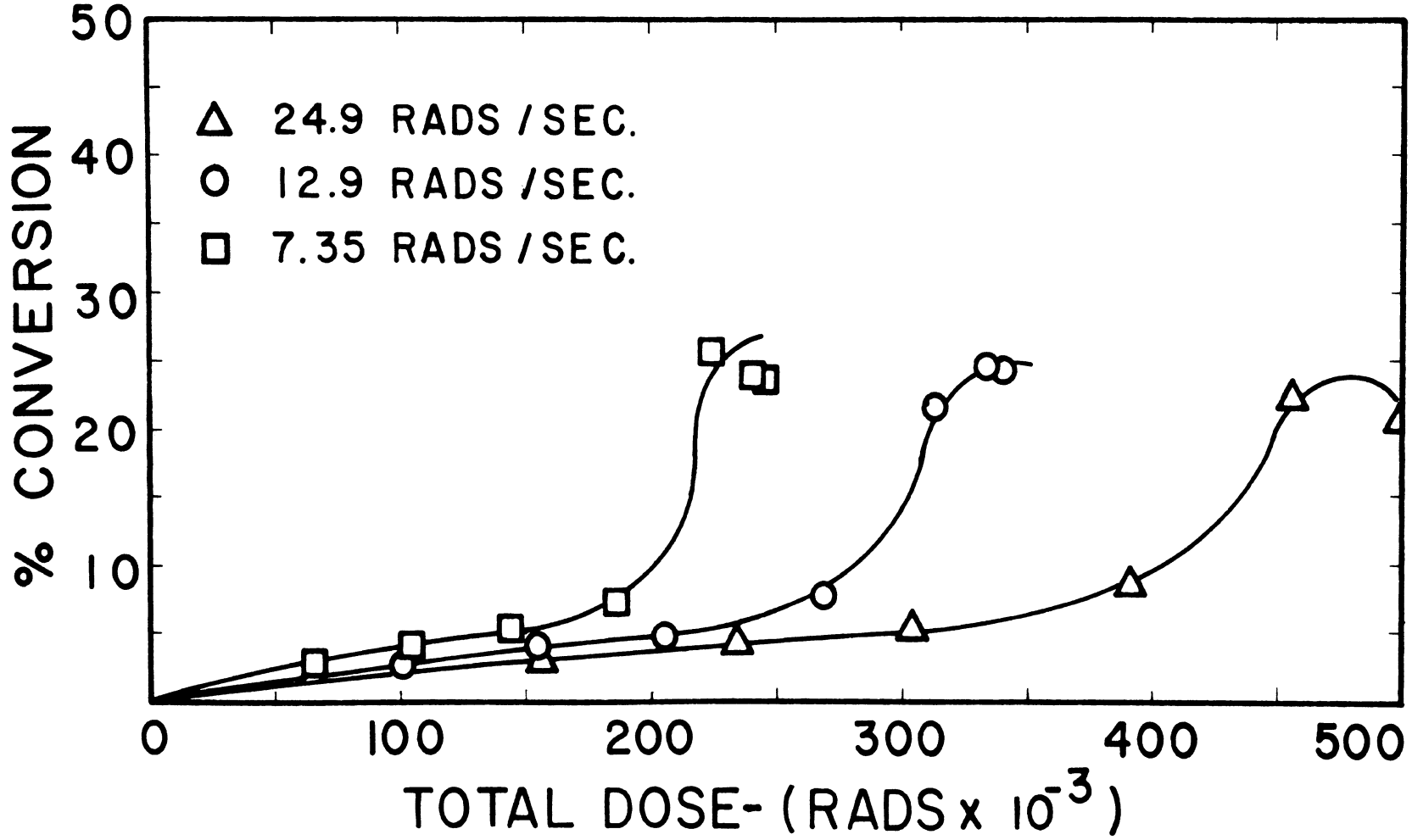

Figure 12. Formation of Inserted Polymer in Air as a Function of Dose Rate @ 25°C.

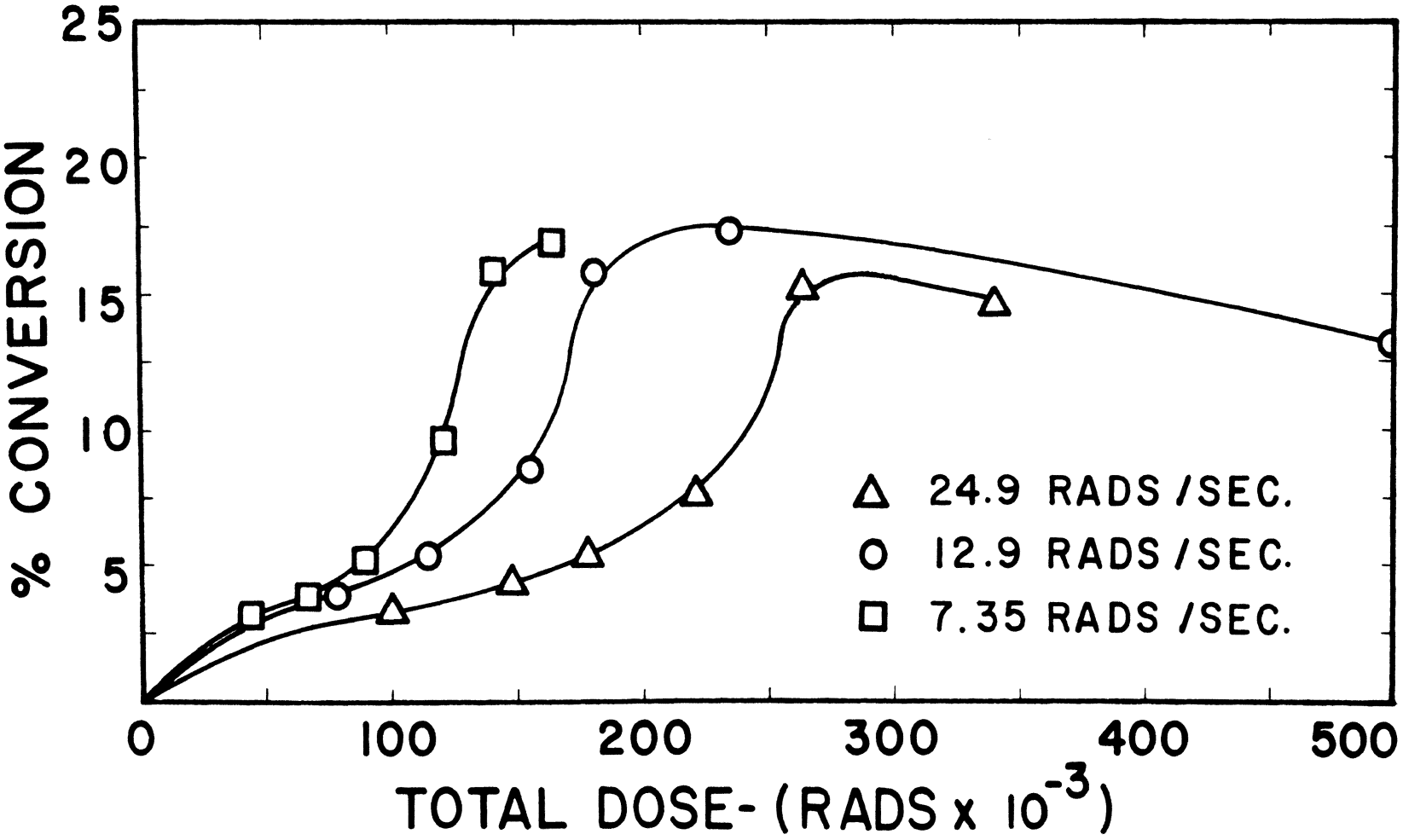

Figure 13. Formation of Inserted Polymer in Air as a Function of Dose Rate @ 50°C.

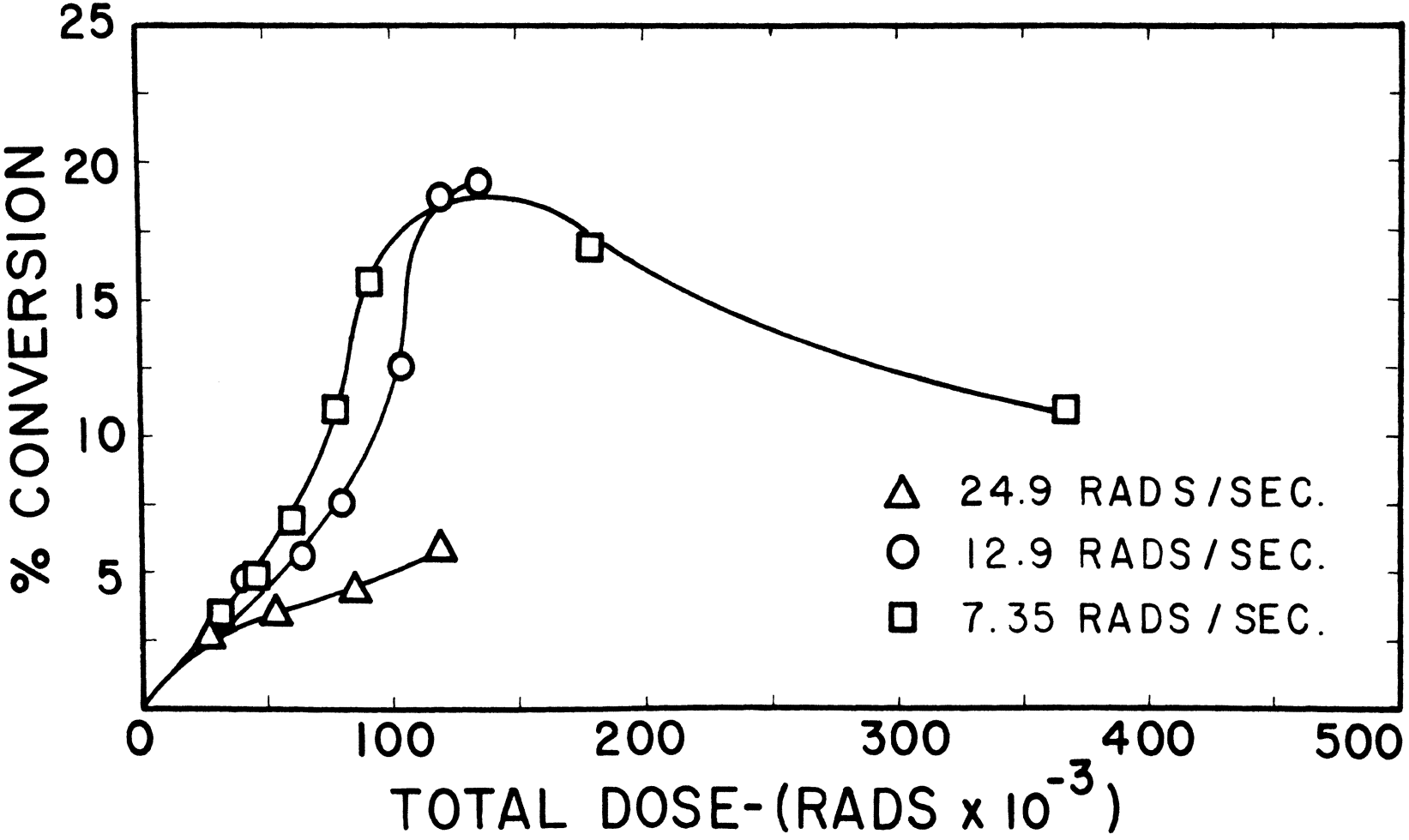

Figure 14. Formation of Inserted Polymer in Air as a Function of Dose Rate @ 75°C

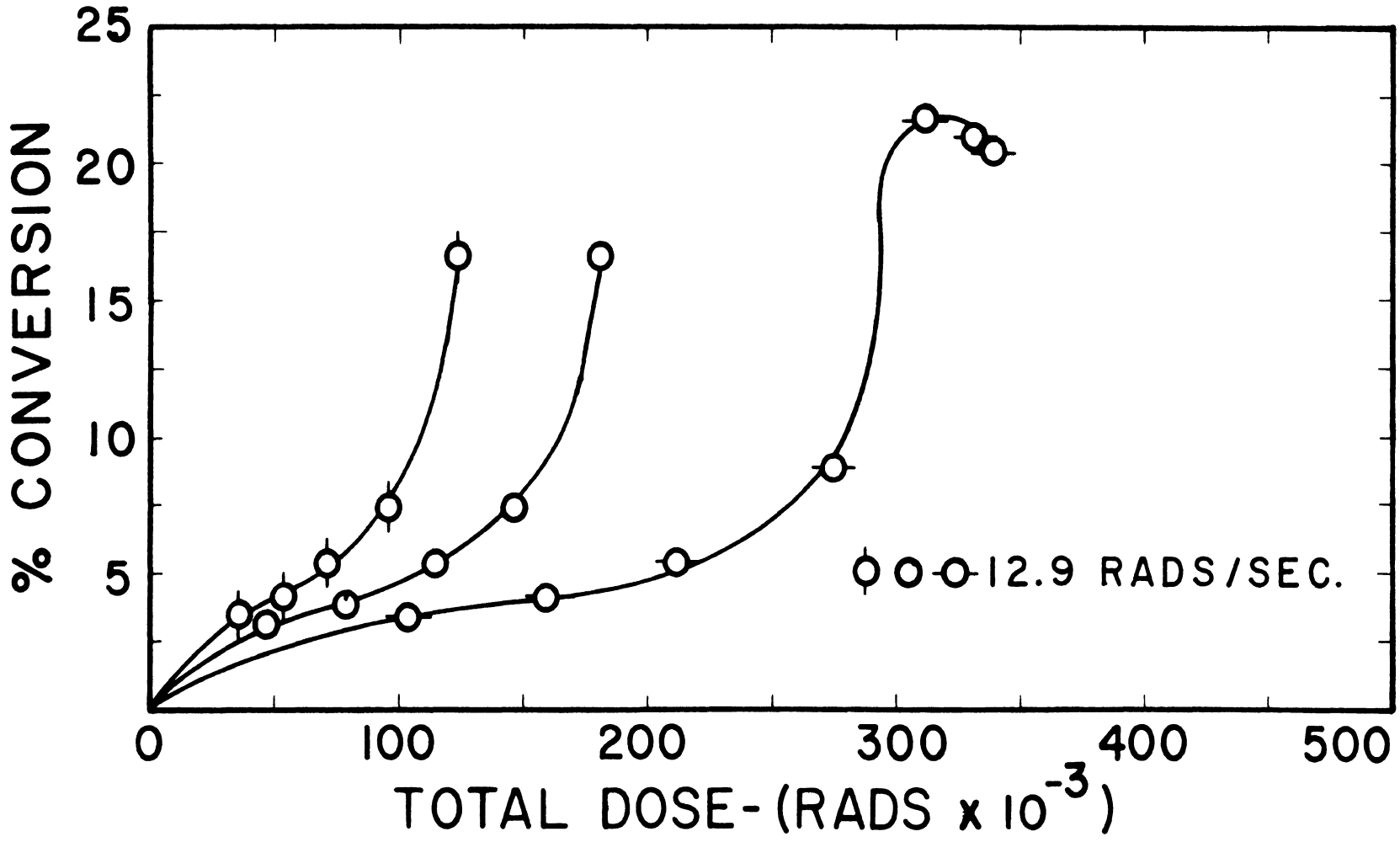

Figure 15. Formation of Inserted Polymer in Inert Gas at 25 (-O-), 50 (O) and 75°C (O).

the clay which then decreases with time. From data obtained (Figure 16) at room temperature without any type of initiator, it is seen that polymerization does take place in the presence of the clay composite. From DTA-TGA and ignition analysis, and using the appropriate calculations (Appendix B) it was found that after 24 hours, 1.3 per cent conversion to polymer had occurred. However in weighing the mixture of monomer-clay, there is an error limit of $\pm$ 1 per cent which could account for the percentage conversion found. Therefore from the general shape of the curves and taking into account the limits of experimental error there appears to be sufficient justification for drawing the kinetic curves for the insertion polymer through zero.

A comparison of the percentage conversion of the homopolymer and inserted polymer at their endpoints is shown in Table XI. The following may be said concerning these results:

1. the percentage conversion of homopolymer was always larger than that of the inserted polymer for the experimental conditions employed,

2. at the same dose rate, the percentage conversion of homopolymer increases, but the percentage conversion of inserted polymer decreases as temperature increases (25^{o}C to 75^{o}C),

3. the comparison of the percentage conversion in inert gas and air showed no differences in the experimental range studied.

In comparing the percentage conversion within each respective system (homopolymer or inserted polymer), it is seen that at a constant

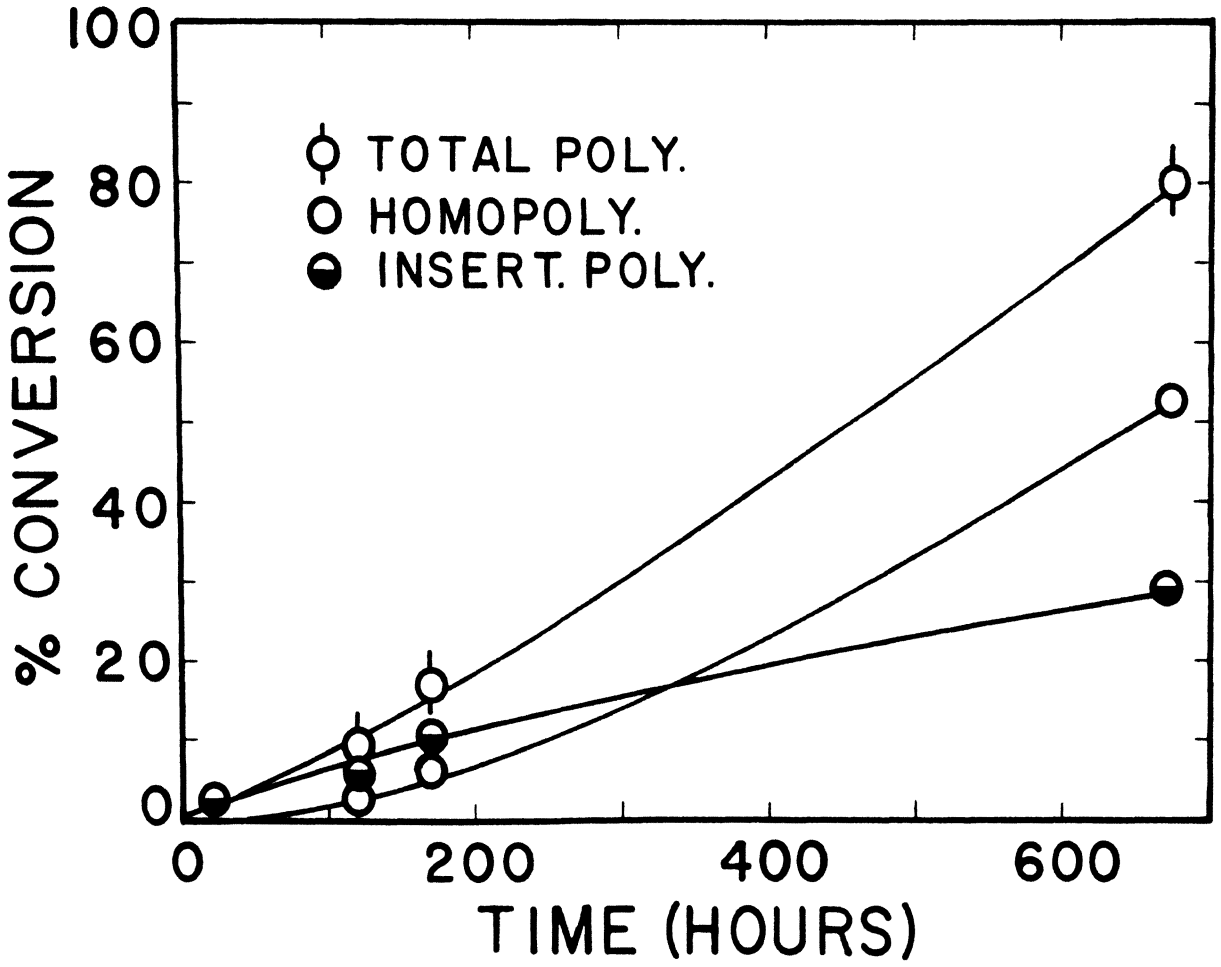

Figure 16. Polymerization of Composite Polymer at Room Temperature

temperature, the conversion of polymer was approximately the same regardless of dose rate.

A plot of $dP/dD = kI^n$ in Figure 17 using initial rate data shows that the order of reaction changes as the temperature increases. Table XII tabulates the calculated initial reaction rate constants. False conclusions can be drawn from this data. At 75°C, the data show that the apparent reaction order is zero and that the percentage conversion is independent of dose rate. However, upon looking at the entire conversion curve in Figure 14 it is seen that the percentage conversion of the insertion polymer is dependent upon the dose rate after the initial reaction has started.

TABLE XI

PER CENT CONVERSIONS OF HOMO AND INSERTED POLYMER AT THEIR ENDPOINTS

Temp. (°C)	Homopolymer			Inserted Polymer		
	25	50	75	25	50	75
Dose Rate (rads/sec.)						
(air) 24.9	56	60		22	15	
(air) 12.9	46	59	70	22	16	19
(air) 7.35	47	55	67	26	16	16
(IG) 12.9	53	61	65	22	17	17

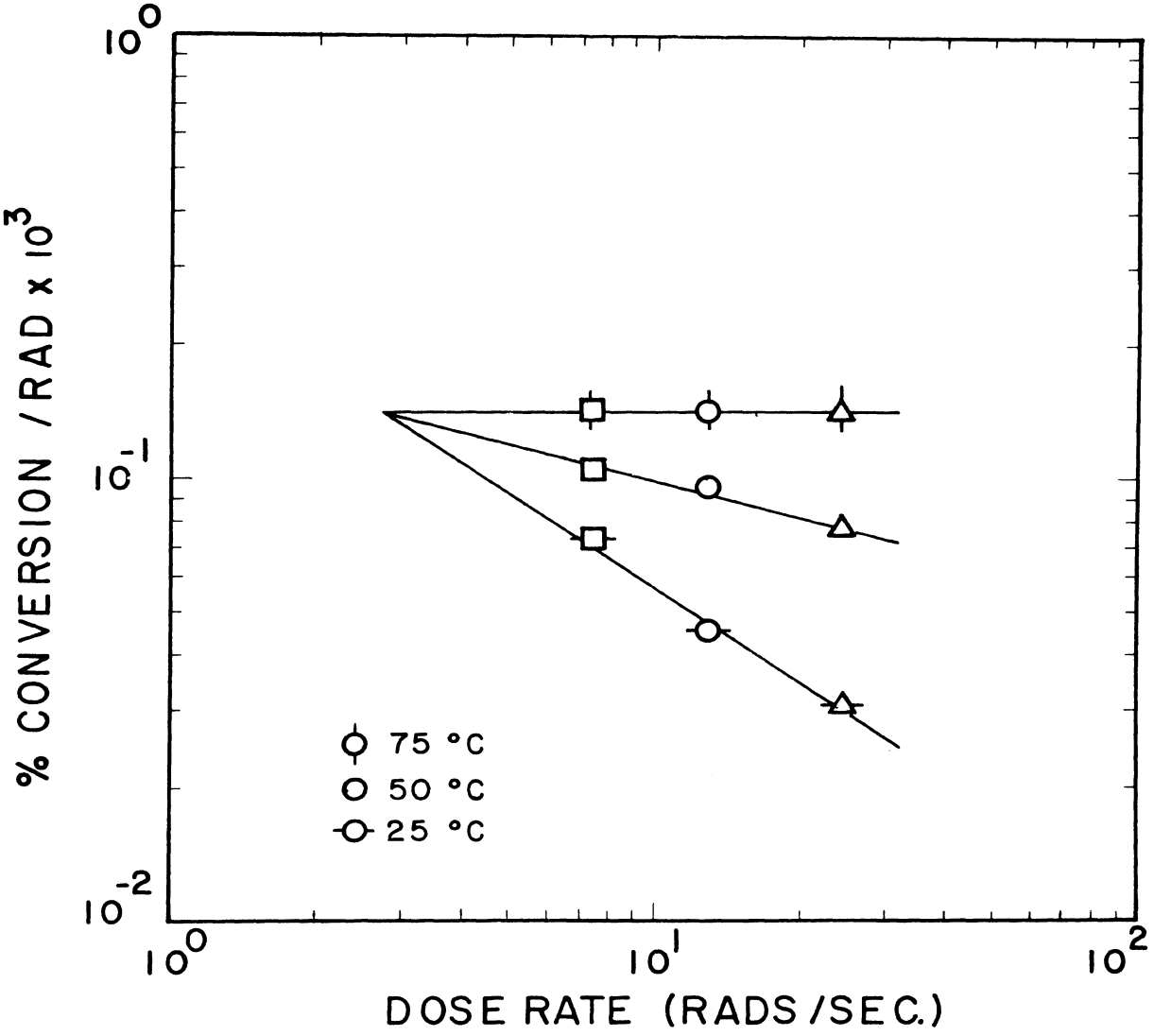

Figure 17. Per Cent Conversion vs. Dose Rate of Inserted Polymer.

TABLE XII

APPARENT REACTION ORDERS OF INSERTED POLYMER AT VARIOUS TEMPERATURES

Temperature ^{o}C	Apparent Reaction Order n
25	-0.702
50	-0.201
75	0.0

When an Arrhenius plot of the type similar to the homopolymer using initial rate data is drawn as in Figure 18, it is seen that the apparent energy of activation is not a constant value and that the formation of inserted polymer is dose rate dependent. Table XIII shows these apparent activation energies at the various dose rates. The inert atmosphere reaction has an apparent activation energy which is .8 kilocalories per mole (1/3 as much as the apparent activation energy in air at the same dose rate).

These data indicate at least two possible explanations; (1) that there is a change in mechanism of polymerization at the surface of the clay as a function of dose rate, and (2) that the data can be explained by physical monomer and polymer population changes at the surface of the clay which are related to the dose rate. A change in polymerization mechanism does not appear reasonable in view of the fact that the activation energies for the

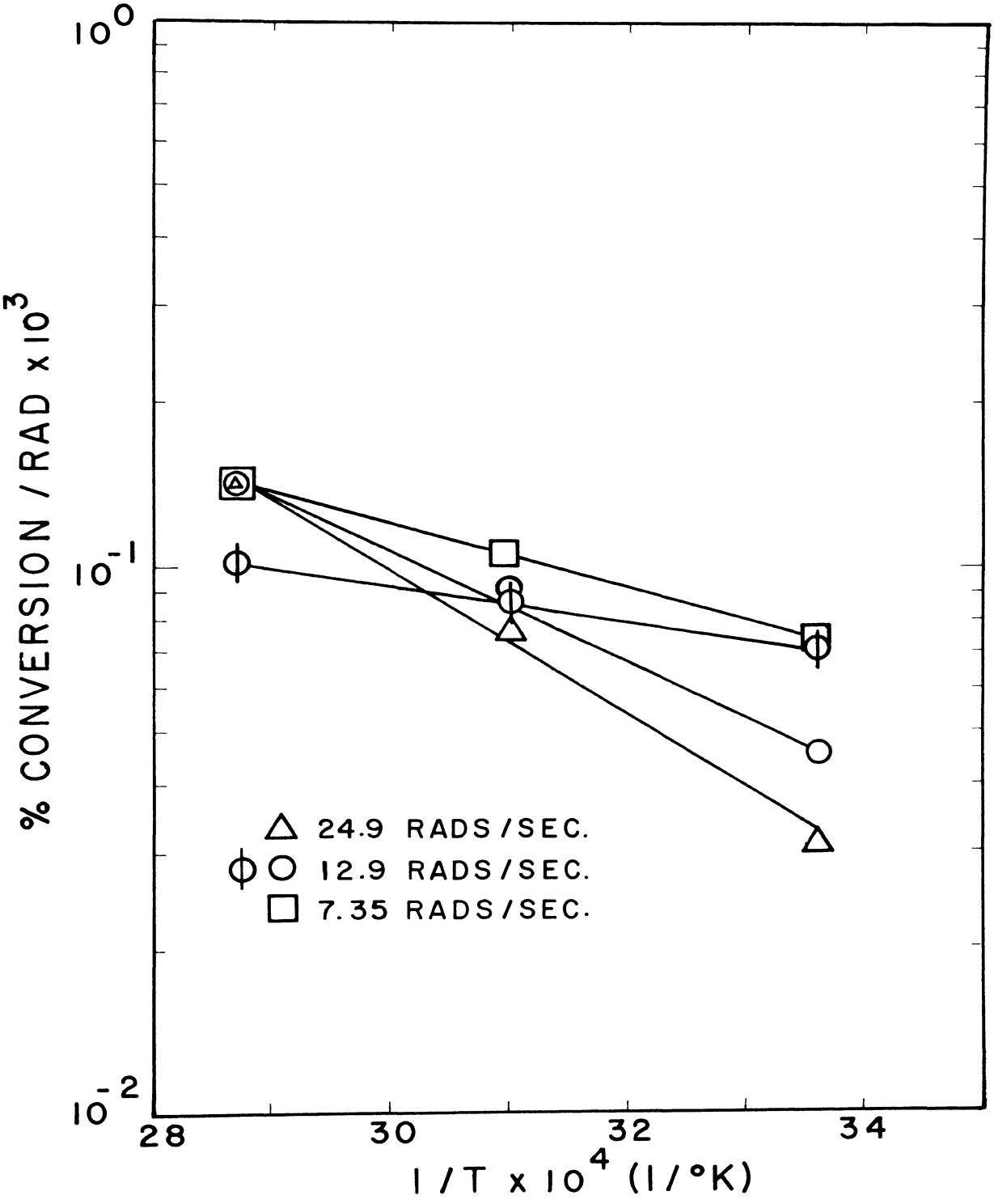

Figure 18. Activation Energy of Inserted Polymer in Air (△ , ○ , □) and Inert Gas (⌀).

TABLE XIII

ACTIVATION ENERGY OF INSERTED POLYMER
AT VARIOUS DOSE RATES

System	Dose Rate (rads/sec.)	dP/dD[a] 25 (°C)	50 (°C)	75 (°C)	ΔE^* (kcal./mole)
Inserted-Air	24.9	.031	.077	.143	6.4
	12.9	.045	.096	.143	4.8
	7.35	.073	.104	.143	2.8
Inserted Inert Gas	12.9	.070	.085	.101	1.6

[a] dP/dD based on initial reaction rates (% conversion per rad x 10^3)

homopolymer showed that the mechanism was the same at all dose rates and temperatures. It will be shown that the characterization of both homo and inserted polymers are also consistent with each other. However, the amount of energy necessary to form a net amount of polymer per unit dose on the surface of the clay may change as dose rate changes. This change in energy requirements could be caused by a depolymerization reaction which would proceed at a faster rate at the higher dose rate. The amount of energy necessary to overcome this larger depolymerization reaction to form the same amount of polymer per unit dose at the clay surface would thus be increased. If the above were true, the rate of formation of inserted polymer would be lower at the higher dose rates for the same total dose. This can be seen in the conversion curves. Thus it appears evident that the catalytic effect of the clay surface is effected by both dose rate and temperature. However, without some knowledge of clay site-gamma interactions as a function of dose rate and temperature, a quantitative explanation of this data can not be presented.

3. Total polymer kinetic analysis. The total polymer content is a summation of the soluble homopolymer and inserted polymer. Even though it has been shown that the inserted polymer behaves differently than the homopolymer, it is necessary to study the overall kinetics of the reaction. In practical applications, the overall rate of conversion of the monomer-clay mixture to a useable product would be the engineers main concern.

Figures 19, 20, 21 and 22 show that for the early stages of polymerization the inserted polymer gives the total polymer conversion curves a slight

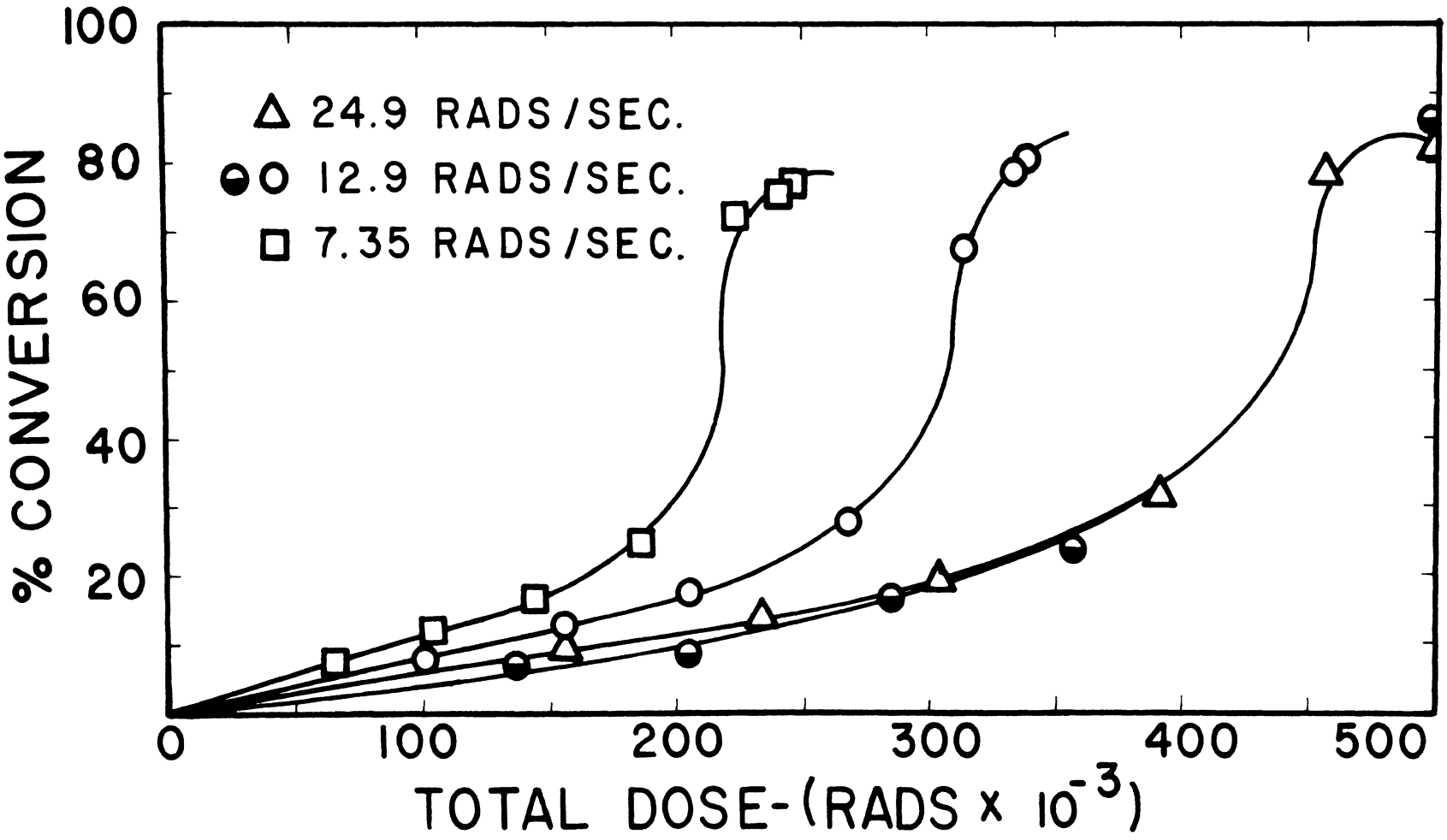

Figure 19. Formation of Total Polymer (△, ○, □) and Bulk Polymer (◒) in Air as a Function of Dose Rate @ 25°C.

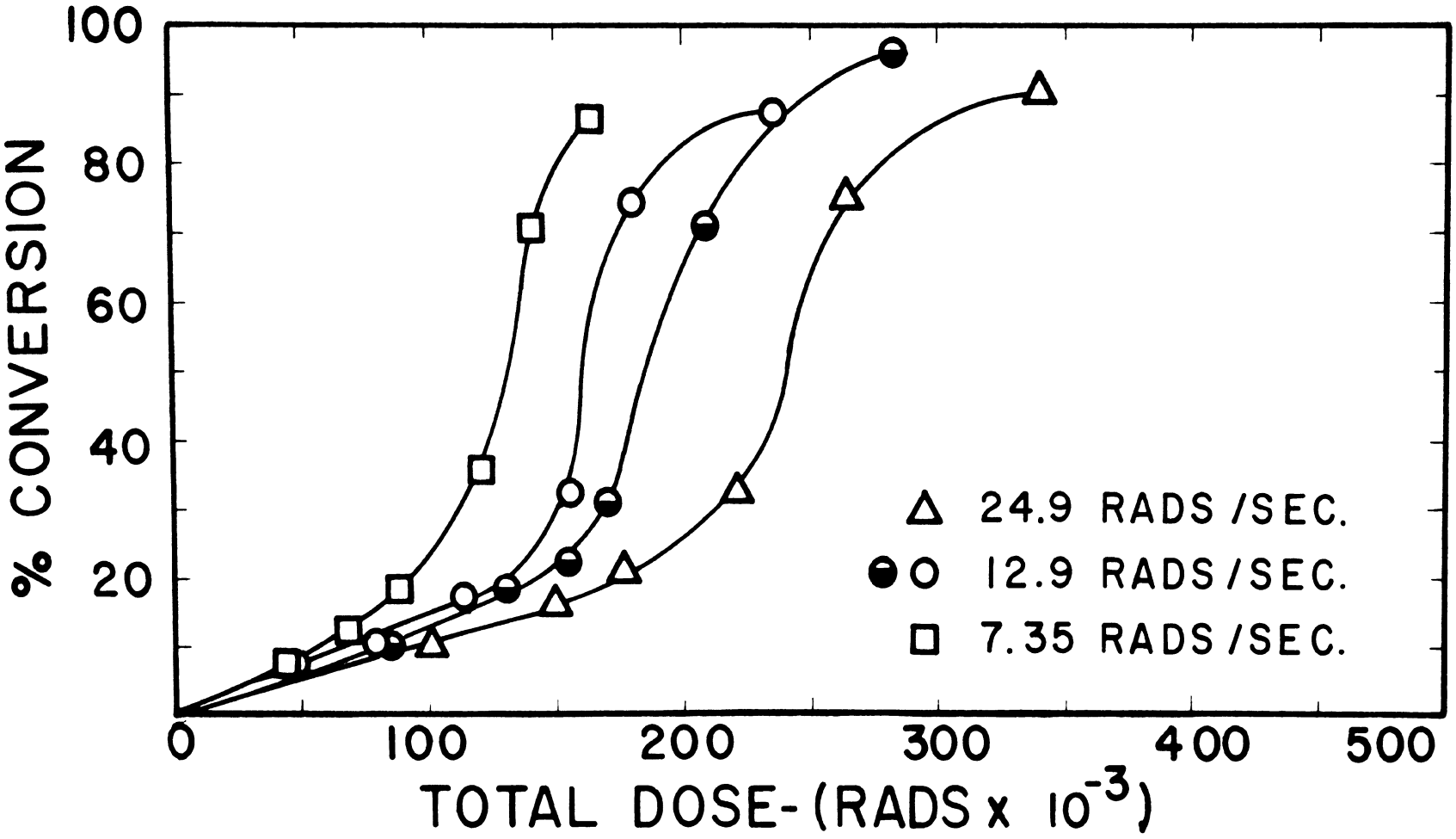

Figure 20. Formation of Total Polymer (△, ○ , □) and Bulk Polymer (◒) in Air as a Function of Dose Rate @ 50°C.

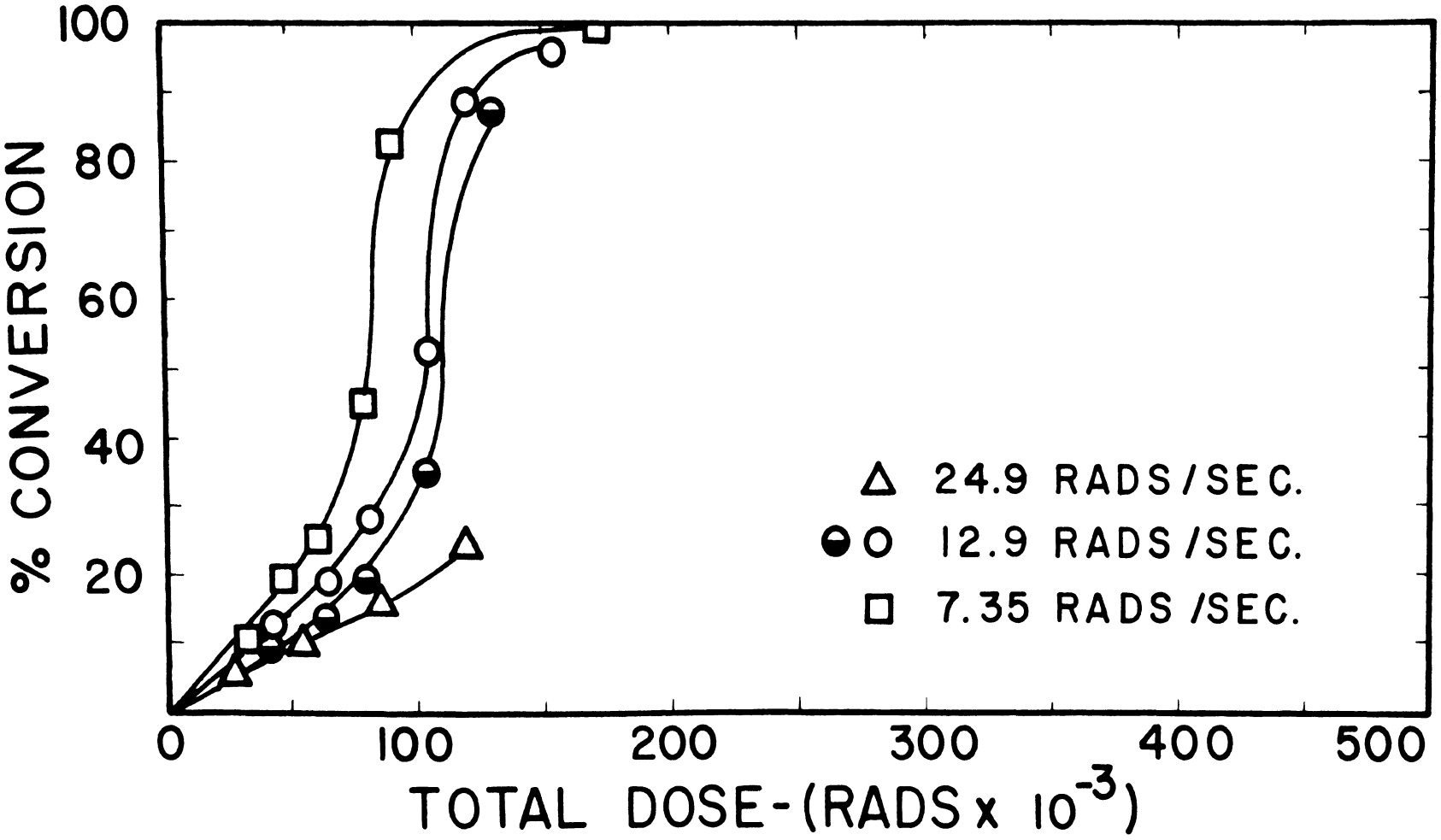

Figure 21. Formation of Total Polymer (△ , ○ , □) and Bulk Polymer (◒) in Air as a Function of Dose Rate @ 75°C.

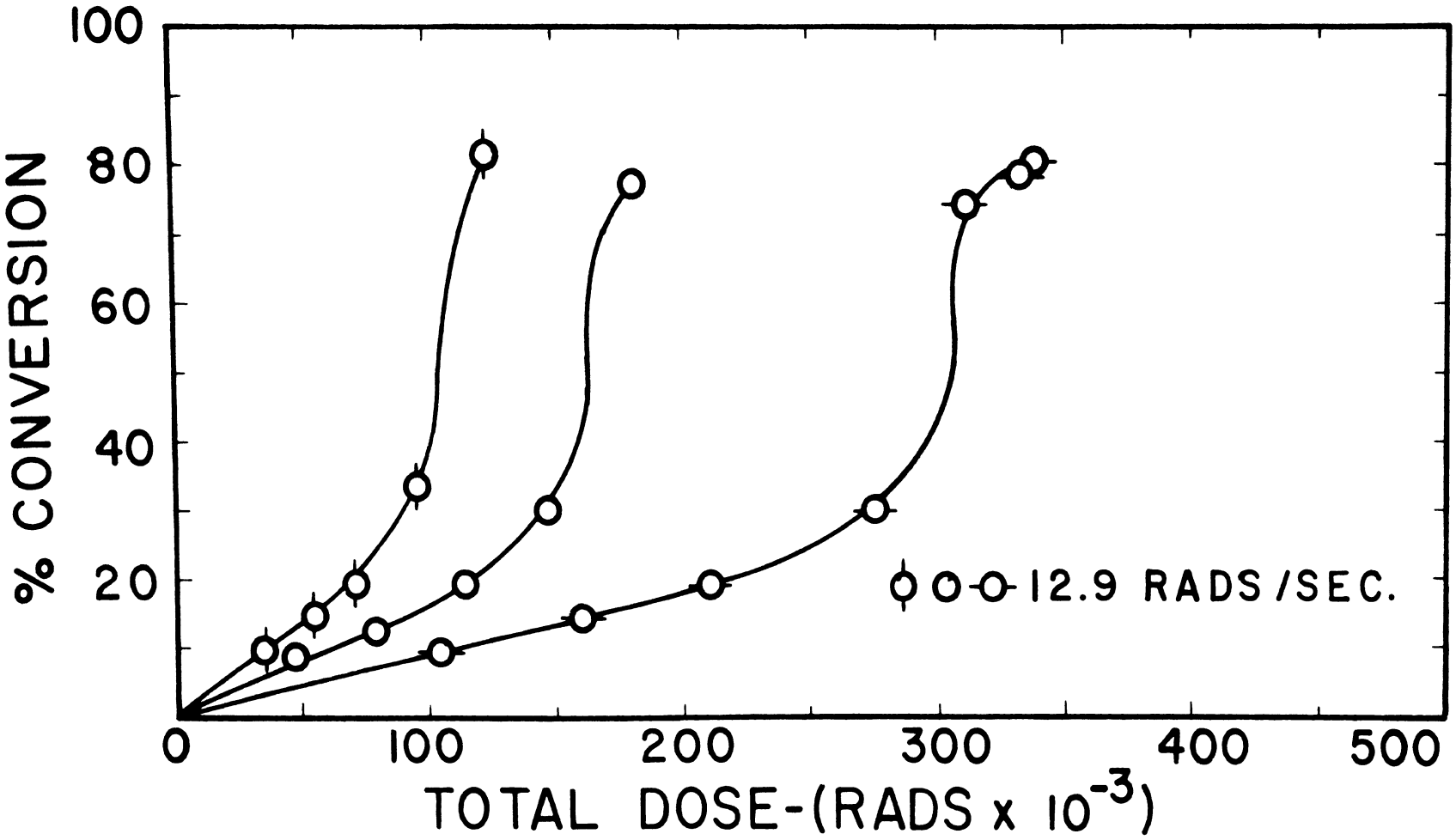

Figure 22. Formation of Total Polymer in Inert Gas at 25 (-O-), 50 (O) and 75°C (O).

concave downward trend. This trend is the influence asserted by the formation of inserted polymer in the early stages. However as polymerization proceeds and the homopolymer polymerization becomes more in evidence, the S-shaped curve characteristic of homopolymerization takes form.

In comparing the total composite polymerization with the bulk polymerization for the middle dose rate, it is seen from Figure 19 at 25°C, and 12.9 rads per second that the clay accelerates the polymerization and the polymer attains 80 per cent conversion almost 125,000 rads or 2.7 hours before the bulk polymer does. However from Figures 20 and 21 as the reaction temperature increases, the acceleration of polymer formation by the clay decreases until at 75°C the bulk and total composite polymer attain 80 per cent conversion at the same total dose. Figure 22 shows that the total percentage conversion of composite in the inert gas atmosphere has all the same shape of curve as the "in air" polymerization.

In all cases, the conversion of monomer to polymer in the composite is greater than the bulk until at least 50 per cent conversion for the same total dose.

If the reaction for the total polymer is plotted (Figure 23) as a $dP/dD = kI^n$, relationship, it is shown that the overall reaction approaches that of a free radical mechanism as shown in Table XIV. The dependence of the initial (dP/dD) rate approaches -0.5 for all temperatures and shows that the overall reaction proceeds via a free radical mechanism.

An Arrhenius plot of the initial rate data for the total polymer is shown in Figure 24. Straight lines have been drawn through the point with

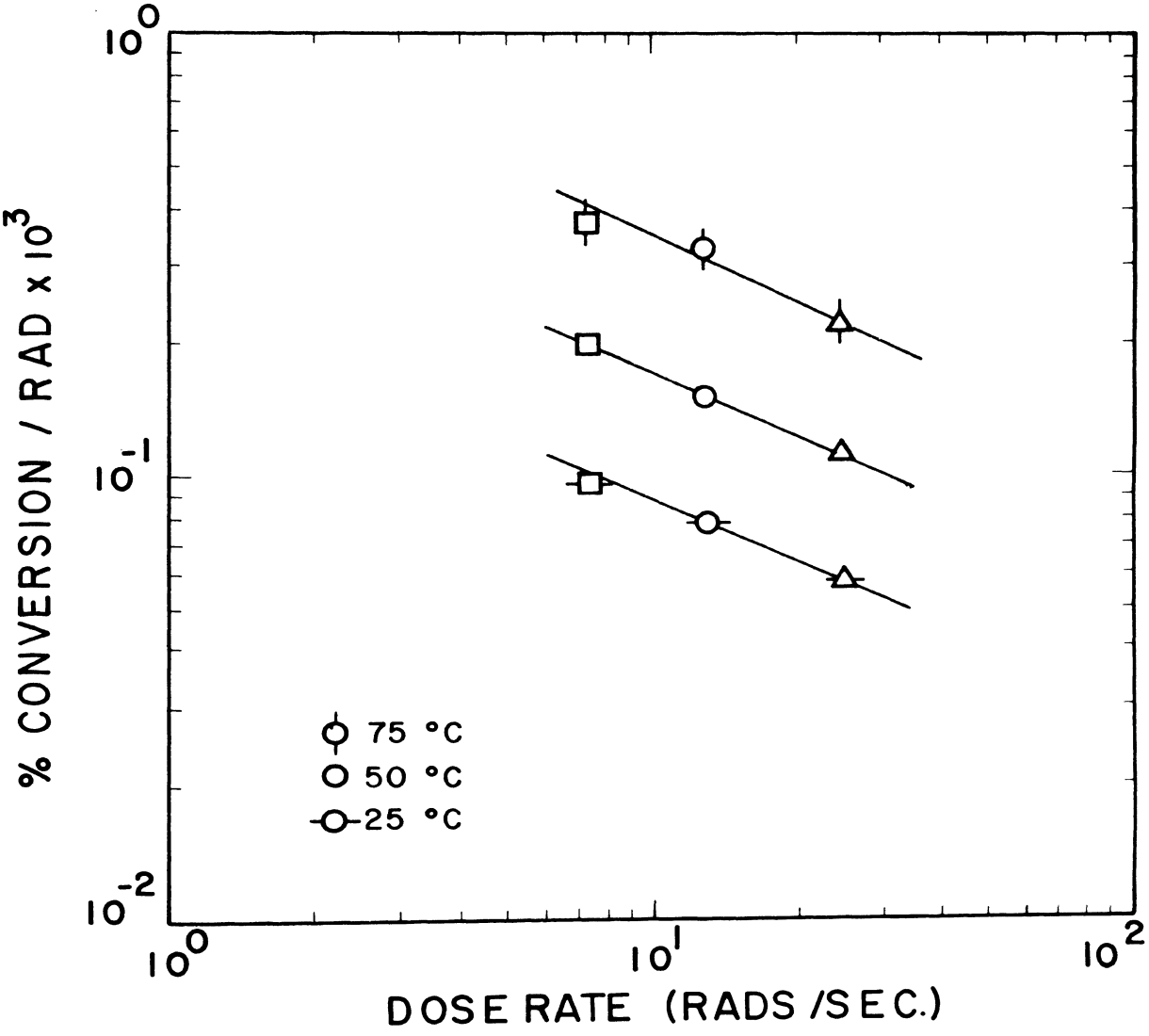

Figure 23. Per Cent Conversion vs. Dose Rate of Total Polymer.

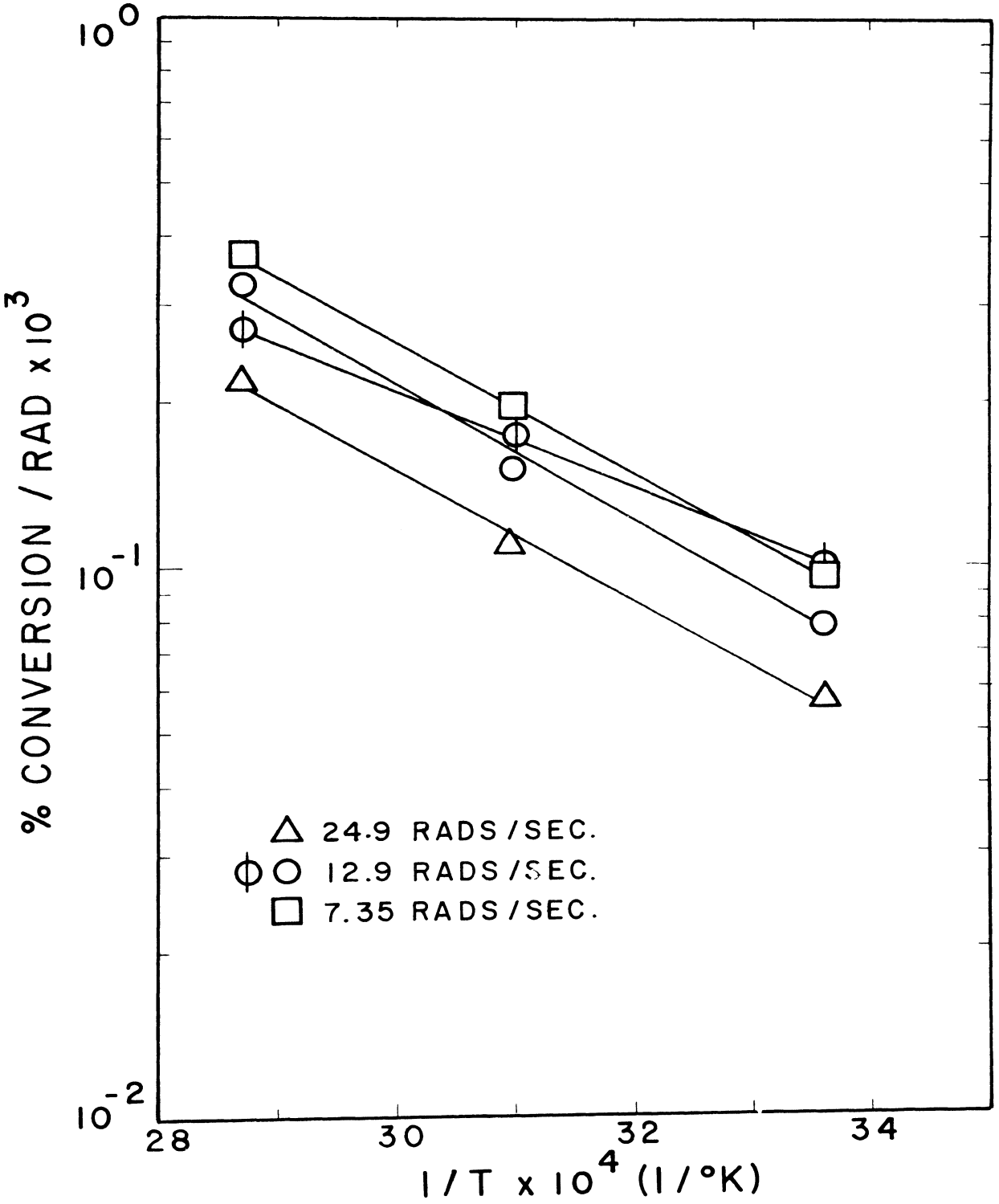

Figure 24. Activation Energy of Total Polymer in Air (△ , O , □) and Inert Gas (ϕ).

TABLE XIV

APPARENT REACTION ORDERS OF TOTAL POLYMERS AT VARIOUS TEMPERATURES

Temperature ^{o}C	Apparent Reaction Order n
25	-0.48
50	-0.49
75	-0.50

the results shown in Table XV. There is a possibility that there is some curvature in the point for the "in air" composites due to the influence of the inserted polymer. The inert gas polymerization shows a true isokinetic relationship. The activation energy of all the composites are approximately 1 kilocalorie per mole less than the activation energy for the bulk polymer in air and 2 kilocalories per mole less than the bulk polymerization in an inert gas atmosphere.

A further discussion of mechanistic possibilities will be presented in Part II of the discussion along with the characterization data.

The calculations and tabulated results for all the conversion data at the various dose rates will be found in Appendix B.

TABLE XV

ACTIVATION ENERGY OF TOTAL POLYMER
AT VARIOUS DOSE RATES

System	Dose Rate (rads/sec.)	dP/dD[a] 25 (°C)	50 (°C)	75 (°C)	ΔE^* (kcal./mole)
Total-Air	24.9	.0575	.112	.220	5.4
	12.9	.078	.150	.325	5.6
	7.35	.095	.195	.368	5.4
Total-Inert Gas	12.9	.100	.174	.270	4.0

[a] dP/dD based on initial reaction rates (% conversion per rad x 10^3)

IV. RESULTS AND DISCUSSION-PART 2

A. Clay Analysis

1. X-ray study. X-ray spectra of undried clay, dried clay, irradiated dried clay and the insoluble composite after removal of homopolymer were obtained as explained in the Experimental Section. A spectrum of dried kaolin clay is shown in Figure 25. The curves of all spectra taken appeared to be identical and no shifting of peaks was observed. On the basis of the X-ray data it was assumed that there were no major disruptions in the structure of the clay lattice caused by either drying or irradiation. However, this data gives no information concerning the number of changes in character of the active polymerization sites.

2. Particle size analysis. Particle size distributions are shown in Table XVI. The distributions of undried, dried and dried-irradiated clay indicated no breakdown in apparent particle size during irradiation. The micrographs obtained by scanning electron microscopy (SEM) show that the actual numbers obtained are not correct and that the sizes of clay agglomerates are being measured. The agglomerates are composed of many individual clay particles.

3. Surface area determination. The surface area determination was accomplished as explained in Experimental Section F-1-d. The specific surface area of irradiated clay was found to be 16.64 meters^2 per gram as compared to 16 $\pm$ 1.0 formed in the literature[34].

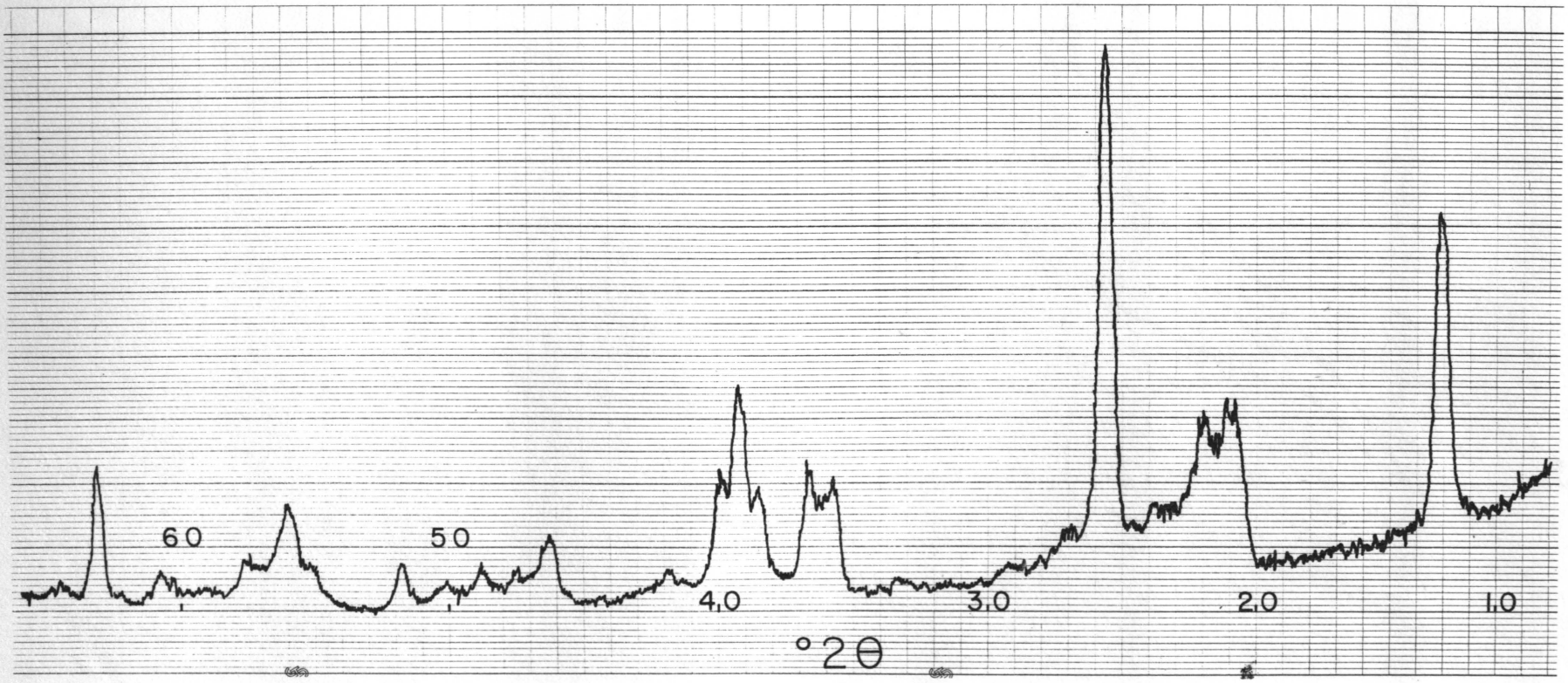

Figure 25. X-ray Spectrum of Dried Kaolin Clay

4. Thermal analysis of clay . Using DTA-TGA analysis the kaolin clay was found to be stable through 400°C. However in the range of 475 to 500°C, the clay underwent a normal transition due to the loss of hydroxyl groups from its lattice. This analysis was important in determining the amount of inserted polymer in the composite (Appendix B).

These analyses of the clay indicate that the irradiation by gamma-rays had no effect on the overall structure, average particle size and the average specific surface.

TABLE XVI

ANALYSIS OF PARTICLE SIZE DISTRIBUTION FOR VARIOUS TREATMENTS OF KAOLIN CLAYS

Clay System	% less than 10 μM diameter	% less than 4.6 μM diameter
Undried	85.6	50.0
Dried	79.9	50.0
Dried-Irradiated	82.9	50.0

B. Infrared Spectroscopy of Polymers

Infrared spectroscopy was used to determine whether or not any gross changes occurred in the structure of the PMMA caused by irradiation or if there was a difference in the structure of the homopolymer and inserted composite of the polymer. An example of the spectra obtained is shown in Figure 26. No differences in the spectra for the homopolymer were noticed for any of the various irradiation times, reaction temperatures or dose rates. There was also no difference in the spectra when the homopolymer and inserted polymer were compared.

C. Thermal Analysis

Thermal analysis was performed on the total composite, inserted composite, homopolymer and bulk polymer. As shown in Table XVII, the comparison of all systems in air for all polymerization temperatures show that there was substantially no difference in the decomposition temperatures of the different polymers. These decomposition temperatures fall in the range of 305-315^{o}C. Decomposition beyond this temperature is rapid. The experiments using the argon atmosphere showed an increase in decomposition temperature of 10 to 20^{o}C above the temperature in air due to the absence of the oxidizing atmosphere and difference in heating rate. The final decomposition temperature of all systems was 390-400^{o}C at the same heating rate in air.

In comparing the irradiated systems with chemically initiated commercial PMMA, it was found that irradiation had increased the decomposition

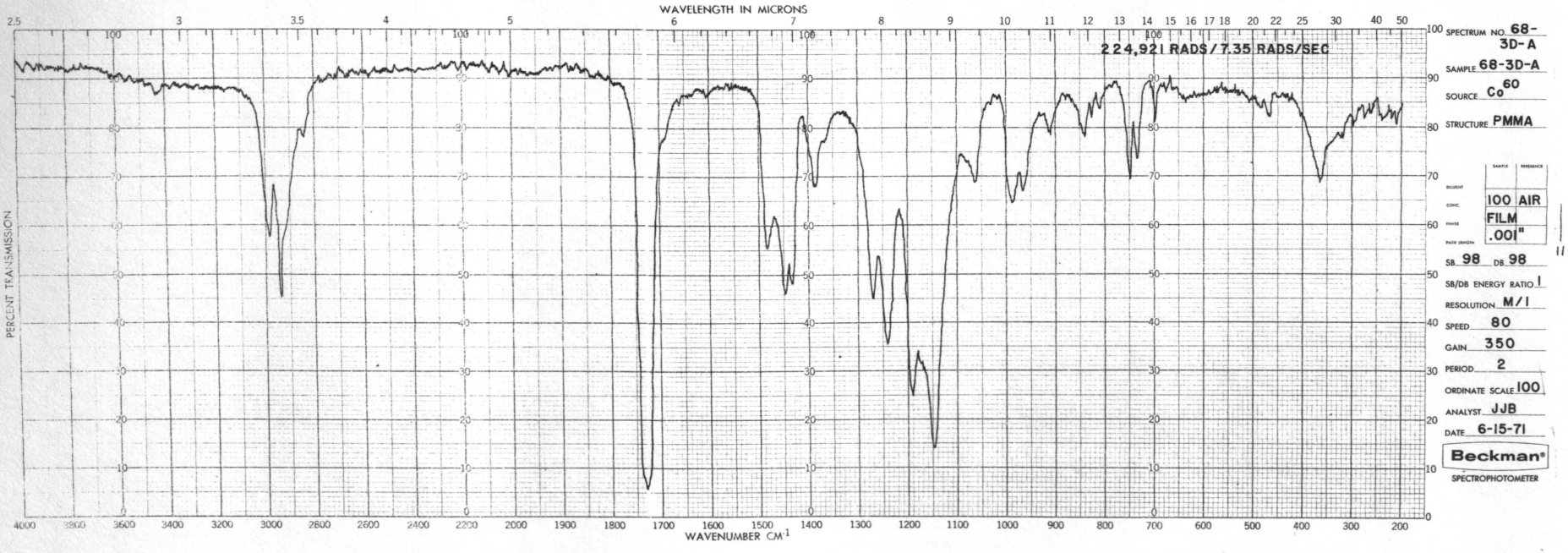

Figure 26. Infrared Spectrum of Irradiated Homopolymer

TABLE XVII

DECOMPOSITION TEMPERATURES OF VARIOUS SYSTEMS USING AIR AND ARGON ATMOSPHERES

Component	Polym. Reaction Temperature °C	Atmosphere	Heating Rate (°C/min.)	Decomposition Temperature
Total Composite	50	Air	10	310
	25	Argon	6	330
Inserted Composite	50	Air	10	310
	25	Air	10	305
	75	Argon	10	320
	25	Argon	6	320
Homopolymer	50	Air	10	300
Bulk Polymer (irradiated)	75	Air	10	315
	50	Air	10	310
	25	Air	10	310
	25	Argon	6	330
Bulk Polymer (chemical)		Air	10	280

temperature 20°C above that of the commercial polymer (at the same experimental conditions).

D. Intrinsic Viscosity Determinations

1. Polymerization comparison of bulk and composite systems. In the formation of polymer in the bulk system, initial polymer chains form which then migrate through the reaction media (largely monomer). In some cases these chains have been shown to actually settle to the bottom of a reaction vessel. After a sufficient amount of polymer has formed, the system becomes a gel. At this point, further polymer molecular weight is attained by the diffusion of successive monomer units to the active chain ends. This diffusion process is named the "Trommsdorff effect." High molecular weight polymers are obtained by this process.

In the case of monomer-clay mixtures a stable paste exists before polymerization begins and the initial polymer chains formed have limited freedom to migrate to other parts of the system or settle to the bottom of the reaction mixture. A diffusion controlled mechanism therefore probably starts at a lower percentage conversion.

Chemically initiated systems have no tendency toward chain breakdown during polymerization. Two opposing reactions occur when gamma irradiation is used. The polymerization reaction is actually a net process of polymerization and depolymerization. After the polymer becomes a gel, further irradiation increases the depolymerization reaction and decreases the molecular weight of the reaction. The ultimate molecular weight of

polymers formed via gamma initiation would therefore be expected to be less than for the chemically initiated commercial system. However, the molecular weights of the composite polymers formed in this study were considerably higher than those polymers produced in the bulk by normal laboratory synthesis techniques and existing commercial processes.

2. Intrinsic viscosity and molecular weight determinations. Intrinsic viscosities reported in Table XVIII and Table XIX were determined on the different polymers at their endpoints and at various times before their endpoints by accepted laboratory procedures as outlined in Experimental Section F-3-d. Because of the high molecular weights of the polymers special handling precautions were followed. Some of the polymers required dissolution times in excess of one week at ambient temperature. Both benzene and toluene were good solvents (the constant "a" in the Mark Houwink relationship >0.7) for polymethylmethacrylate and presented no special problems concerning polymer stability in solution. Initial work was done using toluene because of its inertness and ease of handling. Benzene was used in later work because it was thought that a similar molecule of smaller size would be a more effective solvent. Molecular weights calculated from intrinsic viscosities in these two solvents agree within 5 per cent of each other. The dissolution process could not be hastened by heating (to more than 40-50^{o}C) for fear of degrading the polymer[35]. Solutions could not be agitated beyond a gentle stirring because of possible degradation of the polymers by localized shear stresses[36, 37]. The dissolution was therefore

TABLE XVIII

INTRINSIC VISCOSITY DATA AT ENDPOINTS FOR HOMO AND BULK POLYMERS

Trial		k'	k''	k' + k''	$\overline{M}_v \times 10^{-6}$	Temp. °C	Atm.	Solvent[a]	Dose Rate (rads/sec.)	Total Dose (rads x 10^{-3})
68-3D-A	4.17	.242	.226	.468	2.84	25	Air	B	7.35	225
68-5B-B-C	3.50	.338	.160	.498	2.26	25	Air	B	12.9	313
68-5-C	3.42	.447	.070	.517	2.19	25	Air	B	24.9	457
74-3D-B	5.80	.414	.113	.527	4.38	50	Air	B	7.35	140
74-3B-C	4.55	.406	.097	.503	3.18	50	Air	B	12.9	183
74-7-A	4.21	.274	.210	.484	2.87	50	Air	B	24.9	264
73-1D-B	5.94	.312	.174	.486	4.52	75	Air	B	7.35	90
73-5B-D	6.71	.198	.279	.477	5.30	75	Air	B	12.9	120
73-4-A	2.27	.456	.064	.520	1.27	75	Air	B	24.9	119
69-5B-C	4.45	.307	.180	.487	3.09	25	Ar	B	12.9	311
75-3B-A	4.89	.388	.116	.504	3.50	50	Ar	B	12.9	180
68-5B-B-O	3.50	.338	.160	.498	2.26	25	Air	B	12.9	313
68-5B-B-24	4.38	.292	.198	.490	3.03	25	Air	B	12.9	313
68-5B-B-72	4.51	.311	.171	.482	3.14	25	Air	B	12.9	313

[a] B = Benzene
T = Toluene

Trial		k'	k''	k' + k''	$\bar{M}_v \times 10^{-6}$	Temp. °C	Atm.	Solvent[a]	Dose Rate (rads/sec.)	Total Dose (rads $\times 10^{-3}$)
68-4B-D-M[b]	1.23	.288	.206	.494	.57	25	Air	B	12.9	357
74-3-B-D[b]	6.30	.258	.235	.493	4.88	50	Air	B	12.9	210
73-5B-C[b]	6.28	.340	.153	.495	4.86	75	Air	B	12.9	130

[a] B = Benzene
T = Toluene

[b] Bulk Polymer

TABLE XIX

INRTINSIC VISCOSITY DATA APPROACHING ENDPOINTS FOR HOMO AND BULK POLYMERS

Trial	$[\eta]$	k'	k''	k' + k''	$\overline{M}_v \times 10^{-6}$	Temp. °C	Atm.	Solvent[a]	Dose Rate (rads/sec.)	Total Dose (rads x 10^{-3})
66-5D-F	.16	.345	.151	.496	.88	25	Air	T	7.35	72
66-4D-F	1.10	.375	.137	.512	.81	25	Air	T	7.35	109
66-2D-F[b]	1.17	.370	.140	.510	.88	25	Air	T	7.35	146
68-3D-A[b]	4.17	.242	.226	.468	2.84	25	Air	B	7.35	225
66-5B-E	.90	.407	.115	.522	.61	25	Air	T	12.9	99
66-4B-E	.91	.390	.132	.522	.62	25	Air	T	12.9	152
66-2B-E	.98	.382	.135	.517	.69	25	Air	T	12.9	208
68-5B-B-O[b]	3.50	.338	.160	.498	2.26	25	Air	B	12.9	313
66-2-I	.76	.340	.156	.496	.48	25	Air	T	24.9	147
66-6-4-D-I	.77	.372	.136	.508	.49	25	Air	T	24.9	230
68-5-C[b]	3.42	.447	.070	.517	2.19	25	Air	B	24.9	457
66-2-A-I[c]	.72	.281	.192	.473	.45	25	Air	T	24.9	194
66-3-A-I[c]	.68	.284	.202	.486	.41	25	Air	T	24.9	402
66-4-A-I[c]	.83	.339	.158	.497	.55	25	Air	T	24.9	512
70-RT-7 Days	8.50	.341	.154	.495	7.29	25	Air	B	0	0

[a] B = Benzene
T = Toluene

[b] At endpoint

[c] Bulk Polymer

allowed to occur with a minimum of heating and stirring. Attempts were made to determine the intrinsic viscosity of all of the polymers reported in this study. In some instances the polymers did not completely dissolve and in other cases, where the data showed the polymers were not dissolved, the data were considered to be unreliable and will not be reported.

The molecular weights were calculated using literature values for the constants in the Mark Houwink equation:

$$[\eta] = KM_v^a$$

For benzene[38] $K = 5.2 \times 10^{-5}$ $a = 0.76$

For toluene[39] $K = 7.0 \times 10^{-5}$ $a = 0.71$

The use of these constants have been found to be applicable to PMMA having molecular weights of $2\text{-}4 \times 10^6$.

The following general trends were drawn from the endpoint data in Table XVIII:

1. the net viscosity average molecular weight ($\overline{M}_v$) of composite polymers produced at a constant temperature was greater for the 7.35 dose rate than for the molecular weight of the polymers produced using dose rates of 12.9 and 24.9 rads per second

2. at a constant dose rate, the $\overline{M}_v$ of the composite polymers increased as temperature increased (25 to 75^oC)

3. there were essentially no differences in the molecular weights of the composite polymers formed in the presence of an inert gas (argon) than for those produced at similar temperatures and dose rates in air

4. trials 68-5B-B-O, -24 and -72 represent a composite polymer that was polymerized in air at 25°C using a dose rate of 12.9 rads per second, but where dissolution was started immediately after the endpoint (-0), after 24 hours (-24) and after 72 hours (-72). Published data[10] indicated that polymerization could continue after irradiation if a sufficient amount of unconverted monomer remained. The molecular weight data indicate that the monomer reacted with the existing growing chain ends in the absence of radiation and formed higher molecular weight polymers.

5. the $\overline{M}_v$ of both irradiated composite and bulk polymers was higher than the same system formed by the use of a chemical initiator (5×10^5)[40].

6. the $\overline{M}_v$ of the bulk polymer tended to increase as reaction temperature increased.

The following trends can be stated for polymers which approach the endpoint at various expermental conditions (Table XIX):

1. at a constant temperature and dose rate, only slight increases in $\overline{M}_v$ of the polymer were in evidence until the endpoint was reached. The tremendous increase in $\overline{M}_v$ at the endpoint showed the importance of the Trommsdorff effect

2. at a constant temperature, the $\overline{M}_v$ of the polymer was higher as dose rate decreased

3. trial 70-RT-7days was obtained for a sample which was polymerized at ambient temperature in air for seven days in the complete absence of any radiation. The resulting polymer had a higher molecular weight than any of the polymers formed in the presence of radiation ($\overline{M}_v = 7.2 \times 10^6$) In this

instance depolymerization and degradation reactions would not be expected to occur.

The values of k' and k'' reflect the extent of polymer solvent interactions. These values as shown in the table do not have a direct relationship to the molecular weight. However, as the $\bar{M}_v$ increased most of the k' 's increased above the normal .30 to .35 for the solvents used showing that the polymer was becoming more difficult to place into solution. The values of k' could also reflect the changes in the molecular weight distribution and tacticity. The results of this section will be amplified in the gel permeation chromatograph analysis.

E. GPC Analysis

Gel permeation chromatography was originally planned to be used to determine the weight and number average molecular weights and the molecular weight distribution of the bulk, composite and inserted polymers. A discussion on how the chromatograms were obtained is found in Appendix C. The molecular weights obtained from the samples were much higher than anticipated and difficulties were encountered in obtaining the necessary chromatograms for analysis. Therefore, the results discussed will be that molecular weight obtained from the peak of the chromatograms as shown in Figure 27.

From the peak molecular weights (M_p) shown in Figures 28, 29, 30 and 31, the following can be stated:

1. at a constant dose rate, the M_p was larger at the same dose up to the gel point as the temperature increased (25^oC to 75^oC)

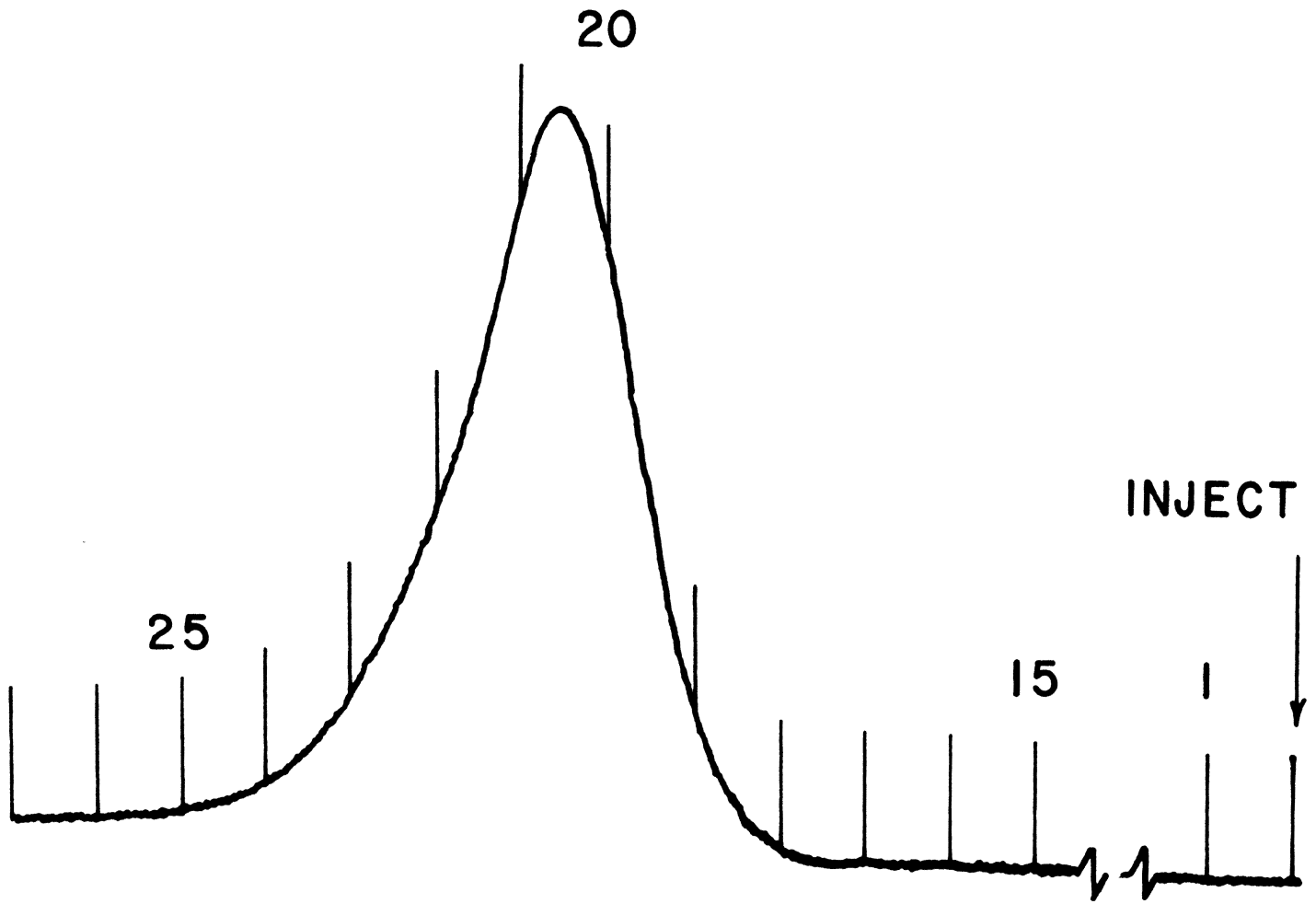

Figure 27. GPC Chromatogram of Homopolymer

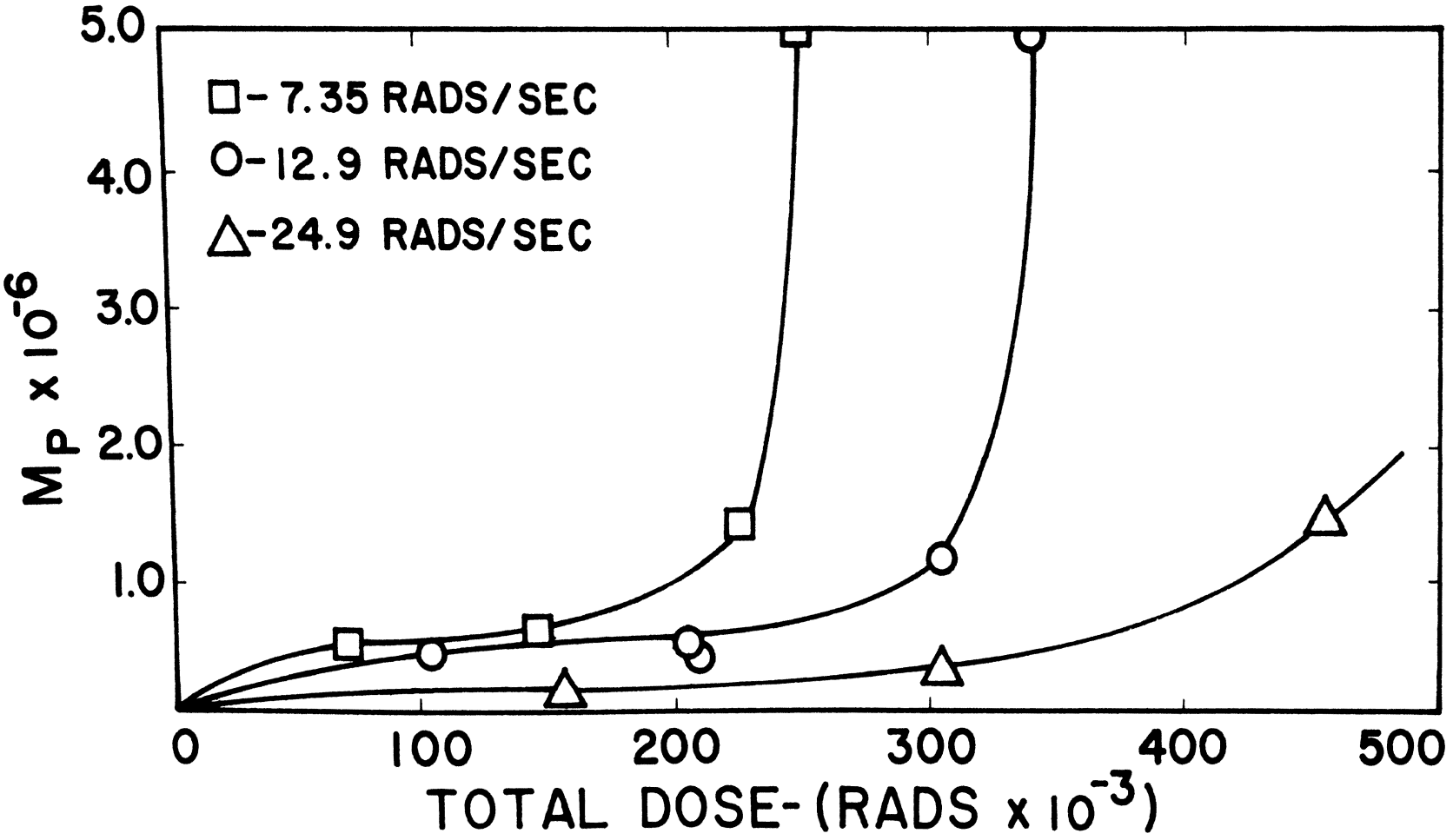

Figure 28. Peak Molecular Weight of Homopolymer in Air as a Function of Dose Rate @ 25°C

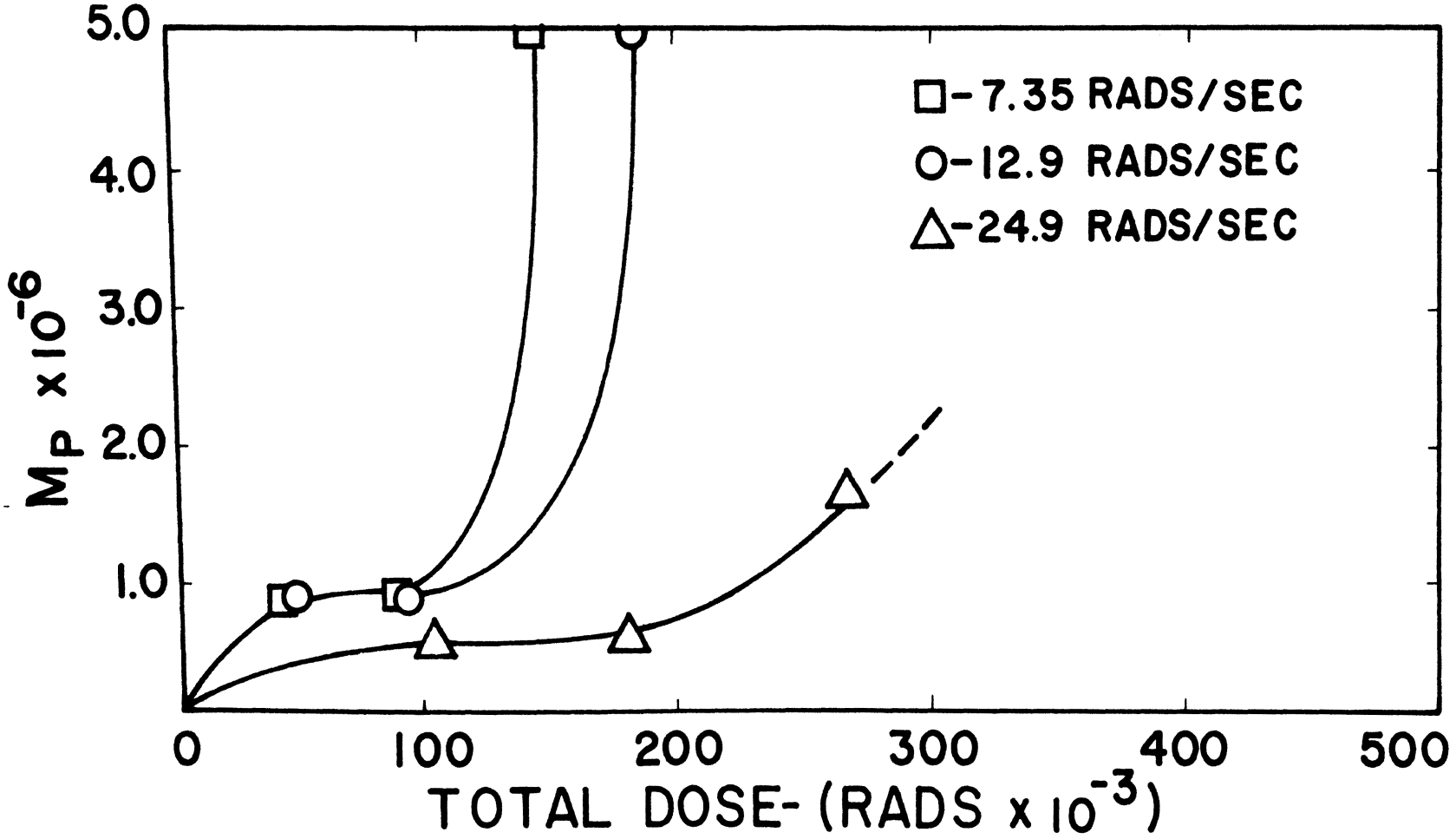

Figure 29. Peak Molecular Weight of Homopolymer in Air as a Function of Dose Rate @ 50°C

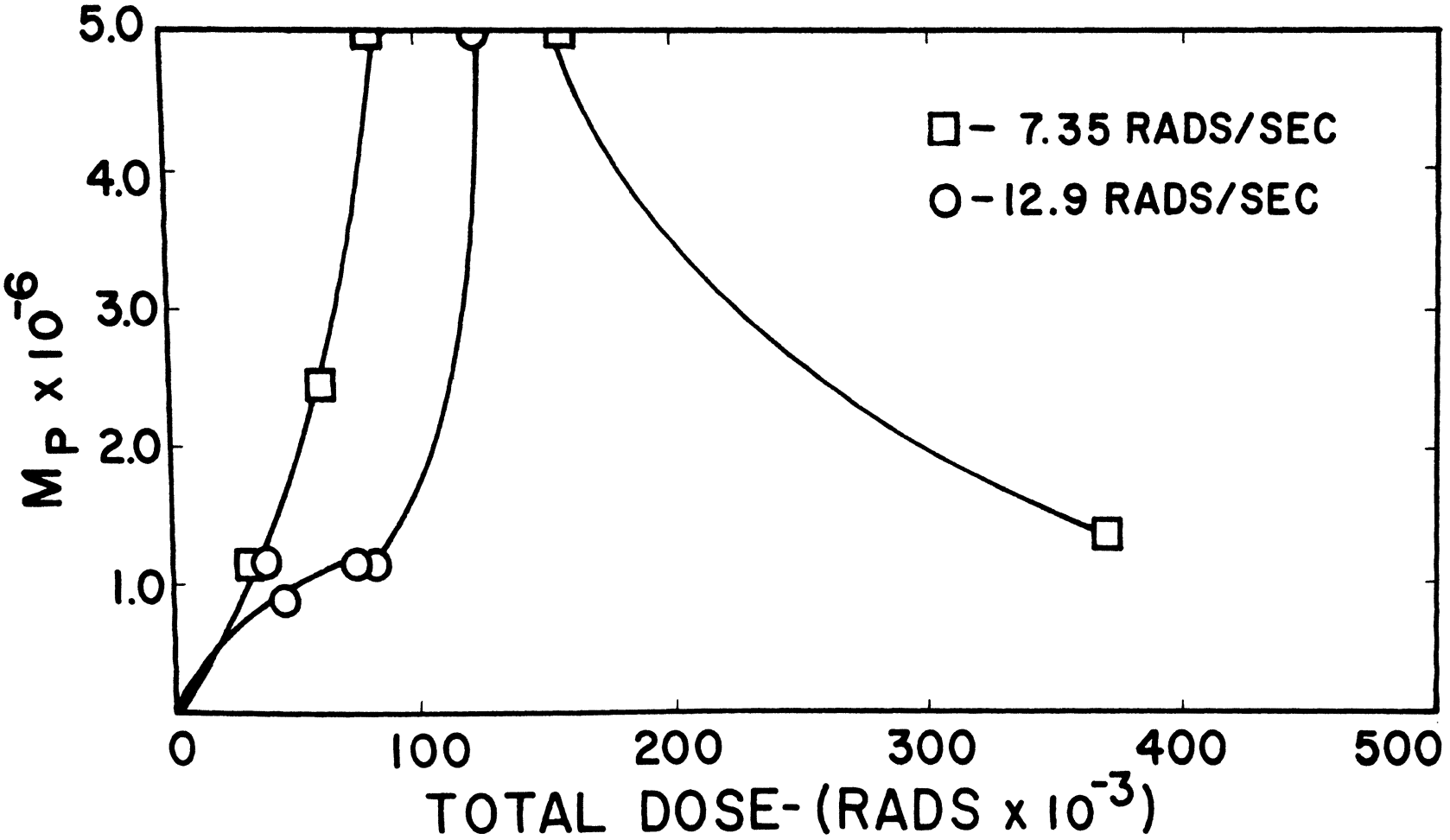

Figure 30. Peak Molecular Weight of Homopolymer in Air as a Function of Dose Rate @ 75°C

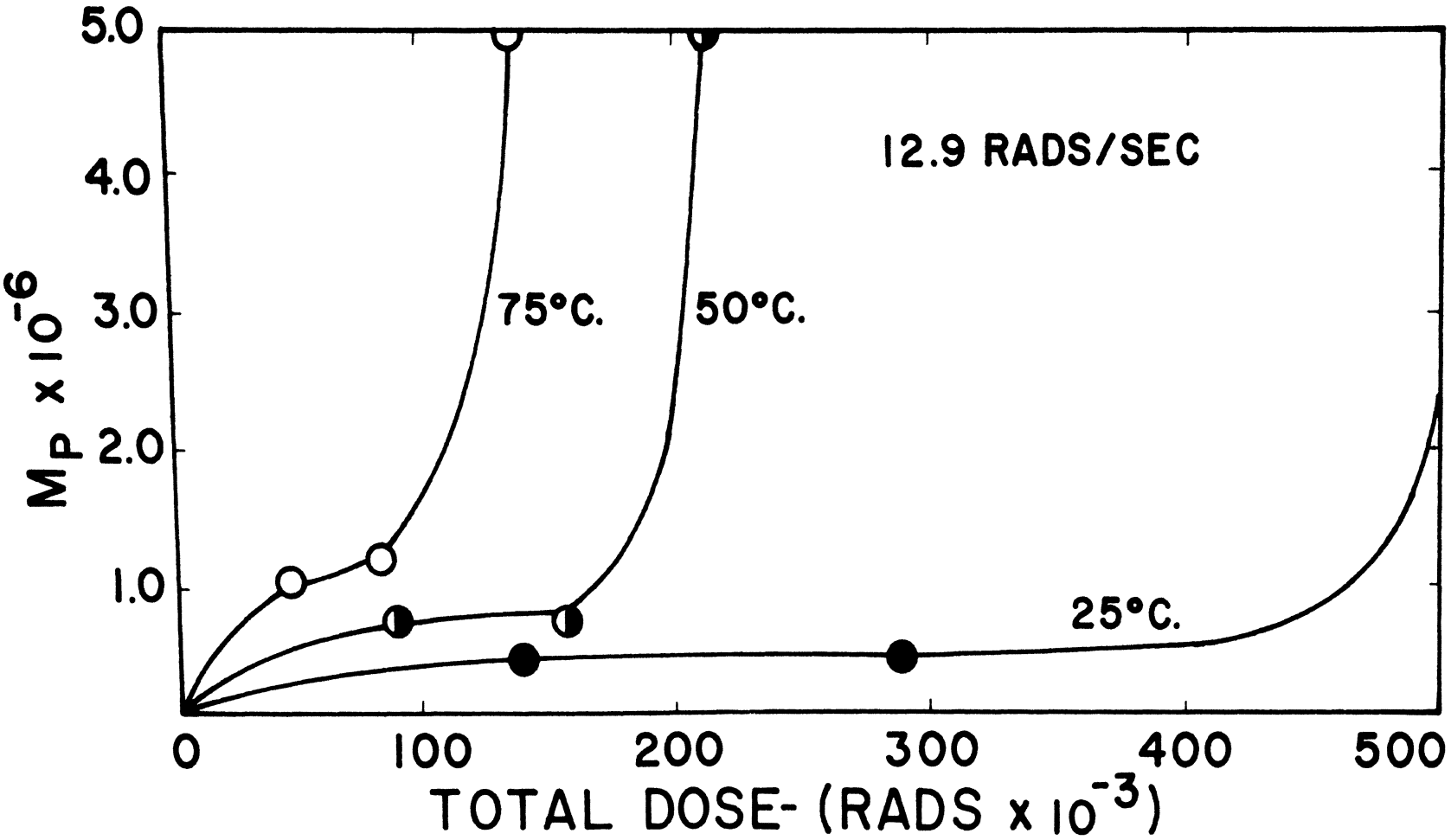

Figure 31. Peak Molecular Weight of Homopolymer in Inert Gas at Various Temperatures

2. at a constant temperature, the M_p was larger at any given dose as the dose rate decreased (24.9 to 7.35 rads per second)

3. the peak molecular weights at the endpoints exceeded the resolution of the calibration curve.

Chromatograms were also obtained on certain samples of the inserted polymer. The results of these chromatograms indicated that there were substantially no differences in the peak molecular weights or the chromatograms for the inserted and homopolymers.

The above results were measures of that portion of the polymer that passed through the columns. The chromatograms obtained for the polymers at their endpoint were not Gaussian, but were skewed to the low molecular weight side of the curve. This in effect said that the columns could not separate the very high molecular weight polymer and that this material was passing through the column as a "slug of polymer." This slug could actually be polymer which has formed a gel inside the columns and could not penetrate into the pores of the column. These high molecular weight polymers or gels were present in such amounts that even at concentrations of 0.1 per cent, actual plugging of the columns occurred. Lower concentrations of polymer solutions could not be used due to the fact that the differences in the indexes of refraction of the polymer and solvent were so close that any lower concentration could not be seen on the chromatogram. This plugging was indicated by the pressure build-up in the column. The plugging effect was the main reason for stating that it was possible that not all of the polymer passed through the columns.

The calculation of a molecular weight distribution and weight and number average molecular weights was attempted by the method of Tung[41]. The weight average molecular weights obtained were low by a factor of 10 in comparison with the viscosity average molecular weights. These two molecular weights should be close to one another with the weight average molecular weight actually being higher.

These differences could be the result of the following:

1. the standard calibration curve was non linear

2. no standards were available which could be used for calibration at the very high molecular weight

3. no correction was made for the skewing of the chromatogram because of the higher concentration of polymer needed for analysis. It was therefore decided not to report these results as they do not reflect the true nature of the average molecular weights or their distributions.

At the time this work was performed the necessary columns were not available to separate polymers of the molecular weights obtained for the PMMA-kaolin clay system. All samples were retained and the necessary information for actual molecular weights and molecular weight distributions will be obtained and reported when funds become available to purchase the required columns.

F. Nuclear Magnetic Reasonance (NMR) Studies

NMR spectra were obtained on selected samples of the bulk, homo and inserted polymers. Figure 32 shows the pertinent portions of spectra for a bulk polymer and an inserted polymer. These spectra were obtained in o-dichlorobenzene at 150^{o}C using trimethyl silane as an internal standard.

In interpreting the spectra for PMMA, consideration must be given to the influence of both the adjacent and nearest neighboring α-methyl groups on the methylene protons. The signals generated reflect the sterospecificity of the polymer chain. The optical configuration of two adjacent monomer units which are the same are classified as isotactic [(I) placements] . Those having different configurations are classified as syndiotactic [(S) placements] . When three adjacent monomer units are considered, either isotactic pairs of placements (II), syndiotactic pairs (SS), or heterotactic pairs (IS_vSI) can be formed. The measurement of triads of placements was not pertinent to this work and the data reported are based upon placement pairs. As seen in the figure the signals at 8.64, 8.78 and 8.88 represent the pairs of placements II (isotactic). IS_vSI (Heterotactic), and SS (syndiotactic), respectively. The values calculated for are in agreement with those values reported by Reinmoller and Fox at 8.62 , 8.75 and 8.85 for the same pairs of placements[28]. The pair placements for a given set of samples were evaluated from the areas under the above peaks and the tacticity of the polymer calculated from the following relationships:

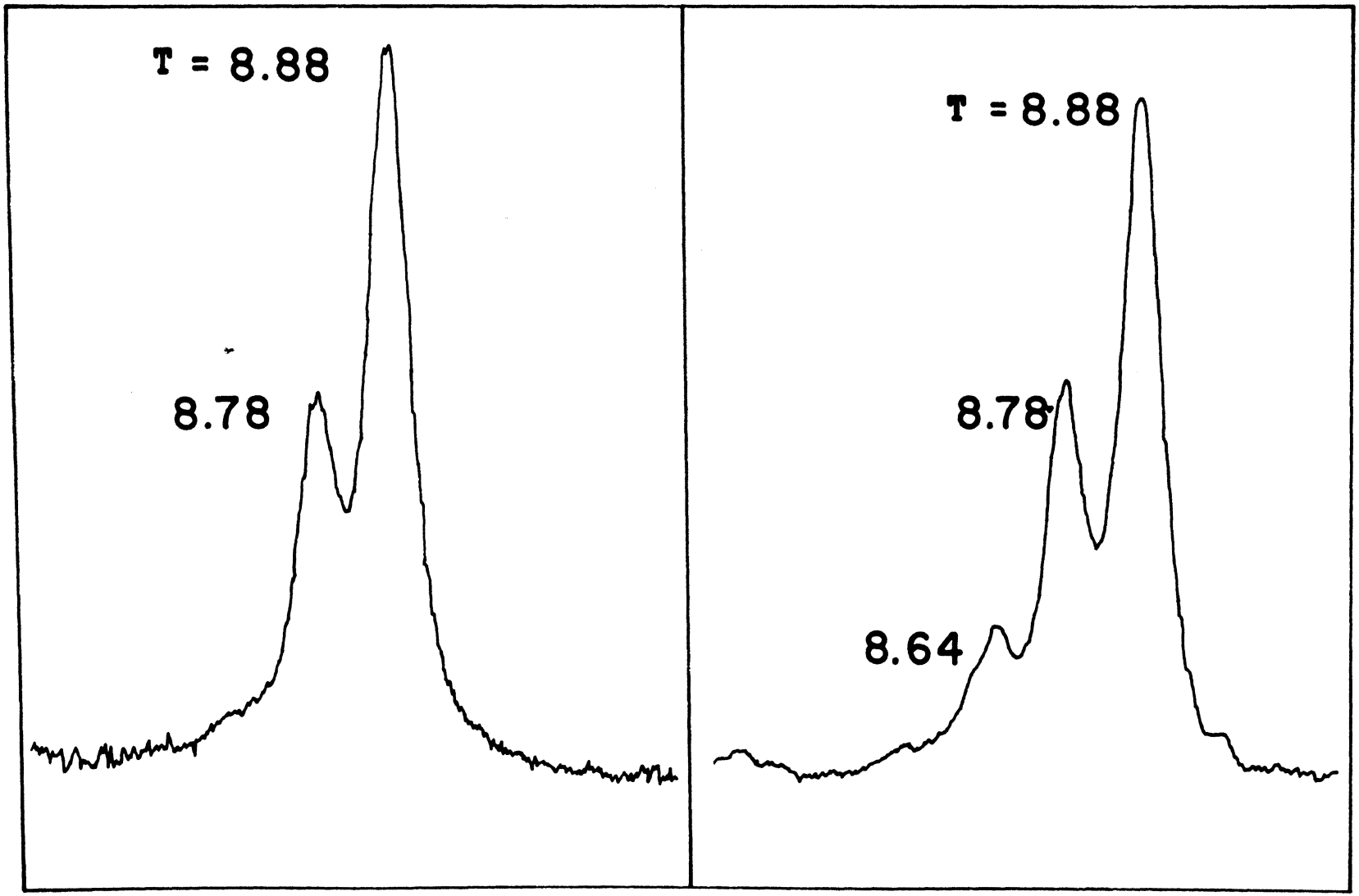

Figure 32. NMR Spectrum of Bulk and Inserted Polymer

$$P(I) + P(S) = 1 \quad (1)$$

$$P(II) + P(IS_vSI) + P(SS) = 1 \quad (2)$$

$$P(IS) = P(SI) = 1/2\, P(IS_vSI) \quad (3)$$

$$P(S) = P(SS) + P(SI) = P(SS) + P(IS) \quad (4)$$

$$P(I) = P(II) + P(SI) = P(II) + P(IS) \quad (5)$$

These relationships follow from general statistical considerations and have been shown to be valid regardless of the particular distribution and polymerization mechanism[28]. Table XX gives data and results for a series of polymers formed under different conditions at 12.9 rads per second. Spectrum 74-3B-D and the data presented in the table show that the bulk polymer is highly syndiotactic and lies in the normal range expected for a free radical polymerization. This tacticity is consistent with the interpretation of the kinetic data. Spectrum 68-5B-B is typical for the homo and inserted polymers. In all cases a change in the stereospecificity has occurred. The table shows that the isotacticity has increased in both the homopolymer and inserted polymers. While these changes are statistically significant, the polymers are still largely syndiotactic, indicating that a free radical mechanism prevails.

The changes in tacticity are relevant when the data are compared to that reported by Blumstein, et. al.[21]. They determined the tacticity of PMMA which was polymerized by adsorbing MMA on sodium montmorillonite and then exposed to X-rays. The ratio of monomer to clay was small and was assumed to constitute a monolayer. The resulting polymer was referenced as insertion polymer and was recovered for analysis by digestion with

TABLE XX

NMR DATA IN o-DICHLOROBENZENE AT 150°C [a]

System	Trial No.	P(II)	P(IS$_V$SI)	P(SS)	P(I)	P(S)
Bulk-50°C	74-3B-D	.05	.300	.650	.20±.02	.80±.02
Homopolym.-25°C	68-5B-B	.069	.336	.595	.24±.02	.76±.02
Homopolym.-50°C	74-3B-C	.112	.357	.469	.29±.02	.71±.02
Homopolym.-75°C	73-5B-D	.066	.384	.550	.26±.02	.74±.02
Inserted Polym.-25°C	68-5B-B	.142	.315	.543	.30+.02	.70±.02
Inserted Polym.-75°C	73-5B-D	.092	.315	.557	.27±.02	.73±.02

[a] Dose rate = 12.9 rads per second.

hydrofluoric acid. The tacticity of the polymers formed was largely isotactic where P(I) was about 0.59. They concluded that the mechanism which leads to the isotactic sterospecificity was confined to the surface of the mineral and that P(II) and P(SS) were not temperature dependent. The sodium montmorillonite surfaces possessed exchangeable cation sites which were distributed on the negatively charged lamellae and could associate with the MMA through the carbonyl pendant ester group. The population of exchangeable ions was sufficient to coordinate large numbers of MMA molecules by dipole-ion interactions. Monomers which were coordinated in this manner would be expected to have limited mobility. However the molecules could exhibit greater degrees of freedom depending upon the orientation of the surrounding molecules. Those monomer molecules which were associated on the lamellae surface and which were in the correct orientation could only form isotactic placements. The growing chain would then be determined by the proportions of associated to unassociated monomer units. The interaction between the lamellae surface and the non-associated monomer was assumed to be insignificant and that the monomer would behave as if polymerized in the bulk.

In the 50-50 weight ratios reported here there was always a preponderance of unassociated monomer molecules. Therefore, the fraction of monomer which could associate is small. If the above mechanism was completely valid for the present system one would expect that the homo polymer (that dissolved from the composite) would have the same tacticity as polymer formed in the bulk polymerization. The data presented in Table XX

indicates that both the homopolymer and the inserted polymer have increased isotacticity and that they are essentially of the same magnitude. The kaolin clay used in the present study has fewer (unsaturated) cations concentrated on the crystal edges than sodium montmorillonite (concentrated on the lamellae surface). This fact could account for the lower tacticity of the inserted polymer.

The above mechanism does not account for changes in tacticity of the soluble portion of the composite reported here. A verified explanation of this phenomena can not be given at this time. However, the following postulation is offered as a possibility. Realizing that the homopolymer is predominantly syndiotactic, the increase in isotacticity could be the result of a mixed free radical-ionic polymerization mechanism. The ionic portion could be the result of exchangeable counter ions from the clay which could in some manner associate the monomer to give short range II placements. These, if incorporated into the growing chain would account for the increase of isotacticity of the homopolymer.

Another possible explanation to account for the homopolymer tacticity is to consider the possibility of polymer-monomer exchange on the clay surface[42]. It is postulated that the initial monomer on the clay surface can be held by dipole-ion, hydrogen bonding or dipole-dipole interactions. A series of II placements result in an initial polymer chain having increased isotacticity. As the chain grows in length and establishes its stereo-helix, the strain exerted in sections of the chain by a particular conformation of the polymer can

overcome the surface interaction and break the growing polymer away from the surface. Another possible happening is that energy is given to the polymer chain by the radiation. If this happens, then segments of the chain could reach an excited state or absorb enough energy to break away from the clay surface. If these reactionswould occur, a mobile monomer unit could immediately diffuse to the surface and the process would be repeated until the gel point was reached. From this point the polymerization process would be diffusion controlled and no further exchange could take place. The result would be that both the homo and bulk polymer would have essentially the same tacticity.

G. Physical Appearance of Samples

1. Bulk Polymer. The bulk polymer system when irradiated retained the clear, transparent properties of common plexiglass. However, in some cases offgassing occurred in the polymer and gas bubbles were noted througout the system.

2. Composite. The composite samples showed a variation in structure in the finished product. Some samples were solid throughout, but many samples had voids or pinholes. These voids could be caused by a number of things such as improper filling of sample container or offgassing of the polymer. The offgassing is prevalent in this irradiation polymerization because when the bulk polymer and composite were heated to 200^{o}C, small bubbles appeared which were indicative of offgassing.

Figure 33 shows an example of an air void which was found in almost

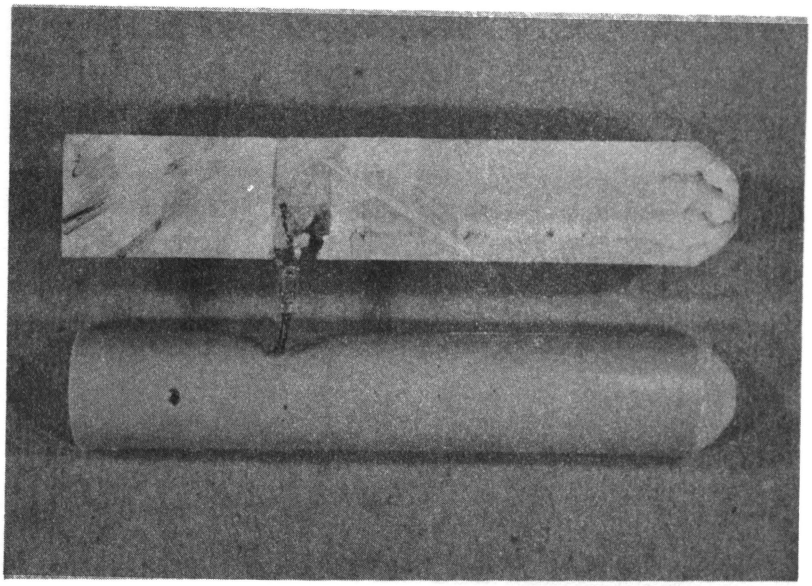

Figure 33. Inserted Thermocouple in Composite Sample

all composite studies around the inserted thermocouple. These voids could have been created when the composite was hand packed into the sample container. It was noticed that most times the voids were found beneath the thermocouple. The thermocouple thus served as an obstruction to the mixture. The bulk samples all had the thermocouples firmly implanted with no air voids around it. The effect of the filling due to the higher viscosity of the composite is believed to be the main reason for the gross void formation around the thermocouple. During the polymerization reaction, all samples contracted from the wall of the sample container. This contraction of sample could also occur at the thermocouple in itself and thus cause the voids.

H. Mechanical Properties

A comparison was made of the bulk polymer and composite at various reaction temperatures at a dose rate of 12.9 rads per second. The total doses obtained were approximately 100,000 (25^{o}C), 70,000 (50^{o}C) and 60,000 (75^{o}C) past the system endpoints. The doses were reduced as the temperature increased because of depolymerization effects on the samples, however the dosage was necessary to insure that the samples were polymerized fully. No unreacted monomer was evident in any of the systems. These doses are not to be construed as optimum doses and were just used to see if gross differences exist in the mechanical properties of the polymers.

Results of the compression tests are shown in Table XXI along with composite compressive strengths for other polymer system. The following

TABLE XXI

COMPRESSIVE STRENGTH DATA

Polymer	Compressive Strength ($Psi \times 10^{-3}$)	Sample Size
Bulk-Irradiated	16.4 ± 0.6	10
50-50 Composite-Irradiated	18.3 ± 0.4	22
50-50 Composite-Chemical	17.3 ± 0.5 [40]	11
Bulk-Chemical [43]	11-16	
Epoxy-various fillers	15-25	
Furane-asbestos filler	10-13	
Melamine-Formaldehyde-cellulose filler	25-45	
Phenol-Formaldehyde-glass fiber	17-70	
Phenolic-mineral filler	29-34	
Polyester-chopped glass	15-30	
Silicones-glass fiber	10-15	
Urea-Formaldehyde cellulose filler	25-45	

comments can be made.

1. The compressive strengths of all samples polymerized at 25, 50 and 75°C were the same, within experimental error.

2. Within the time limits of these experiments the compressive strengths were the same for different total doses beyond the endpoint.

The results reported in the above table represent average values of samples prepared under different conditions of temperature and total dose. The addition of the clay to the polymer system did not result in a decrease in compressive strength. A small increase in strength was actually noted. In most polymer systems, the addition of anything except fibrous fillers results in a decrease of mechanical properties. Therefore, the addition of the clay had a beneficial effect on this system and that further improvements could possibly be obtained through the use of fibrous materials, particularly the addition of kaolin fibers.

I. Scanning Electron Microscope Studies (SEM)

Throughout this study composite samples were examined by SEM. It was concluded that SEM did not reveal any major differences in any of the samples regardless of the dose rate, total dose or temperature employed. Several general features were noted and are described in the following paragraphs.

Figure 34 shows a typical composite fracture surface. These micrographs revealed numerous bulk agglomerates (20-100 μ) surrounded by a more uniform matrix. Higher magnification micrographs showed that

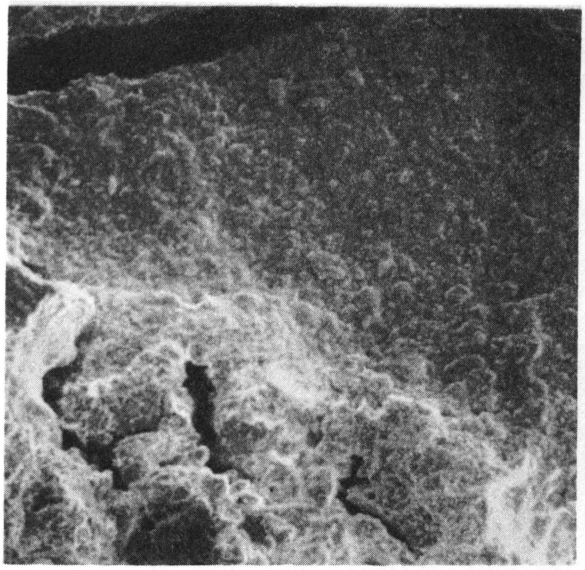

100x

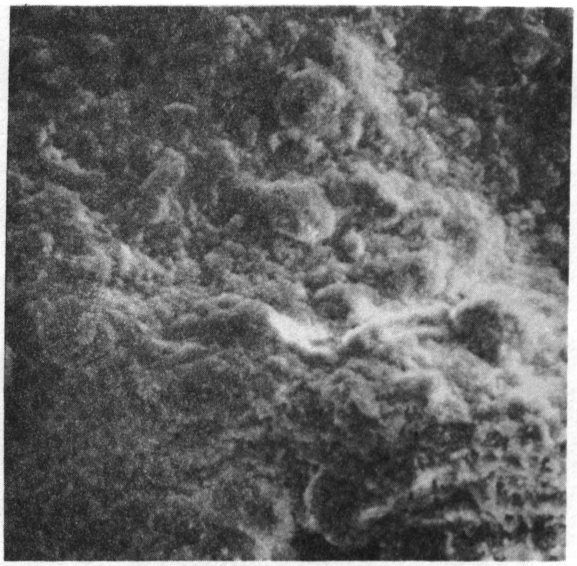

300x

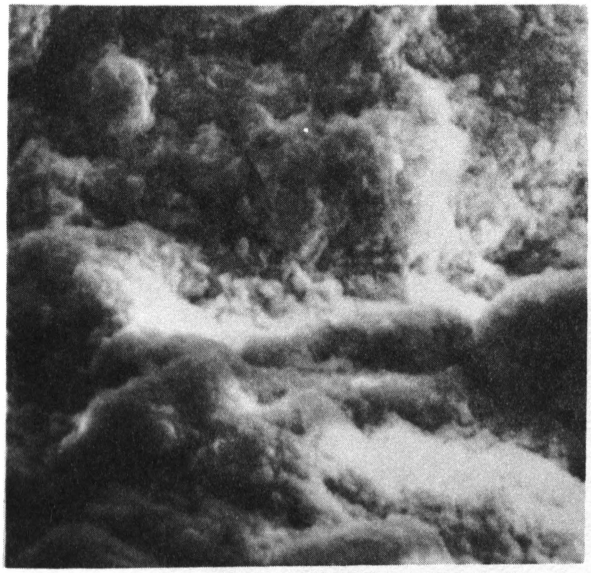

1000x

3000x

1μ = 0.04 inches for 1000x

1μ = 0.133 inches for 3000x

Figure 34. Micrograph of Total Composite

the large agglomerates were made up of smaller agglomerates (2-6 μ). A sufficient number of micrographs were recorded to conclude that the clay agglomerates were wetted. A number of different mixing procedures were tested (including high shear blending, high frequency mechanical vibrating and ultrasonic waves) in an attempt to better disperse the clay. None of the approaches were successful. The size of the individual clay particles were beyond the resolution limits of the SEM. It was therefore concluded that the particle size analysis reported reflects only the dimensions of the clay agglomerates in air.

Figures 35 and 36 are representative of the inserted polymer-clay surfaces after the homopolymer had been dissolved. These micrographs show a surface composed of agglomerates ($\geq$20 μ) which have been smoothed through the dissolution process. No surface detail is evident since the entire surface is covered with a thin layer of polymer which has been smoothed by the solvent extraction process.

Figure 37 shows the inserted clay-polymer surface after digestion with hydrofluoric acid. The residue remaining shows the clay agglomerates in more detail. The smooth portions of the surface are bits of polymer-clay which were apparently uneffected by the acid treatment.

In general, the SEM showed that the PMMA-kaolin clay composites were more uniform in structure than other types of polymer based composites which have been investigated in this and other laboratories[44].

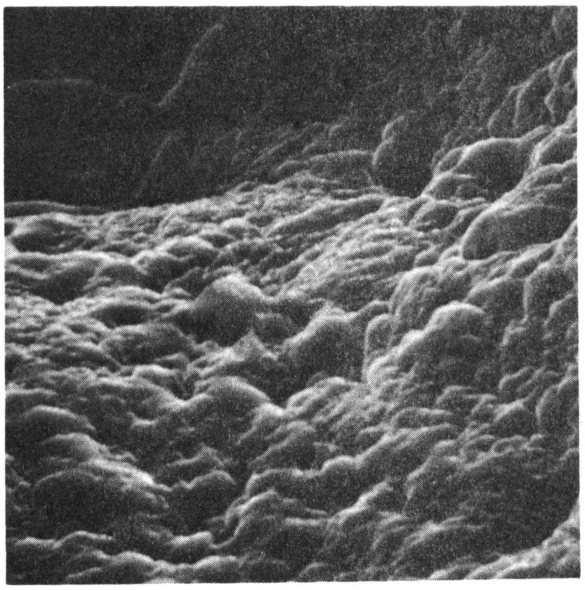

300x

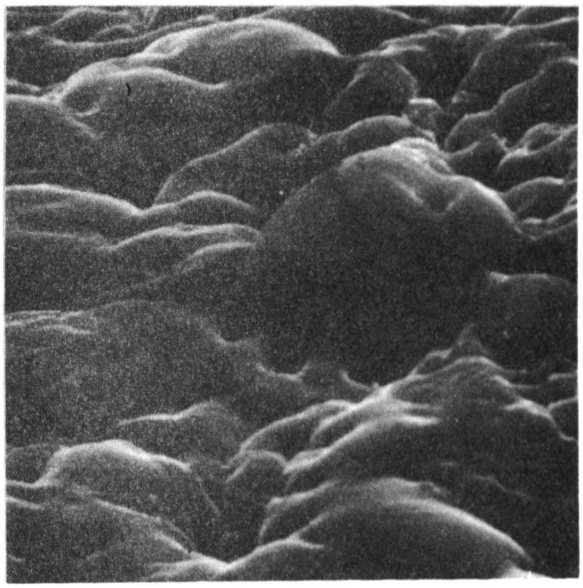

1000x

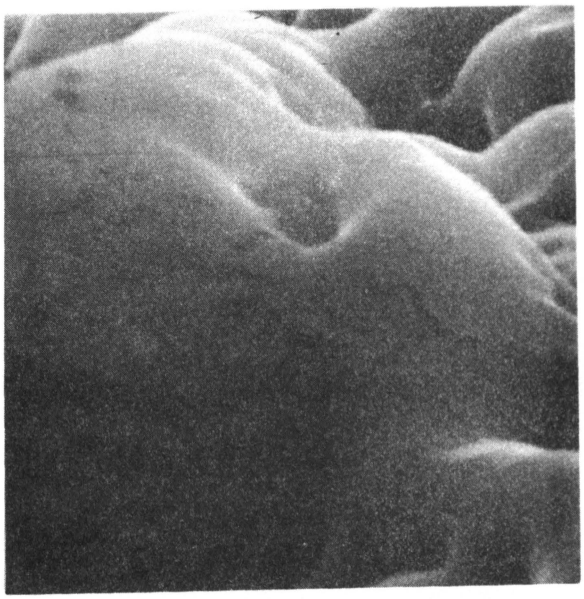

3000x

1μ = 0.04 inches for 1000x

1μ = 0.133 inches for 3000x

Figure 35. Micrograph of Insoluble Composite

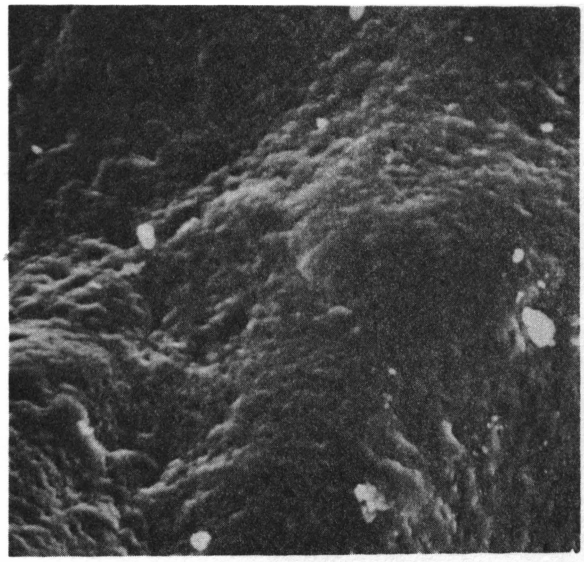

100x

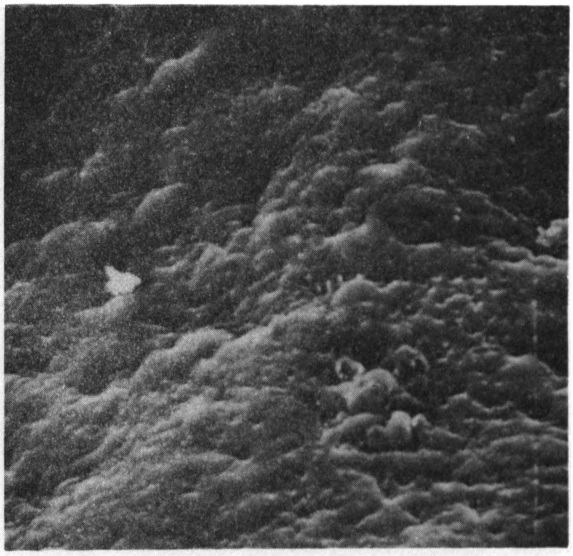

300x

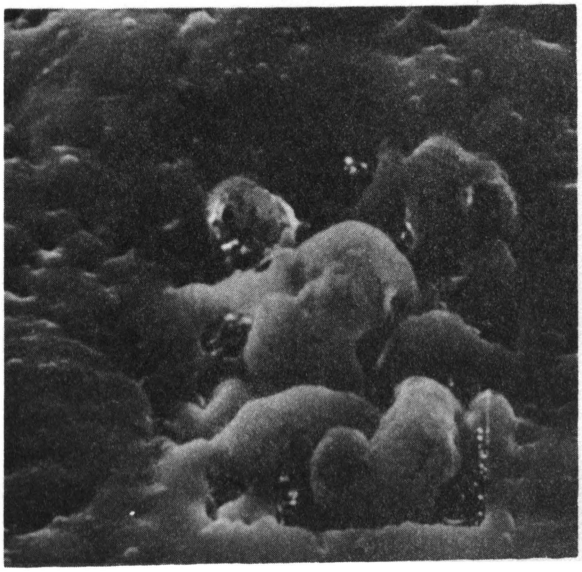

1000x

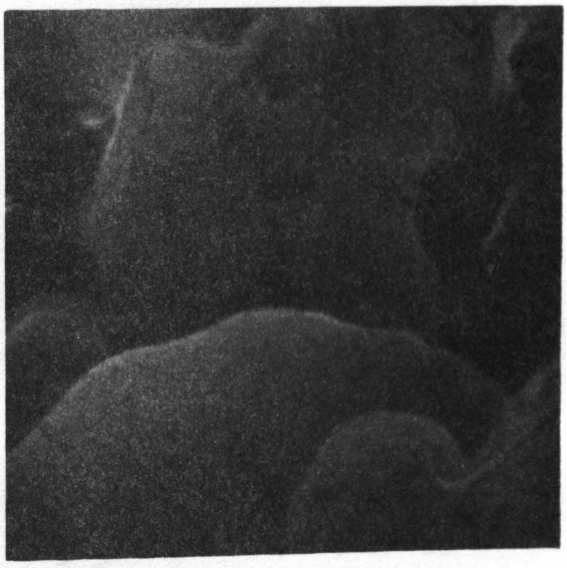

3000x

1μ = 0.04 inches for 1000x

1μ = 0.133 inches for 3000x

Figure 36. Micrograph of Insoluble Composite

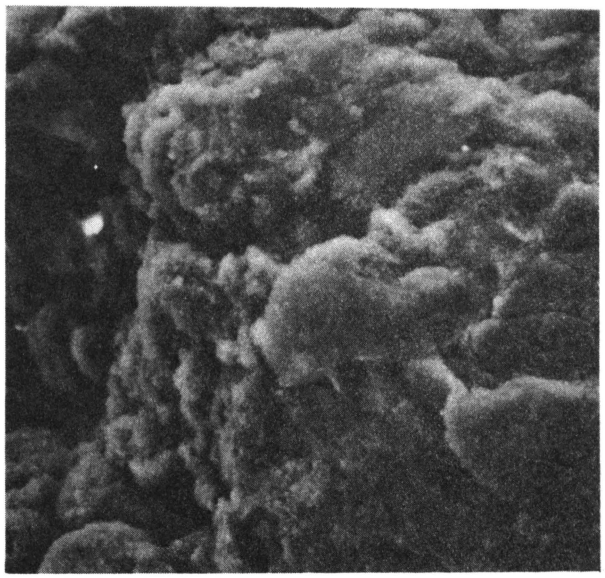

300x

1000x

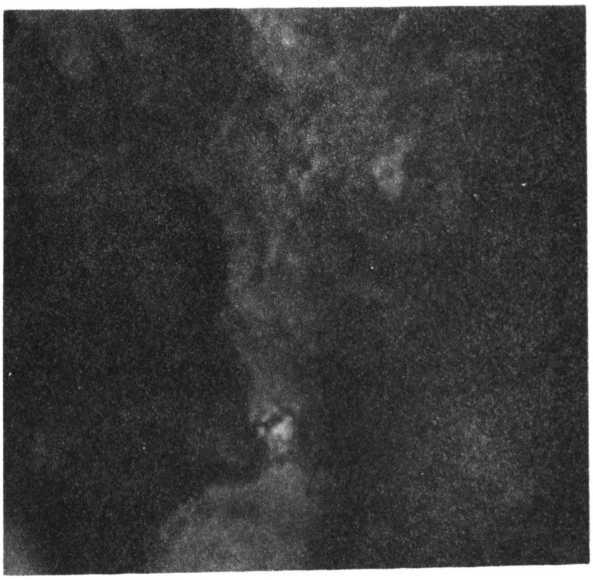

3000x

1μ = 0.04 inches for 1000x

1μ = 0.133 inches for 3000x

Figure 37. Micrograph of HF Treated Composite

V. CONCLUSIONS

As a result of this study, the following conclusions were made:

1. At the same dose rate, the kaolin clay had a catalytic effect on the polymerization process at 25°C as compared to the bulk polymerization. This effect decreased as temperature increased.

2. Polymerization of the composite at the same dose rate in air or in an inert gas showed no differences in the total dose necessary to reach the endpoint.

3. The polymerization of the composite was less affected by the presence of inhibitors than the bulk polymerization.

4. Two types of polymer were produced in the composite. One type (homopolymer), could be extracted by common organic solvents; the other type (inserted) could only be extracted by destroying the clay structure through hydrofluoric acid treatment.

5. At the endpoint the percentage conversion of homopolymer was always larger than that of the inserted polymer for the experimental conditions employed.

6. At the endpoint as temperature increased and at the same dose rate, the percentage conversion of homopolymer increased, but the percentage conversion of inserted polymer decreased.

7. A kinetic analysis showed that the apparent activation energy for polymerization in the composite was less than that for the bulk polymerization.

8. There were no apparent structural changes in the clay after irradiation. SEM micrographs showed that the clay did not exist as individual particles, either in the natural state or in the composite. The clay was actually composed of agglomerates of smaller particles.

9. No differences in the homo or inserted polymers were found by infrared analysis.

10. DTA-TGA measurements (in air) showed the decomposition of the irradiated polymer to be 30^{o}C higher than was found for chemically initiated bulk polymer.

11. Abnormally high molecular weights were determined for the irradiated polymer. For the same dose rate, the $\overline{M}_v$ of both the composite and bulk polymers increased as temperature increased. No differences were found in the $\overline{M}_v$'s of the composite polymers formed in either air or inert gas at the same temperature and dose rate. Large increases in molecular weight did not occur until after the endpoint was reached. Molecular weights of the polymers increased after the irradiation source was removed.

12. High molecular weight polymer was formed in the composite in the absence of radiation over much longer time intervals.

13. GPC analysis showed that the peak molecular weight of homo and inserted polymer was the same. These analyses also confirmed the viscosity measurement trends as a function of dose rate, total dose and temperature.

14. NMR studies showed that both the homo and inserted polymers were more isotactic than the bulk polymer.

15. The addition of the clay did not decrease the compressive strength of the polymer system, but actually increased it to a small extent.

VI. ADDITIONAL WORK

The results of this project indicate that additional work is necessary for a more complete understanding of the MMA-kaolin clay polymerization process. The following areas are suggested for investigation:

1. The nature of the clay surface requires characterization in order to identify the number and type of active sites which participate in the polymerization reaction.

2. A mechanistic study should be conducted in conjunction with (1) to determine why the tacticity of the homo and inserted polymer are the same.

3. A detailed kinetic study should be made at higher dose rates in view of the larger radiation sources available in industry.

4. The effects of pressure on reducing the number and sizes of voids in the composite should prove useful. Preliminary work with chemically initiated systems under pressure have shown this to be a feasible approach.

5. The effects of adding kaolin fibers to the composite to improve the mechanical properties.

6. A series of tests should be carried out to determine the effect of stopping the radiation before or at the endpoint and allow the remaining monomer to polymerize without the degrading effects of radiation on the high molecular weight polymers.

7. A copolymer-kaolin clay study should be undertaken to determine if composites can be produced which will yield specific properties based upon monomer structure.

VII. ENGINEERING APPLICATIONS

Some of the possible general applications and uses that the composite could have are:

1. A possible substitute for thermosetting materials which are currently being used for fabrication and reinforcement applications. This could be possible because:

a. The preliminary studies show that the mechanical properties are in the same range.

b. Costs are less

c. Less handling problems

d. Exotherms during the polymerization process are substantially lower than either chemically initiated MMA or crosslinked systems requiring an activator.

e. Fibrous fillers can be added to increase mechanical properties to compete with large scale commercial composites.

2. The composite properties can be changed for specific purposes. Some of these are:

a. Flame retardency - work with chemically initiated systems showed that the flame retardency can be incorporated by means of halogenated

materials. The amount of flame retardency can also be varied.

b. Color - the system will accept dyes and pigments.

c. Fungicides and antioxidants can be incorporated into the system.

d. Ultraviolet absorbers can be incorporated to slow the degradation of the polymer.

3. Stock made of the composite can be:

a. Machined, milled and sharpened with tolerances being held.

b. Made with superior impact strength.

The above comments have been generalized. In order to utilize the composite for a specific application, some applied research must be done which should encompass the following:

1. Mold design.

2. Radiation source, dose rate, total dose and temperature.

3. Concentration of monomer in the clay.

4. Type of blending, handling, distilling and drying equipment necessary to prepare the mixtures.

5. Determine if the process should be batch or continuous.

6. Should the process be stopped before the endpoint and allowed to proceed in the absence of radiation. The depolymerization effect is thus decreased.

7. Safety precautions for all stages of processing.

8. Economic evaluation of the process.

VITA

James Jackson Beeson was born on May 18, 1945, in Bloomsburg, Pennsylvania. He received his primary education in St. Charles, Missouri and Berwick, Pennsylvania. The author's secondary education was received in Berwick, Pennsylvania. He has recieved his college education from the University of Missouri-Rolla, Rolla, Missouri. He received a Bachelor of Science in Chemical Engineering from the University of Missouri-Rolla, Rolla, Missouri in June 1967. He also received his Master of Science in Chemical Engineering from the University of Missouri-Rolla, Rolla, Missouri in May 1969.

He has been enrolled in the Graduate School of the University of Missouri-Rolla, Rolla, Missouri since September 1967. He has held in the Department of Chemical Engineering the Sinclair Research Fellowship from September 1967 to June 1968 and a Graduate Teaching Assistantship from September 1968 to June 1969. From September 1969 to June 1970 the author held an Atomic Energy Research Fellowship. He has held a Graduate Research Assistantship from the Graduate Center for Materials Research from September 1970 to the present.

APPENDIX A

Dosimetry

This appendix shows the calculation of the malor absorptivity, and mass energy absorption coefficients for all dosimetry.

1. Molar absorptivity calculation. The molar absorptivity was calculated using three different molar concentrations of ferric sulfate dissolved in 100 milliliter Erlynmeyer flasks using 0.8 N H_2SO_4. The absorbance as measured at 304 mμ (using a 1 centimeter pathlength) was plotted as a function of ferric ion concentration and the molar absorptivity determined from the slope of the resulting line by the method of least squares. The data used and absorptivity obtained are shown in Table XXII.

TABLE XXII

DETERMINATION OF MOLAR ABSORPTIVITY

Amount $Fe_2(SO_4)_3$ gms.	Molarity (moles/liter)	Absorbance
.0295	.00061	1.343
.0113	.00023	.511
.0049	.00010	.223

Absorptivity = 2198 + 3

2. Mass energy absorption coefficients. Mass energy absorption coefficients were determined at 1.17 and 1.33 MeV. The mean of these coefficients was taken to determine the average mass energy absorption coefficient of each element. Each total coefficient was determined by summing the elemental coefficients as seen in the following equation[45]:

$$\left(\frac{\mu_{en}}{\rho}\right) = \Sigma F_p \left(\frac{\mu_{en}}{\rho}\right)_{E_p}$$

where: F_p = Fractional weight of element in sample

$\left(\frac{\mu_{en}}{\rho}\right)_{E_p}$ = Mass energy coefficient of element p (cm^2/gram) used in the calculations.

The elemental coefficients used in the dosimetry calculations are shown in Table XXIII with the resulting coefficients shown in Table II.

TABLE XXIII

ELEMENTAL MASS ENERGY ABSORPTION COEFFICIENTS

Element	μ/ρ_{en} (1.17 MeV) ($cm.^2$/gm.)	μ/ρ_{en} (1.33 MeV) ($cm.^2$/gm.)	Average μ/ρ_{en} ($cm.^2$/gm)
C	.0263	.0271	.0267
H	.0523	.0539	.0531
O	.0262	.0270	.0266
Al	.0253	.0261	.0257
Si	.0261	.0269	.0265
0.8 N H_2SO_4	.0290	.0299	.0294

APPENDIX B

Calculation and Results of the Percentage Conversion of Bulk, Homo, Inserted and Total Polymer

1. Bulk polymer. The percentage conversion of bulk polymer was calculated making the assumption that the weight of monomer originally present in the composite equals the weight of polymer (polym) plus monomer (mon) after irradiation. Calculations were made according to the following equation:

$$\% \text{ Conversion}_{\text{Bulk}} = \frac{\text{wt polym (100)}}{\text{wt}_{\text{mon orig}}}$$

2. Homopolymer. In determining the percentage conversion of homopolymer, the same basic assumption was made that the weight of polymer plus monomer in the composite after the desired time of irradiation equaled the initial weight of monomer in the system. The initial weight of monomer was then equal to one-half the total composite (tot comp) weight. The percentage conversion of homopolymer was then found by the following equation:

$$\% \text{ Comversion}_{\text{Homopolymer}} = \frac{\text{wt polym (100)}}{(0.5)\,(\text{wt}_{\text{tot comp}})}$$

3. Inserted polymer. The percentage conversion of the inserted polymer was obtained by calcination at 1000^{o}C of the remaining insoluble composite after removing the homopolymer. One problem which occurred

was that the clay also lost weight during the firing due to the loss of structural hydroxyl groups between 475 and 500°C. The weight loss from the dried clay (300°C) was found by calcinating four different weights of clays to 1000°C and determining the weight loss. From a plot of the weight loss of clay as a function of the original weight of clay, the ratio of weight loss of clay per gram of original material was obtained from the slope. This ratio (k) will be used in the material balance for the inserted polymer. The results of this procedure are shown in Table XXIV.

TABLE XXIV

WEIGHT LOSS OF CLAY AS A FUNCTION OF STARTING MATERIAL

Weight clay original (gms.)	Weight loss of clay (gms.)	k $\frac{\text{wt. clay lost}}{\text{wt. clay orig.}}$
1.9858 ± 0.0002	.2623	.1321
1.0528 ± 0.0002	.1393	.1323
.4824 ± 0.0002	.0637	.1321
.2220 ± 0.0002	.0293	.1320

$k_{avg.} = .1321$

The following assumptions were made in determining the percentage conversion of inserted polymer ($polym_{ins}$):

1. $wt\ polym_{ins}\ orig = wt\ polym_{ins}\ lost$

2. $wt\ comp_{ins}\ orig = wt\ clay\ orig + wt\ polym_{ins}\ orig$

3. $wt\ comp_{ins}\ lost = wt\ clay_{OH}\ lost + wt\ polym_{ins}\ lost$

4. $\dfrac{wt\ comp_{ins}\ lost}{wt\ comp_{ins}\ orig} = Z$

The calculations were obtained as follows:

By placing (4) into (3)

$$(Z)\,(wt\ comp_{ins}\ orig) = wt\ clay_{OH}\ lost + wt\ polym_{ins}\ lost$$

By clay calculation and (1)

$$Z\,(wt\ comp_{ins}\ orig) = k\,(wt\ clay\ orig) + wt\ polym_{ins}\ orig$$

By substitution for $wt\ comp_{ins}\ orig$ from (2) and rearranging

$$\frac{wt\ polym_{ins}\ orig}{wt\ clay\ orig} = \frac{(Z-k)}{(1-Z)}$$

The above material balance was applied to an aliquot of the total composite sample. Therefore the percentage conversion is

$$\%\ Conversion = \left(\frac{wt\ polym_{ins}\ orig}{wt\ clay\ orig}\right)_{\substack{ins\\comp}} \left(\frac{wt\ clay}{wt\ mon}\right)_{\substack{orig\\comp}} \qquad (100)$$

However $\left(\dfrac{wt\ clay}{wt\ mon}\right)_{\substack{orig\\comp}} = 1$ for a 50 - 50 composite

Therefore the final equation is:

$$\% \text{ Conversion} = \left(\frac{\text{wt polym orig}}{\text{wt clay orig}}\right)_{\substack{\text{ins} \\ \text{comp}}} (100)$$

TABLE XXV

CONVERSION STUDIES OF COMPOSITE POLYMER IN AIR AND INERT GAS AT 25°C

	Approximate Endpoint						
	1/3	1/2	2/3	7/8	1	1+	1++
	50-50 COMPOSITE-AIR @ 25°C @ 24.9 RADS/SEC.						
Dose (rads x 10^{-3})	156	234	304	392	457	500	534
Homopolymer (% conversion)	6.3	9.5	14.4	22.7	55.9	61.9	63.1
Inserted polymer (% conversion)	3.4	4.3	5.3	8.5	22.4	21.0	22.6
Total polymer (% conversion)	9.7	13.8	19.7	31.2	78.3	82.9	85.7
	50-50 COMPOSITE-AIR @ 25°C @ 12.9 RADS/SEC.						
Dose (rads x 10^{-3})	100	156	205	268	313	335	340
Homopolymer (% conversion)	4.9	8.9	12.2	20.1	45.7	54.3	56.2
Inserted polymer (% conversion	2.9	4.0	4.8	7.6	21.6	24.7	24.2
Total polymer (% conversion)	7.8	12.9	17.1	27.7	67.3	79.0	80.4
	50-50 COMPOSITE-AIR @ 25°C @ 7.35 RADS/SEC.						
Dose (rads x 10^{-3})	67	105	144	188	225	243	248
Homopolymer (% conversion)	4.4	7.6	11.0	17.4	46.8	52.0	53.1
Inserted polymer (% conversion)	2.8	4.2	5.2	7.2	25.8	23.8	23.6
Total polymer (% conversion)	7.2	11.8	16.2	24.6	72.6	75.8	76.7
	50-50 COMPOSITE-INERT GAS @ 25°C @ 12.9 RADS/SEC.						
Dose (rads x 10^{-3})	103	160	211	275	311	332	337
Homopolymer (% conversion)	6.4	10.0	14.0	21.3	52.5	58.1	60.2
Inserted polymer (% conversion)	3.4	4.1	5.3	8.9	21.6	20.8	20.3
Total polymer (% conversion)	9.8	14.1	19.3	30.2	74.1	78.9	80.5

TABLE XXVI

CONVERSION STUDIES OF COMPOSITE POLYMER IN AIR AND INERT GAS AT 50°C

	Approximate Endpoint						
	1/3	1/2	2/3	7/8	1	1+	1++
	50-50 COMPOSITE-AIR @ 50°C @ 24.9 RADS/SEC.						
Dose (rads x 10^{-3})	101	149	177	223	264	341	1043
Homopolymer (% conversion)	7.1	12.1	16.1	25.0	60.3	75.5	88.7
Inserted polymer (% conversion)	3.3	4.5	5.5	7.7	15.2	14.7	9.6
Total polymer (% conversion)	10.4	16.6	21.6	32.7	75.5	90.2	98.3
	50-50 COMPOSITE-AIR @ 50°C @ 12.9 RADS/SEC.						
Dose (rads x 10^{-3})	47	78	115	155	183	236	511
Homopolymer (% conversion)	4.0	7.6	11.9	23.9	58.8	70.3	79.6
Inserted polymer (% conversion)	3.0	3.9	5.3	8.5	15.9	17.4	13.2
Total polymer (% conversion)	7.0	11.5	17.2	32.4	74.7	87.7	92.8
	50-50 COMPOSITE-AIR @ 50°C @ 7.35 RADS/SEC.						
Dose (rads x 10^{-3})	43	67	89	122	140	156	
Homopolymer (% conversion)	4.8	8.6	13.1	27.4	55.0	69.3	
Inserted polymer (% conversion)	3.1	3.8	5.0	9.5	15.9	17.0	
Total polymer (% conversion)	7.8	12.4	18.1	36.9	70.9	86.3	
	50-50 COMPOSITE-INERT GAS @ 50°C @ 12.9 RADS/SEC.						
Dose (rads x 10^{-3})	48	78	115	147	180		
Homopolymer (% conversion)	4.8	8.7	13.8	22.8	61.1		
Inserted polymer (% conversion)	3.2	3.9	5.3	7.4	16.6		
Total polymer (% conversion)	8.0	12.6	19.1	30.2	77.7		

TABLE XXVII

CONVERSION STUDIES OF COMPOSITE POLYMER IN AIR AND INERT GAS AT 75°C

	Approximate Endpoint						
	1/3	1/2	2/3	7/8	1	1+	1++
	50-50 COMPOSITE-AIR @ 75°C @ 24.9 RADS/SEC.						
Dose (rads x 10^{-3})	27	55	85	119			
Homopolymer (% conversion)	2.7	7.0	11.6	18.7			
Inserted polymer (% conversion)	2.6	3.6	4.4	5.9			
Total polymer (% conversion	5.3	10.6	16.0	24.6			
	50-50 COMPOSITE-AIR @ 75°C @ 12.9 RADS/SEC.						
Dose (rads x 10^{-3})	42	64	81	104	120	164	
Homopolymer (% conversion	7.6	13.2	20.6	40.4	69.6	76.7	
Inserted polymer (% conversion)	4.9	5.7	7.5	12.6	18.7	18.8	
Total polymer (% conversion)	12.5	18.9	28.1	53.0	88.3	95.5	
	50-50 COMPOSITE-AIR @ 75°C @ 7.35 RADS/SEC.						
Dose (rads x 10^{-3})	31	46	60	79	90	179	368
Homopolymer (% conversion)	7.2	11.5	18.5	33.9	67.0	83.1	88.4
Inserted polymer (% conversion)	3.4	4.9	6.8	11.0	15.6	16.9	10.9
Total polymer (% conversion)	10.6	16.4	25.3	44.9	82.6	100.0	99.3
	50-50 COMPOSITE-INERT GAS @ 75°C @ 12.9 RADS/SEC.						
Dose (rads x 10^{-3})	36	54	72	95	124		
Homopolymer (% conversion)	5.9	10.5	14.3	26.0	65.0		
Inserted polymer (% conversion)	3.4	4.1	5.3	7.5	16.6		
Total polymer (% conversion)	9.3	14.6	19.6	33.5	81.6		

TABLE XXVIII

CONVERSION STUDIES OF BULK POLYMER AT VARIOUS TEMPERATURES

	Approximate Endpoint					
	1/3	1/2	2/3	7/8	1	1+
	BULK POLYMER-AIR @ 25°C @ 12.9 RADS/SEC.					
Dose (rads x 10^{-3})	137	206	285	357		520
Polymer (% conversion)	6.2	8.1	16.7	23.4		86.2
	BULK POLYMER-AIR @ 50°C @ 12.9 RADS/SEC.					
Dose (rads x 10^{-3})	87	133	155	177	210	274
Polymer (% conversion)	10.3	18.2	22.7	31.0	71.8	96.0
	BULK POLYMER-AIR @ 75°C @ 12.9 RADS/SEC.					
Dose (rads x 10^{-3})	42	63	80	104	130	170
Polymer (% conversion)	9.1	14.0	19.8	34.5	87.3	100

TABLE XXIX

CONVERSION STUDIES OF COMPOSITE POLYMER AT ROOM TEMPERATURE WITHOUT IRRADIATION

Time (hours)	0	24	120	168	672
Homopolymer (% conversion)	0.0	0.0	2.4	6.5	52.2
Inserted Polymer (% conversion)	0.0	1.3	3.0	6.0	24.0
Total Polymer (% conversion)	0.0	1.3	5.4	12.5	76.2

APPENDIX C

Gel Permeation Chromatography

This separation method involves column chromatography in which the stationary phase is a heteroporous, solvent swollen, polymer network, varying in permeability over many orders of magnitude.

A deaerated solvent stream is divided; a polymer sample is added to one-half the solvent stream. This stream flows into a sample column packed with styagel, a rigid crosslinked poly-(styrene) gel. The sample solution contains both high and low molecular weight materials. As the polymer moves down the column the smaller molecules diffuse more rapidly into the gel pores. Larger molecules are excluded to more pores and thus follow a shorter path. Therefore, the larger molecules are eluted first and the smaller ones follow. The time required for a molecule to elute through a column is related to the size or molecular weight of the molecule.

The polymer is detected by a differential refractometer, an instrument capable of detecting changes in the refractive index of a solution of one part of polymer in 10,000 of solvent. A typical GPC chromatogram is shown in Figure 27.

APPENDIX D

Intrinsic Viscosity and Molecular Weight Determinations

All intrinsic viscosity data was calculated using the equations of Huggins[46]:

$$\eta_{sp}/c = [\eta] + k' [\eta]^2 c$$

and Kraemer[47]:

$$\ln \eta_r /c = [\eta] - k'' [\eta]^2 c$$

where:

η_{sp}/c = reduced viscosity = $(t-t_o)/t_o$

η_r = relative viscosity = t/t_o

c = concentration of solution (gms. per dl.)

$[\eta]$ = intrinsic viscosity (dl. per gms)

k', k'' = constants

t, t_o = Efflux times in viscometer of polymer solution and solvent respectively.

A plot of the reduced or inherent viscosity as a function of concentration (c) will obtain a plot as shown in Figure 38. The intrinsic viscosity is defined as that point where the reduced and inherent viscosity approach zero. Therefore by finding the reduced and inherent viscosities at different concentrations of polymer and extrapolating to zero concentration, the intrinsic viscosity may be found.

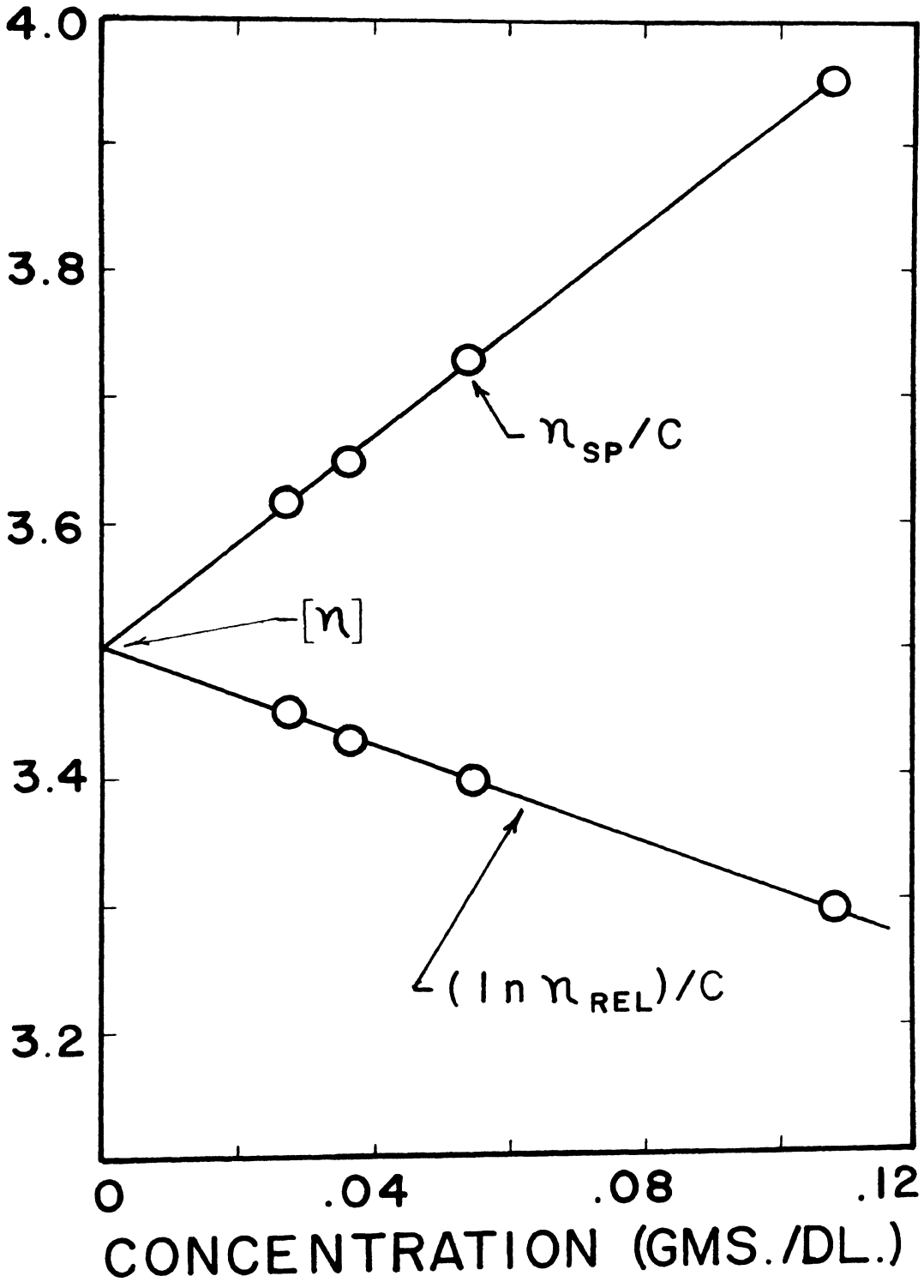

Figure 38. Intrinsic Viscosity Curve

BIBLIOGRAPHY

1. Chapiro. A. Radiation Chemistry of Polymeric Systems. New York: Interscience Publishers, Vol. XV (High Polymers), 1962, 121-123.

2. Worrall, R. and Charlesby, A., "Effect of Additives on the Radiation Induced Polymerization of Isobutene," Int. J. Appl. Rad. and Isotopes, 4, 84-88 (1958).

3. Charlesby, A., Pinner, S. H. and Worrall, R., "Analysis of Radiation-Induced Ionic Polymerization of Isobutene," Proc. Roy. Soc. (London), A259, 386-402 (1960).

4. Dalton, F. L., Glawitsch, G. and Roberts, R., "The Effect of ZnO on the Radiation-Initiated Polymerization of Isobutene at -78°C," Polymer, 2, 419-428 (1961).

5. Mezhirova, L. P., Sheinker, A. P. and Abkin, A. D.,"Influence of Semiconductor Additives on the Radiation Polymerization of Acrylonitrile and Methylmethacrylate," Doklad. Akad. Nauk. SSSR, 153 (6), 1378-1380 (1963).

6. Worrall, R. and Pinner, S. H., "Heterophas Radiation Polymerization of Isobutene and Methyl Methacrylate," J. Polym. Sci., 34, 229-242 Nottingham Symp. (1959).

7. Charlesby, A. and Morris, J., "Enhanced Ionic Polymerization of Styrene Induced by Radiation," Proc. Roy. Soc. (London), A273, 387-399 (1963).

8. Charlesby. A. and Morris, J., "Radiation-Induced Ionic Polymerization of Styrene: Effect of Additives," J. Polym. Sci., Part C, 4, 1127-1133 (1963).

9. Kristal'nyi, E. V. and Medvedev, S. S., "Polymerization of Isobutylene by Gamma-Radiation in the Presence of Solid Substances," Vysokomol. Soyed., 7 (8), 1377-1382 (1965).

10. Kornienko, T. P. Polishchuk, U. N. Zelenchukova, T. G., and Polyakov, M. V., "Investigation of the Influence of Mineral Additives on the Radiation Polymerization of Vinyl Monomers," Radiation Chemical Materials Symposium of Polymers Moscow 1964, 69-74 (Pub. 1966).

11. Uskov, I. A., Tertykh, L. I., Solomko, V. P. and Polischuk, U. N., "Radiation Polymerization MMA and Styrene in the Presence of Mineral Fillers," Vysokomol. Soed., 8 (1), 26-30 (1966) Polym. Sci. USSR, 8, 24 (1966).

12. Tsetlin, B. L. Rafikov, S. R., Plotnikova, L. I. and Glazunov, P. Ya., "Radiation Grafting of Polymers Chains onto the Surface of Inorganic Particles," Proceedings of the All-Union Conference on Radiation Chemistry. Second Moscow, Oct. 10-14, 1960, 529-523 (Pub. 1964).

13. Nahin, P. G., "Organoclays Bonded to Polyethylene by Ionizing Radiation," (Union Oil Co. of Cal., Brea, Cal.).

14. Morozov, Yu. L., Plotnikova, L. I. Rafikov, S. R. and Tsetlin, B. L., "Study of the Kinetics of Radiation Graft Polymerization from the Vapour Phase on Mineral Powders," Vysokomol. Soed., A9 (8), 1627-1634 (1967).

15. Yuan, H. C., Hsu, W. W., Wang, V. P., Wu, C. C., Shieh, J. S., Chang, M. L., "Gamma-Ray Induced Polymerization of Unsaturated Polyester in Red Mud," Symp. Utilization Large Radiation Sources and Accelerators in Ind. Proc. - Munich, 18-22 (August 1969).

16. Kornienko, T. P. and Zelenchukova, T. G., "On the Mechanism of Radiation Polymerization of Vinyl Monomers in the Presence of Mineral Additives," Theoretical Experiments in Chemistry, 6 (4), 553-556 (1970).

17. Blumstein, A., "Polymerization of Adsorbed Monolayers. I. Preparation of the Clay-Polymer Complex," J. Polym. Sci., Part A, 3, 2653-2664 (1965).

18. Blumstein, A., "Polymerization of Adsorbed Monolayers. II. Thermal Degradation of the Inserted Polymer," J. Polym. Sci., Part A, 3, 2665-2672 (1965).

19. Blumstein, A. and Billmeyer, F. W. Jr., "Polymerization of Adsorbed Monolayers. III. Preliminary Structure Studies in Dilute Solution of the Insertion Polymers," J. Polym. Sci., Part A-2, 4, 465-474 (1966).

20. Blumstein, A., Blumstein, R. and Vanderspurt, T. H., "Polymerization of Adsorbed Monolayers. IV. The Two-Dimensional Structure of Insertion Polymers," J. Coll. Interface Sci., 31 (2), 236-247

21. Blumstein, A., Malhotra, S. L. and Watterson, A. C., "Polymerization of Monolayers. V. Tacticity of the Insertion Poly(methyl methacrylate)," J. Polym. Sci., Part A-2, 8, 1599-1615 (1970).

22. Raff, R. A. V., "The Grafting of Organic Polymers onto Inorganic Surfaces," AEC Contract No. AT(45-1)-2043.

23. Attix, F. H., Roesch, W. C. and Tochilin, E. Radiation Dosimetry. New York: Academic Press Inc., Vol. II (Instrumentation) 1965, 167-197.

24. Ibid., p. 189.

25. Ibid., p. 193.

26. Ibid., p. 229.

27. Currier, J. Personal Communication. International Minerals and Chemical Corporation Libertyville, Ill.

28. Reinmoller, M. and Fox. T. G., "Determination of Diastereosequence Distribution Statistics From Data on Triad and Pair Populations: Anionic Polymethyl Methacrylate," ACS Polym. Preprints, 17 (2), 987-998 (1966).

29. Reinmoller, M. and Fox, T. G., "Penultimate Effect on the Stereospecificity of Free Radical Polymethyl Methacrylate," ACS Polym. Preprints, 17 (2), 999-1004 (1966).

30. Detrick, C. A. and Kelly, J. L., "Effects of Certain Factors on the Radiation-Induced Polymerization of Methyl Methacrylate," Ind. Eng. Chem. Process Des. Develop., 9, (2), 191-194 (1970).

31. Chapiro, A. Radiation Chemistry of Polymeric Systems. New York: Interscience Publishers, Vol. XV. (High Polymers), 1962, 129-140.

32. Ballantine, D. S. Colombo, P., Glines A., and Manowitz, B. Chem. Eng. Symposium Series, 50, 267-270 (1954).

33. Okamura, S. Oishi, Y. and Inagaki, H., Bull. Ins. Chem. Research, Kyoto Univ., 14, 103 (1957).

34. Grim, R. E. Clay Mineralogy. New York: McGraw-Hill Book Co., 1968, 265.

35. Chen, Y. C., "Thermal Degradation of Polymethyl Methacrylate in Solution in Various Solvents," M.S. Thesis, Univ. of Mo.-Rolla (1965).

36. Niu, T. F., "Degradation of Polystyrene Solutions by Capillary Shear," M.S. Thesis, Univ. of Mo.-Rolla (1970).

37. Sarmasti, A. A., "Shear Degradation of Polystyrene in Toluene," M.S. Thesis, Univ. of Mo-Rolla (1970).

38. Brandrup, J. and Immergut, E. H. Polymer Handbook. New York: Interscience Publishers, 1966, IV-26.

39. Ibid, p. IV-28.

40. Mayhan, K. G. and Thompson, L. F., Personal Communication, GCMR, Univ. of Mo.-Rolla.

41. Tung, L. H., "Correction of Instrument Spreading in Gel Permeation Chromatography," J. App. Polym. Sci., 13, 775-784 (1969).

42. Bertrand, G, Personal Communication, Univ. of Mo-Rolla (1971).

43. Parker, F. R. Materials Data Book. New York: McGraw-Hill, 1967, 339-340.

44. Illinois Institute of Technology Research Institute SEM Symposia, 1968, 1969, 1970, 1971.

45. Attix, F. H., Roesch, W. C. and Tochilin, E. Radiation Dosimetry. New York: Academic Press Inc., Vol. II (Instrumentation), 1965, 231.

46. Huggins, M. L., J. Am. Chem. Soc., 64, 2716 (1942).

47. Kraemer, E. O., Ind. Eng. Chem., 30, 1200 (1938).